PALEOCEANOGRAPHIC SHIFTS IN THE GULF OF ALASKA OVER THE PAST 2000 YEARS: A MULTI-PROXY PERSPECTIVE

By

Molly McCall Boughan

RECOMMENDED:

_____
Dr. Sathy Naidu

_____
Dr. Terry E. Whitledge

_____
Dr. Bruce Finney
Advisory Committee Chair

_____
Dr. Katrin Iken
Head, Program in Marine Science and Limnology

APPROVED:

_____
Dr. Denis Wiesenburg
Dean, School of Fisheries and Ocean Sciences

_____
Dr. Lawrence Duffy
Dean of the Graduate School

_____
Date

PALEOCEANOGRAPHIC SHIFTS IN THE GULF OF ALASKA OVER THE PAST 2000 YEARS: A MULTI-PROXY PERSPECTIVE

A

THESIS

Presented to the Faculty

of the University of Alaska Fairbanks

in Partial Fulfillment of the Requirements

for the Degree of

MASTER OF SCIENCE

By

Molly McCall Boughan, B.S.

Fairbanks, Alaska

December 2008

Abstract

The Gulf of Alaska (GOA) is a dynamic region influenced by climate variability on time scales ranging from days to millennia. Recent regime shifts suggest interdecadal GOA primary productivity patterns, yet it is unclear whether such fluctuations extend beyond the instrumental record. This thesis examined the nature of prevalent climatic and oceanographic patterns before the twentieth century using several marine sediment core proxies for paleoproductivity and paleoceanography. Sediment cores were from two locations: Bay of Pillars, Kuiu Island, in southeast Alaska (56.63˚N, 134.35˚W), and a central midshelf location (GAK4) along the Global Ecosystem Dynamics (GLOBEC) Seward Line (59.25˚N, 148.82˚ W). Proxy data from these cores include: percentages of organic carbon, nitrogen and biogenic opal; organic carbon-to-nitrogen ratios; stable isotope ratios from sediment organic matter ($\delta^{13}C$ and $\delta^{15}N$) and foraminifera tests ($\delta^{13}C$ and $\delta^{18}O$); and foraminifera faunal analysis. Bay of Pillars proxy data suggest that the onset of the Little Ice Age (LIA) ca. 1200 AD coincides with pulses of decreased salinity and increased productivity. GAK4 proxy data indicate increased productivity and decreased terrestrial input over the past century; as well as fresher surface water was during the latter portion of the LIA (1716 – 1894) and positive Pacific Decadal Oscillation phases.

Table of Contents

Page

Page

Page

Page

List of Figures

Page

Page

Page

List of Tables

Page

List of Appendices

Page

Acknowledgments

Funding for part of this research was provided by NOAA through CIFAR (cooperative agreement NA17RJ1224) project 06-043 (Paleoecologic and Paleoceanographic Studies of Marine Bays in Southeast Alaska) to Dr. Bruce Finney

Special thanks to the following for aid in processing proxy data: Andrea Krumhardt, Celia Sapart, and Dr. Amy Hirons at the Marine Geology Lab, Institute of Marine Science (University of Alaska Fairbanks); to Tim Howe, Norma Haubenstock and Dr. Mat Wooller at the Alaska Stable Isotope Facility (University of Alaska Fairbanks); and to Dr. John Jaegar at the University of Florida Stable Isotope Mass Spec Lab.

Many thanks to my advisor, Dr. Bruce Finney, and committee members, Dr. Sathy Naidu and Dr. Terry Whitledge for their keen insight, knowledge and endless patience; and Madeline Scholl and Christina Neumann for keeping track of it all. Most of all, thank you Hays, Ula, Tulie, and Darby for not kicking me to the curb for all the weekends I spent finishing this thesis.

1.0 Introduction

Gulf of Alaska (GOA) ocean circulation and biological processes are driven by a complex myriad of forces that vary on multiple spatial and temporal scales (Weingartner *et al.* 2002). For example, optimum primary productivity on the GOA shelf is dependent upon the occurrence of intermittent winter and spring storm events to draw nutrients to the surface. However, excess storm events during the same time frame can hinder summer productivity by inhibiting solar radiation and diminishing stratification (Strom *et al.* 2006). A delicate and poorly understood balance exists among the forces that drive atmospheric-oceanic interaction within the GOA, which could become altered if anthropogenic climate change continues to increase in influence.

Shifts in oceanic temperature, salinity or circulation patterns can have profound effects on the marine ecosystem. The diverse and lucrative fisheries found in this region changed rapidly in 1976 – 1977 (Francis *et al*. 1998, Anderson and Piatt 1999, Hare and Mantua 2000, Litzow 2006), apparently in response to physical changes. The ability to predict future ecological shifts would be very valuable (Overland and Stabeno 2004). The purpose of this thesis is to examine paleoecological conditions in the GOA before the instrumental record. Have changes similar to those described above happened in the past? If so, have they occurred in a

predictable manner? Or, are the recent changes a response to the broad warming trend observed throughout Alaska and the greater Pacific basin?

1.1 Oceanographic Setting

The rugged coastline bordering GOA is comprised of numerous fjords, bays and inlets, which are the result of repeated glacial advancement and retreat. The present coastline has one of the highest sedimentation rates on earth, ranging from >1 m y^{-1} in fjords to ~2 cm y^{-1} on the continental shelf (Anderson and Molnia, 1989). Estimated sedimentation rates based on magnetic susceptibility and radiocarbon dates from the two cores in this study were: 0.06 cm y^{-1} in SE Alaska; and 0.46 cm y^{-1} at the mid-continental shelf.

Rapid sedimentation in the GOA is largely a result of the extreme elevation of coastal mountains, the high amount of precipitation that falls on the coast due to the proximity of the Aleutian Low, and the active tectonic plates underlying the region (Jaeger *et al*. 1998). Rivers transport large amounts of melt water and sediment to the GOA during summer to late fall. This accounts for rapid deposition of lithogenic sediments, though in some areas high productivity also accounts for rapid sedimentation. The melt water forms a seasonal halocline on the surface of the ocean, which extends to an approximate depth of 20 m near the coast; much shallower than the 100 – 150 m pycnocline that exists the rest of the year.

The seasonal halocline and southeast winds drive the swift, narrow Alaska Coastal Current (ACC), which flows west along the inner shelf, adjacent and inland to the Alaska Current and Alaska Stream (Figure 1).

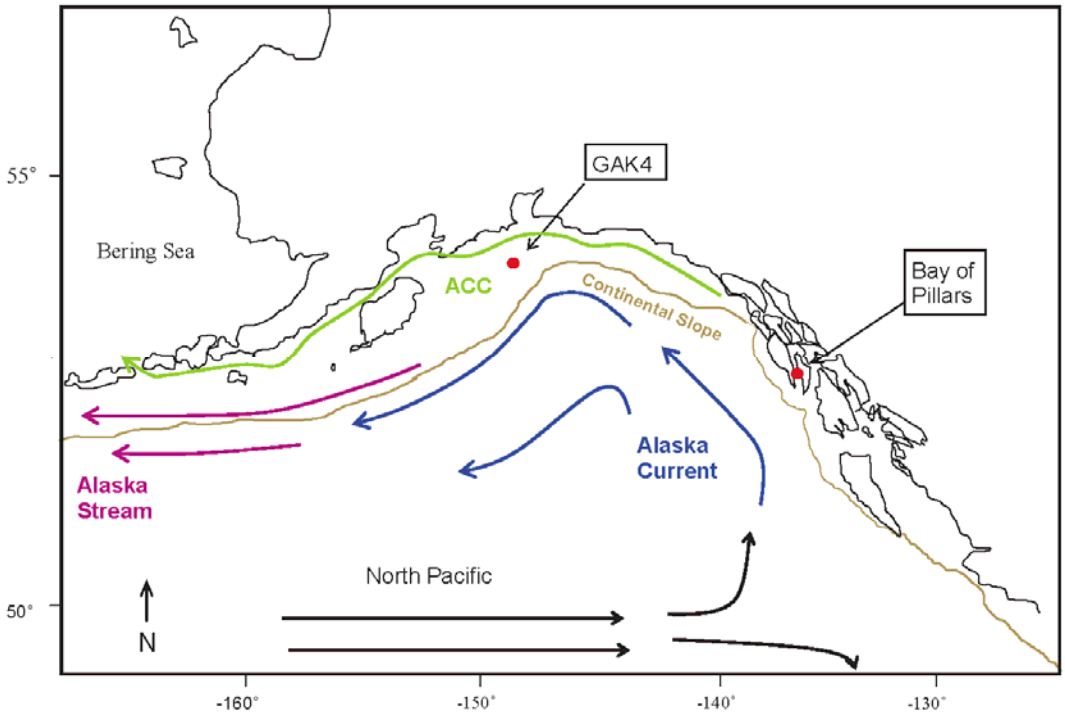

Figure 1 Gulf of Alaska Site Map

Despite downwelling conditions that exist most of the year, productivity in the Gulf of Alaska is very high, up to 300 g C m^{-3} y^{-1} (Sambrotto and Lorenzen 1987). Regional atmospheric and oceanic circulation patterns display strong annual cycles (Childers 2005). The Aleutian Low, a cyclonic low pressure system situated above the GOA,

forms in late fall due to seasonal pressure regimes, which form a vast atmospheric temperature gradient between the warm Pacific Ocean and the frigid continental land mass (Shulski and Wendler 2007). Intensity diminishes during summer months when terrestrial temperatures increase. The Aleutian Low also displays decadal variation in intensity and location (Overland *et al*. 1999). Noted shifts during the past century include 1925, 1948, 1959, 1968, 1977, and 1989 (Shulski and Wendler 2007).

The water column is well-mixed during the winter months due to the strong Aleutian Low; however, during summer months, it is dominated by an influx of riverine freshwater. Stratification allows deep, nutrient-rich water to flow inland, while simultaneously inhibiting these nutrients from reaching the euphotic zone. Several factors, such as intermittent summer storm events, eddy formation, and complex bathymetry will periodically bring these nutrients to the surface during the summer; however, the majority remain at depth to spur early spring blooms the following year. In this sense, a strongly stratified water column promotes continued productivity on the GOA shelf by preventing nutrient depletion (Weingartner *et al.* 2002, Harrison *et al.* 2004, Childers 2005, Childers *et al.* 2005, Strom *et al.* 2006).

As previously mentioned, the Aleutian Low is driven by temperature gradients between the warm Pacific Ocean and the frigid Alaska interior. Therefore, future shifts in atmospheric temperatures could significantly

affect this pressure system. If atmospheric temperatures across Alaska continue to increase, it is plausible that the intensity of the Aleutian Low will decrease because the atmospheric temperature gradient between sea and land will decrease. This could extend the duration of stratified summer months; possibly increasing the summer phytoplankton growth, thus decreasing nutrient availability for spring blooms. However, increasing atmospheric temperatures also increase North Pacific SSTs, which counters, to some extent, any potential decrease in the land-sea temperature gradients. Present observations based on the Aleutian Low Pressure Index (ALPI) indicate the Aleutian Low has decreased from 2002 – 2007 (Beamish *et al*. 1997, http://www.pac.dfo-mpo.gc.ca/sci/sa-mfpd/climate/clm_indx_alpi.htm).

It is uncertain what might occur if both atmospheric and oceanic temperatures continue to rise, but it is possible that a positive feedback loop has formed between GOA atmospheric and oceanic dynamics (Royer *et al.* 2001). Increased SSTs cause increased inland precipitation and milder winters, which eventually increases freshwater run-off. This results in increased stratification and further warming of SSTs.

1.2 Regional Climate Variability

Alaska gyre circulation is directly connected to the entire North Pacific basin as well as the Bering Sea and Arctic Ocean, which eventually

flows into the Atlantic Ocean. Climate patterns that influence the GOA include El Niño Southern Oscillation (ENSO) and the Pacific Decadal Oscillation (PDO). Regional variability directly affects the Alaska gyre by altering the position of the North Pacific Current or the intensity of the Aleutian Low. Trenberth (2001) observed the following from 1977 – 1988: intensified Aleutian Low, increased SST, three El Niño events, and a lack of La Niña events. This period coincides with the well-documented GOA regime shift of 1977 and is characterized by warmer SSTs, increased intensity of the Aleutian Low, and increased productivity (Francis and Hare 1994, Hare and Mantua 2000). Changes in the SST within the Kuroshio Extension have also been linked to GOA regime shifts with warmer trends observed during the 1950s and 1960s, cooler SSTs in the 1970s and 1980s, and an abrupt SST increase in 1998. These time frames coincide with documented GOA regime shifts (Noto and Yasuda, 1999).

1.3 El Niño Southern Oscillation (ENSO)

El Niño Southern Oscillation (ENSO) events are a natural occurrence caused by equatorial oscillations of barometric pressure, which fluctuate between the eastern and western edges of the equatorial Pacific Ocean basin on a timescale of 3 – 7 years. For example, during an El Niño event, atmospheric pressure is higher on the South American coast and lower in the South Pacific, resulting in increased SST and suppressed

upwelling along the South American coast. The intensity of these events fluctuates irregularly, which may link to PDO oscillations. The SST distributions of both patterns are similar, and periods of positive PDO anomaly do appear to coincide with greater El Niño frequency (An *et al.* 2007).

El Niño events affect the NE Pacific by pushing warm subtropical water north to the southern edge of the Alaska Gyre. These events are also marked by an intensified Aleutian Low and increased frequency of storms which aid nutrient mixing. (Harrison *et al*. 2004). There is also a link between El Niño events and increased eddy formation off the Canadian and SE Alaskan coasts (Melsom *et al.* 1999, Childers *et al.* 2005,), which also increases nutrient mixing and productivity.

La Niña events in the GOA have been characterized by decreased SST, increased nitrate and increased salinity (Weingartner *et al*. 2002). In general, though, ENSO effects on the GOA are not consistent and will vary spatially and temporally depending on localized parameters such as atmospheric forcing and storm events. For this reason, it is difficult to draw direct links between ENSO events and broader climatic patterns.

1.4 Pacific Decadal Oscillation (PDO)

The PDO describes the interdecadal recurring pattern of ocean-atmosphere climate variability centered over the North Pacific basin

(Mantua *et al*. 1997). Although this phenomenon was not yet named in 1977, biologists and fisherman were aware of its presence as witnessed by a decrease in shellfish catches and an increase in bottom fish and salmon (Francis and Hare 1994, Hare and Mantua 2000). These biological indicators were later attributed to the PDO warm (or positive) phase, characterized by an increased intensity of the Aleutian Low. This intensity was thought to have resulted in greater offshore upwelling and phytoplankton production in the GOA, although abundant direct monitoring of such changes is lacking. During the same twenty-year period and all other positive PDO phases, the coasts of California, Oregon, and Washington were marked by a decrease in productivity, salmon catches, and SST.

A better understanding of PDO oscillations has been achieved based on SST and atmospheric measurements over the past century. It is presently believed that the PDO shifted in 1890, 1925, 1947, 1977, and, possibly, in 1998 (Figure 2). It is unclear if the 1998 shift represents a change in PDO mode because it may not signal a prominent interdecadal shift. From 2001 – 2005, GOA SSTs have been increasing while sea level pressure (SLP) has been decreasing; however, based on small mesh trawl survey catches, the only notable ecosystem response has been a decrease in cod abundance. Secondary productivity has not yet shown a

decrease, although a lag response of 2 – 4 years has been hypothesized (Litzow 2006).

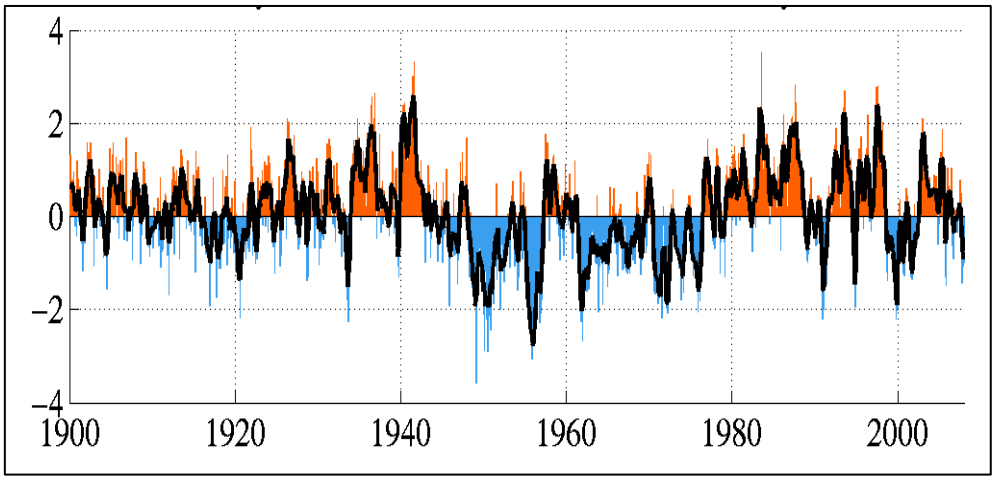

Figure 2 Pacific Decadal Oscillation Index: Monthly Values
Source: Mantua, JISAO University of Washington Website http://jisao.washington.edu/pdo/

While the past century indicates that an approximate 18.2 year cycle has occurred over the past 100 years, proxy studies from tree rings and corals—that extend beyond this record—suggest an irregular pattern of 20 – 50 year oscillations (Minobe 1997, Gedalof and Smith 2001, Gedalof and Mantua 2002, D'Arrigo *et al*. 2005, MacDonald and Case 2005). The foraminifera data in this study are unique because they represent a direct water column proxy for the GOA; whereas tree-ring data are a proxy of past atmospheric conditions and most coral studies have been conducted in lower latitudes.

2.0 Study Area

Cores for this study were chosen on two main criteria: (1) the presence of an adequate number of foraminifera for stable isotope analysis; and (2) representative of AK gyre circulation. Selection of cores from a suite of 16 available sites was based on $CaCO_3$ percentages of sediment and visual inspection under a 10X dissecting microscope at 10 cm intervals. Two locations were selected: a SE Alaskan fjord (Bay of Pillars) and the central, mid-shelf GOA (GAK4) (Figure 1).

2.1 Bay of Pillars, Kuiu Island

Bay of Pillars (56.63˚N, 134.35˚W, 16 m water depth) is located on the east central edge of Kuiu Island, one of approximately 1,000 islands that make up the Alexander Archipelago in Southeast Alaska. This region is considered a temperate rain forest and houses an abundant terrestrial ecosystem (MacDonald and Cook 1996). To the west of Kuiu Island is Chatham Strait and Baranof Island further west; directly east is Kupreanof Island, followed by Petersburg, Alaska, and then additional islands, which adjoin the coastal mountains of British Columbia.

The Bay of Pillars G-2 core is 106 cm in length and extends from approximately 1997 to 260 AD. The sediment from this core consists of diatomaceous, organic-rich, sandy silt. Two cm^3 samples were extracted

continuously down core for sediment analysis; 1 cm^3 samples were extracted every 2 cm for foraminifera analysis. Each centimeter of sediment represents approximately 16 years. Carbon and nitrogen percentages and isotope ratios (sediment organic matter and foraminifera) were sampled every 2 cm (totaling 32 years per sample) and magnetic susceptibility were sampled every centimeter. Only benthic foraminifera species existed in the Bay of Pillars core, which is common in fjord settings due to the fluctuating salinity (Korsun and Hald 2000, Jennings *et al*. 2004). *Elphidium excavatum* (Terquem) was selected for stable isotope analysis as it was the most abundant species.

2.2 GAK 4, Seward Line, GLOBEC Program

The Seward line, a cross-shelf transect of 13 stations located southeast of Seward, Alaska, is one of the most well-monitored locations in the GOA. It is part of the US Global Ecosystem Dynamics Program (GLOBEC) NE Pacific Long-Term Observation Program, designed to define a baseline regional description of the GOA and better understand the driving forces that control it. GAK 4 (59.41˚N, 149.05˚ W, 200 m water depth) is a mid-shelf location, approximately 30 nautical miles (~55 km) south of Seward, Alaska. The length of this gravity core is 166 cm and the approximate time range is from 2003 – 1688 AD. The sediment at this location is fine-grained biogenic silty-clay. Sediment samples were

analyzed continuously every centimeter for most parameters representing approximately 2 year resolution. For foraminiferal analysis, 1 cm^3 samples were extracted every 4 cm starting at the top of the core (2003 AD) through 137 cm (1716 AD), totaling 8 year sample resolution at each depth. Additional foraminifera samples were added at the top of the core to calibrate proxy data with the instrumental record. Stable isotope analysis was conducted on the benthic species *Cassidulina teretis* (Tappan) and the planktonic species *Neogloboquadrina pachyderma* (Ehrenberg). *N. pachyderma* is sometimes referred to as *Globigerina bulloides* var. *borealis* (Brady 1881). The coil direction of *N. pachyderma* has been used in paleoceanographic studies because it is temperature dependent, coiling to the right (dextral) in shallow surface layers (5 – 20 m) warmer than 8˚C; and to the left (sinistral) in well-mixed surface layers (>100 m deep) and cooler than 8˚C (Reynolds and Thunell 1986). In this core, only the left-coiling (sinistral) form was present, which is characterized by a rounded, tightly-coiled coarse test.

3.0 A Multi-proxy Analysis

Paleoenvironmental studies are based on interpretations of proxy data, and thus subject to many assumptions. Therefore, more robust conclusions can be drawn when several proxies are cross-referenced, potentially minimizing the influence of these assumptions. This study

integrates data from both sediment and foraminifera proxies. Sediment proxies include percent organic carbon and organic carbon to nitrogen ratios (OC/N), carbon and nitrogen stable isotopes ($\delta^{13}C$ and $\delta^{15}N$) of organic matter, percent biogenic opal, foraminiferal oxygen and carbon stable isotopes ($\delta^{18}O$ and $\delta^{13}C$), and foraminiferal faunal analysis. Each proxy and the general assumptions associated with it are summarized below and listed in Table 1. Specific assumptions based on results from this study are discussed in the conclusion.

Geochemical analysis was conducted to interpret shifts in productivity and oceanographic conditions over time. The top of the core represents near present conditions while the down core data provide information for prior decades and millennia. The sedimentation chronologies were determined from paleomagnetic and radiocarbon data. The GAK4 core has a higher resolution; therefore, in some cases, correlations can be made to instrumental data.

Table 1 Proxy Summary

Analyte	Proxy	Interpretation
Sediment Organic Matter		
$\delta^{13}C$	Shifts in source (terrestrial vs. marine) and/or productivity	Higher ratios ($\downarrow \delta^{13}C$) indicate increased marine input with respect to terrestrial input. Further fractionation of organic matter can be a result of preferential uptake of the lighter ^{12}C isotope and therefore increased productivity.
$\delta^{15}N$	Presence of phytoplankton blooms; Extent of nitrate utilization	Depleted ratios (increased fractionation) indicate phytoplankton blooms; while heavier ratios can indicate denitrification and/or increased nitrate utilization in the euphotic zone.
TOC	Total plankton biomass	Higher overall cabon indicates higher overall productivity
OC/N	Source: terrestrial vs. marine	Marine C/N is ~4-8; Terrestrial C/N is >20
Percent biogenic opal	Diatom biomass	High % biogenic opal indicates past diatom blooms
Foraminifera		
$\delta^{18}O$	Salinity and/or temperature	Test $\delta^{18}O$ signatures will be higher when surrounding waters are saltier/colder; and lighter when surrounding waters are fresher/warmer.
$\delta^{13}C$	Carbon pump	An efficient carbon pump is represented by enriched planktonic tests and depleted benthic tests.
Faunal analysis	Standing stock & species diversity	Increased dominance of single species & decreased diversity correlates with increased productivity.

3.1 Organic Carbon Content and Organic Carbon/Nitrogen (OC/N) of Marine Sediment

Organic carbon (OC) flux to bottom sediment generally increases during periods of increased productivity within the euphotic zone. Therefore, a higher amount of OC in sediment cores represents an overall increase of biomass, unless diluted by inorganic inputs. However, alternate interpretations include decreased consumption in the euphotic zone

(resulting in increased OC accumulation) or offsite transport by swift surface currents (resulting in decreased OC). For the purpose of this study, it is assumed that down-core increases in OC are the result of increased surface productivity; and decreased OC accumulation is the result of decreased surface productivity.

Due to the proximity of the core locations to the coast, organic carbon-to nitrogen ratios (OC/N) can be used to determine whether sediment organic matter originated from a terrestrial or marine source. Marine algae sources usually have an OC/N ratio of approximately 4 – 8, while terrestrial plants have a ratio of 20 or more due to the presence of cellulose in the vascular plants (Meyers 1994). Down core shifts of OC/N ratios indicate paleoshifts in the source of organic material over time. Therefore, decreased OC/N ratios generally coincide with either increased marine productivity or reduced terrestrial input.

3.2 Carbon Stable Isotopes ($\delta^{13}C$) of Marine Sediment Organic Matter

Stable isotopes of an atom are equal in charge yet differ by atomic weight due to a differing number of neutrons. Marine phytoplankton generally have a $\delta^{13}C$ of ~ -21 ‰ (Naidu *et al*. 1993, Meyers 1994), whereas terrestrial input from Alaska is more negative, around ~ -26 ‰ (Rember and Trefrey 2005). Therefore, the $\delta^{13}C$ signature of bottom

sediment will reflect the majority of the source by shifting between these values.

This proxy is complicated, however, because large variability can exist among phytoplankton based on physiological factors such as growth rate, nutrient availability, uptake mechanisms and cell size (Laws *et al.* 1995); as well as external factors such as temperature and salinity of the water column or the photoperiod in which the phytoplankton formed (Perry *et al.* 1999). Moreover, the $\delta^{13}C$ of marine sediment organic matter does not only reflect phytoplankton and terrestrial sources; it represents particulate organic carbon (POC) from higher trophic levels such as fecal pellets and dissolved organic carbon (DOC) from various sources. The $\delta^{13}C$ of DOC can also vary by biochemical composition, for example, lipids tend to have a depleted signature with respect to the entire organism (DeNiro and Epstein 1977), whereas protein is enriched (Deines 1980).

The $\delta^{13}C$ of phytoplankton is also influenced by the inorganic carbon isotopic signature of the water column in which it formed. When inorganic carbon enters the ocean, it combines with seawater to form carbonic acid, which dissociates and forms bicarbonate, then dissociates again to form carbonate, according to the following equilibrium equation:

$$CO_2 + H_2O \leftrightharpoons H_2CO_3 \leftrightharpoons HCO_3^- + H^+ \qquad (1)$$

This is controlled by the atmospheric partial pressure (pCO_2) which is in approximate equilibrium with the surface layer $[CO_2]_{(aq)}$.

The surface water and atmosphere exchange gases at the air-sea interface through a stagnant "thin film" surface layer approximately 30μm thick. Because the water is considered stagnant and therefore not advective, transport is driven by molecular diffusion. The rate of gas exchange between the atmosphere and surface waters varies by many factors; primarily, wind speed, temperature, and difference in CO_2 concentrations between the atmosphere and ocean surfaces. Gas exchange will increase as wind speed and temperature increases. The exchange of gas between atmosphere and ocean moves in the direction of higher concentration to lower concentration, and the reaction rate will accelerate as the difference in concentrations increases. Currently in the GOA, all three factors (high wind velocity, temperature and atmospheric pCO_2 concentrations) indicate that oceanic uptake of $CO_{2(aq)}$ is likely occurring.

The $\delta^{13}C$ of atmospheric pCO_2 has become depleted since the onset of the Industrial Revolution, from -6.3 ‰ to -7.8 ‰, due to the input of depleted $\delta^{13}C$ of fossil fuels (approximately -26 ‰) (Friedli *et al.* 1986, Keeling *et al.* 1995, Verburg 2007). The estimated $\delta^{13}C$ of surface seawater in this region is approximately 2.3 ‰ (Freeman 2001). This phenomenon, termed the Suess effect (Keeling *et al.* 1979, DeNiro and

Epstein 1978) could be an important factor in this region due to the downwelling dynamics and high latitude location. The marine sediment $\delta^{13}C$ data would also be a good tracer since animals lower in the food chain, which are more likely to be part of the DOC found in marine sediment, are more directly affected than those with a higher trophic level (Schell 2000).

For the purpose of this study, it will be assumed that depleted (more negative) $\delta^{13}C$ ratios represent increased terrestrial input and enriched (less negative) $\delta^{13}C$ ratios represent increased marine input and productivity.

3.3 Nitrogen Stable Isotopes ($\delta^{15}N$) of Marine Sediment Organic Matter

Nitrogen stable isotopes of marine sediment organic matter can be used to infer relative productivity shifts and nitrate utilization within the euphotic zone. Phytoplankton blooms can be detected in marine sediment because the majority of phytodetritic material formed during a bloom will eventually make it to the shelf sea-floor, thus representing a majority of the particulate organic matter (POM). Like carbon, phytoplankton preferentially uptake the lighter isotope (^{14}N) (Altabet and François 1994, Altabet *et al.*1999), therefore the sediment $\delta^{15}N$ signature may also be lighter following a bloom. After sedimentation has occurred, additional fractionation occurs because bacteria also prefer the lighter isotope,

resulting in a possible $\delta^{15}N$ enrichment of the remaining sediment organic matter.

A depleted $\delta^{15}N$ signature can also be used to infer nutrient availability because phytoplankton fractionation increases when nutrients are abundant and growth rates are high (Altabet and François 1994, Teranes and Bernasconi 2000), therefore reflecting lighter $\delta^{15}N$ values. During periods when nutrients are sparse and growth rates slow, fractionation by phytoplankton is less likely to occur (Schell *et al.* 1998), resulting in heavier $\delta^{15}N$ values.

Where nitrogen is a limiting nutrient, the $\delta^{15}N$ is linearly related to the degree of ocean surface water nitrate utilization. As [NO_3] is utilized in the surface, sediment organic matter $\delta^{15}N$ will increase. Once deposited, further enrichment occurs during digenesis (Altabet and François 1994). The opposite can also be observed: under conditions of high nitrate supply, productivity could increase, although [NO_3] may not be depleted, and $\delta^{15}N$ ratios could be decreased or unchanged. Therefore, depending on the interpretation, enriched $\delta^{15}N$ could indicate either high productivity or low nitrate supply. For this study, a lighter $\delta^{15}N$ signature will likely indicate increased productivity in the Bay of Pillars core; however in the GAK4 core, where nitrate is seasonally limited, heavier ratios could infer increased productivity.

3.4 Percent Biogenic Opal of Marine Sediment

Sedimentary biogenic opaline is the sum of the siliceous plankton within the core, which in this region consists primarily of diatoms (Strom *et al.* 2007). Thus, fluctuations that may occur down core indicate changes in diatom abundance over time. Diatoms prefer nutrient-rich waters; therefore, I presume that increased percent biogenic opal correlates with increased paleoproductivity. However, it should be noted that increased silica dissolution occurs with increased diatom frustule surface area (such as chain-forming diatoms) or when interstitial conditions are brackish or alkaline (Barker *et al.* 1994), which could cause misinterpretation.

3.5 Foraminifera proxies

Foraminifera are single cell animals of the Kingdom Protista that secrete a protective test, or shell. Living foraminifera contain cytoplasm, or rhizopodia, that extend through the test to feed on bacteria, diatoms, or dissolved organic matter. Shells are most commonly composed of calcium carbonate ($CaCO_3$-trigonal mineral system), aragonite ($CaCO_3$-orthorhombic mineral system) or agglutinated with organic material. Individual size can range from microns to centimeters.

There have been very few paleoceanographic studies utilizing foraminifera in this study region. Although globally distributed, foraminifera are most diverse and abundant in tropical waters. In addition, calcium

carbonate is typically dissolved in deep waters offshore of this region due to the relatively shallow (500 – 1500 m) carbonate compensation depth (CCD) found in the Pacific Ocean. At depths below the CCD, foraminifera readily dissolve because the deep water becomes undersaturated with respect to $CaCO_3$ minerals in the several hundred years it takes to flow from the southern ocean where it originates. Both core locations in this study are on the shelf, and therefore not affected by the CCD.

3.6 Oxygen Stable Isotopes ($\delta^{18}O$) of Calcium Carbonate Foraminifera Tests

Oxygen isotope ratios of foraminifera tests have been used as paleoceanographic indicators since the 1950's when University of Chicago scholars Harold Urey and Cesare Emiliani first discovered the correlation between glacial periods and oxygen isotopes of foraminifera (Urey *et al.* 1951, Emiliani 1954). Nicholas Shackleton showed that the foraminifer's $\delta^{18}O$ signature of deep water species is mainly a function of the water column $\delta^{18}O$ and therefore more dependent on salinity than temperature (Shackleton 1974). He then went on to advance mass spectrometry technology and prove the usefulness of foraminifera $\delta^{13}C$ signatures to quantify the efficiency of the carbon pump (Shackleton and Pisias 1985).

The $\delta^{18}O$ signature of foraminifera is an indicator of past salinity and temperature parameters of the water in which they grew. In this study, the

emphasis is on salinity because GOA dynamics are driven by seasonal density differences resulting from summer freshwater influx. As glacial or fluvial run-off increase, salinity decreases and the $\delta^{18}O$ signature of water and the foraminifera formed therein will decrease. The carbonate test $\delta^{18}O$ of the foraminifer is in near-equilibrium with the water column $\delta^{18}O$ in which it formed; however, temperature and individual physiology will offset this to some degree. As temperature increases, the $\delta^{18}O$ difference between water column and test will decrease due to thermodynamics. This physiological offset is referred to as the 'vital effect,' and can be influenced by the species and within the species based on size or development stage.

In this study, vital effects are considered negligible based on the following rationale: 1) The size fraction is consistent—stable isotope analysis was conducted for the 125 – 249 μm size fraction only; 2) the species is consistent—stable isotope analysis was conducted separately on one continuous benthic species (*E. excavatum*) from the Bay of Pillars core and one benthic *(C. teretis)* and one planktonic species (*N. pachyderma*) from the GAK4 core; and 3) the paleoceanographic and paleoecolgical change inferred from these data are relative—a direct calculation of SST has not been attempted in this study. However, for the planktonic species *N. pachyderma*, a common vital effect offset of -1.0 ‰ $\delta^{18}O$ has been observed (Bauch *et al.* 1996). This adjustment was made in Figure 8, comparing the predicted water column equilibrium $\delta^{18}O$ with

the calcite $\delta^{18}O$. All other $\delta^{18}O$ data reported in this study have not been corrected for vital effects.

3.7 Carbon Stable Isotopes ($\delta^{13}C$) of Calcium Carbonate Foraminifera Tests

Measuring the carbon isotopic signature of foraminifera tests is useful to infer past changes in the ocean carbon cycle. Spero *et al.* (1997) have linked decreased carbon and oxygen isotopes to increased [CO_3^{2-}] of the water column. Carbonate tests are formed according to the following equation:

$$Ca^{2+} + 2HCO_3^- \rightleftharpoons CaCO_3 + CO_2 + H_2O. \quad (2)$$

When tests are secreted, the $\delta^{13}C_{DIC}$ is incorporated into the $CaCO_3$. Thus, depleted benthic calcite values reflect depleted DIC in sediment due to respiration of organic matter. Planktonic species can reflect a depleted $\delta^{13}C$ signature during periods of high riverine input because the bicarbonate $\delta^{13}C$ signature is depleted relative to open ocean bicarbonate (Anderson and Arthur 1983, Thomas *et al.* 2000). This can also be interpreted to evaluate past upwelling events, indicated by a depleted $\delta^{13}C$ signature, indicative of the depleted $\delta^{13}C_{DIC}$ signature of subsurface water.

The efficiency of the carbon pump can be assessed by comparing planktonic and benthic carbon isotope values. During periods of high surface productivity, the water column will be enriched in $\delta^{13}C$ due to the phytoplankton preferential uptake of ^{12}C, thus resulting in an enriched $\delta^{13}C$ of the planktonic foraminifer test. Benthic species will be depleted in $\delta^{13}C$ relative to the planktonic species because their source of DIC at bottom waters will be mainly respired CO_2 from remineralization of deposited phytodetritus rich in C^{12}. Less productive surface waters are characterized by relatively lighter planktonic and heavier benthic $\delta^{13}C$ signatures in foram species. There is greater disparity in $\delta^{13}C$ values of planktonic and benthic forams when surface water productivity is relatively higher.

The Suess effect should be considered when interpreting $\delta^{13}C$ signatures of foraminifera tests. As previously mentioned, the Suess effect is diminished when mixing of deep open ocean water and surface water occurs (as in case of upwelling events), yet enhanced during downwelling, which is common most of the year on the GOA shelf. Increased atmospheric pCO_2 may have future effects on calcite formation, the $\delta^{13}C$ value in planktonic foram and the entire global carbon cycle. When pCO_2 increases, hydrogen ions $[H^+]$ increase, resulting in decreased pH of surface waters. Acidic surface waters inhibit $CaCO_3$ secretion, thereby decreasing the capacity of the ocean as a carbon sink. The $\delta^{13}C$ of

foraminifera tests would be expected to decrease as anthropogenic atmospheric CO_2 rises.

3.8 Foraminifera Faunal Analysis

The goal of measuring density, in this case the number of individuals per 1 cm^3 of sediment, is to provide another proxy to help quantify paleoenvironmental shifts. Herguera and Berger (1991) estimate that one individual benthic foraminifera is equivalent to 1 mg organic carbon at the surface. The number of benthic individuals can therefore be used as a proxy for productivity in the euphotic zone. Productivity can also be assessed by the general assumption that a community will be more abundant and less diverse as productivity increases. During less productive periods, there may be a decrease in standing stock but an increase in diversity.

4.0 Methods

The Bay of Pillars G – 2 core was collected in 1997 with a light-weight hammer corer from a small skiff (Boston Whaler), which was necessary to navigate the shallow sills. Excellent core top recovery was observed upon extraction. The GAK4 core was collected in 2003 with a Benthos gravity corer from the ship RV *Alpha Helix*.

Once extracted, cores were stored in the Institute of Marine Science geological oceanography laboratory at ~ 3˚C. Upon investigation, the marine sediment cores were split in half lengthwise, visually examined and described, and analyzed down core for magnetic susceptibility. The cores were then sub-sampled to analyze each proxy. Sediment samples were extracted for the analysis of $\delta^{13}C$, $\delta^{15}N$, and percent carbon and nitrogen following methods outlined below. Separate sub-samples were collected and processed for biogenic opal, foraminifera stable isotopes and foraminifera faunal analysis.

4.1 Age Determination

Sediment samples from the Bay of Pillars core were dated by Accelerator Mass Spectrometry (AMS) radiocarbon analysis of terrestrial macrofossils sieved from the core. The age model consisted of a linear fit between the core top (1997) and the 68 – 69 cm radiocarbon date (Table A – 4). The GAK4 core was dated by correlating its paleomagnetic secular variation record to high-resolution records of instrumental data. This analysis was conducted by collaborators John Jaeger (University of Florida) and Joseph Stoner (Oregon State University) (Jaeger *et al*. in preparation).

4.2 Organic Carbon Content and Carbon/Nitrogen (OC/N) of Marine Sediment

Organic carbon and total nitrogen percentages were measured on acid washed samples (technique described below) on a Costech elemental analyzer that is the “front end” of the isotope ratio mass spectrometer. Calibration is done via in house standards at the Alaska Stable Isotope Facility. Analytical precision is ± 5 %.

4.3 Carbon and Nitrogen Stable Isotopes ($\delta^{13}C$, $\delta^{15}N$) of Marine Sediment Organic Matter

Organic matter from sediment samples was analyzed for isotopic composition on the Thermo Electron Finnigan Delta^{plus}XP Continuous Flow Stable Isotope Ratio Mass spectrometer at the University of Alaska Stable Isotope Facility. For all stable isotope analyses, the isotopic signature is reported as follows:

$$\delta^{H}E = \left(\frac{R_{sample}}{R_{Std}} - 1\right) \times 1000; \quad (3)$$

where $\delta^{H}E$ is the heavier element (ie. $\delta^{18}O$, $\delta^{15}N$, $\delta^{13}C$), R_{sample} is the isotopic ratio of the sample and R_{Std} is the standard. The standard for

oxygen and carbon is PeeDee belemnite (PDB); and for nitrogen, it is atmospheric nitrogen (N_2).

Two cm^3 samples were first acid treated with 5 ml 2N HCl, centrifuged and thoroughly rinsed with Nanopure water. After freeze-drying, the CO_3-free sediment was weighed on a microbalance to an approximate weight of 15 µg (or more if organic carbon content was low) and placed in aluminum foil tins. The isotope ratio mass spectrometer is interfaced with the aforementioned Costech elemental analyzer for organic combustion and determination of carbon and nitrogen abundance. The analytical precision for carbon isotopes was ± 0.2 ‰ and ± 0.3 ‰ for nitrogen stable isotopes.

4.4 Percent Biogenic Opal of Marine Sediment

Biogenic opal (silica) percentages were determined based on a procedure modified from Mortlock and Froelich (1989), which utilizes molybdate-blue spectrophotometry. The opal was dissolved in an alkaline solution and extracted from the sediment. The extract was then analyzed in a Spectonic D+, set at 812 nm. The blue wavelength is reported as absorbance, A_s, and applied to the following equation:

$$C_s = F * (A_s - A_o); \quad (4)$$

where C_s is the silica concentration of the sample, A_o is the absorbance of the operational blank, and F = 1/S. S is the slope of a linear repression through five silica standards used in the initial step to turn the extract blue. The silica concentration is reported in mM. This value was then converted to weight percent, which was then multiplied by 2.4 to account for the percent water in the diatom. The final units were reported in weight % opal. This method determines amorphous silica, hence it does not discriminate between silica bound in tests of diatoms and other siliceous organisms such as radiolarians. The standard deviation of sediment samples containing both silica-rich (70 – 100 %) and silica-poor (4 %) is ± 4 – 5 % (Mortlock and Froelich 1989).

4.5 Foraminifera Analysis

Sediment samples were extracted from the cores at 1 cm widths spaced at 4 cm (GAK4) and 2 cm (Bay of Pillars) intervals. These samples were wet-sieved into three size fractions: 63 – 125 μm, 125 – 249 μm, and >250 μm. Each individual size-fraction was then dried and placed in a glass vial to be used for taxonomic analysis. Additional bulk sediment samples (ranging in volume from 2 – 8 cm^3) were extracted from the same depth intervals for picking foraminifera for stable isotope analysis. The 125 – 249 μm size fraction was isolated from the bulk samples to ensure

consistency of individual sizes, thus minimizing vital effects that could be attributed to size.

4.6 Carbon and Oxygen Stable Isotopes ($\delta^{13}C$, $\delta^{18}O$) of Foraminifera

Approximately five individual foraminifera were extracted at each depth with a fine brush using a 10X dissecting microscope. The GAK4 core contained both benthic and planktonic species; therefore, both individual species were picked and analyzed separately for each core depth. Prior to stable isotope analysis, the bulk sediment samples were soaked in tap water for 24 hours to disaggregate then rinsed with additional tap water while sieving; therefore, additional pretreatment to remove organics from the tests was not conducted. Once extracted, the individual foraminifera were analyzed using a Finnigan-MAT 252 system equipped with a Finnigan-Mat Kiel III carbonate preparation device at the University of Florida Stable Isotope laboratory. Analytical precision was estimated by measuring eight standards (NBS-19) with each carousel containing 38 samples and averaged ± 0.05 ‰ for $\delta^{13}C$ and ± 0.08 ‰ for $\delta^{18}O$.

4.7 Foraminifera Faunal analysis

Faunal taxonomic analysis was conducted from an altered protocol provided by Dave Anderson (NOAA Institute of Arctic and Alpine

Research, pers. comm.). Foraminifera from each depth and size fraction were identified and counted under a 10X dissecting microscope. Relative abundance of species was calculated from Buzas and Hayek (2005) as:

$$p_i = \frac{n_i}{N}; \quad (5)$$

where n_i is the number of individuals within a given species and N is the total number of individuals in the community.

The definition of community within the context of faunal analysis refers to a single statistical population. In this study, the community is defined by the depth of the sample and includes all three size fractions.

5.0 Results

Bay of Pillars data are presented in Appendix A, GAK4 data are in Appendix B, and GAK1 water column data can be located in Appendix C. To display broad down-core trends, Figures 3 – 6 include a 6^{th}-order polynomial regression line superimposed on the raw data fluctuations vs. time plots. Again, the time-interval represented by foraminifera counts was 32 years from Bay of Pillars and 8 years for GAK4.

5.1 Organic Carbon Content and Organic Carbon/Nitrogen (OC/N) Ratios of Marine Sediment

Organic carbon percentages were extremely high for the Bay of Pillars core (Figure 3a), approximately 7.3 – 10.0 %; and GAK4 values ranged from 0.7 – 1.6 % (Figure 3b). The OC/N ratios were similar for both locations: 10 – 12.5 for Bay of Pillars and 9 – 13.5 for GAK4 data (Figures 3a – b). The Bay of Pillars sediment record shows three periods of time with lower carbon percentages and increased OC/N ratios: 1000 – 100 AD, 1550 – 1600 AD and 1800 – 1910 AD (Figure 3a). The GAK4 data (Figure 3b) display decadal fluctuations with a prominent OC/N decrease from 1920 – 2003 AD.

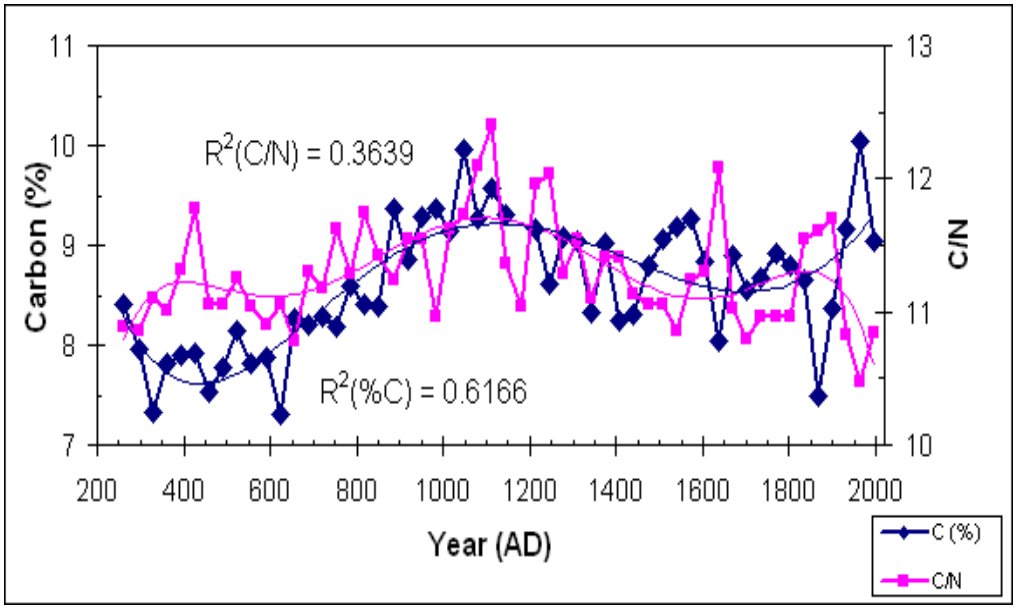

Figure 3a Bay of Pillars Percent Carbon and OC/N Ratios of Marine Sediment Organic Matter

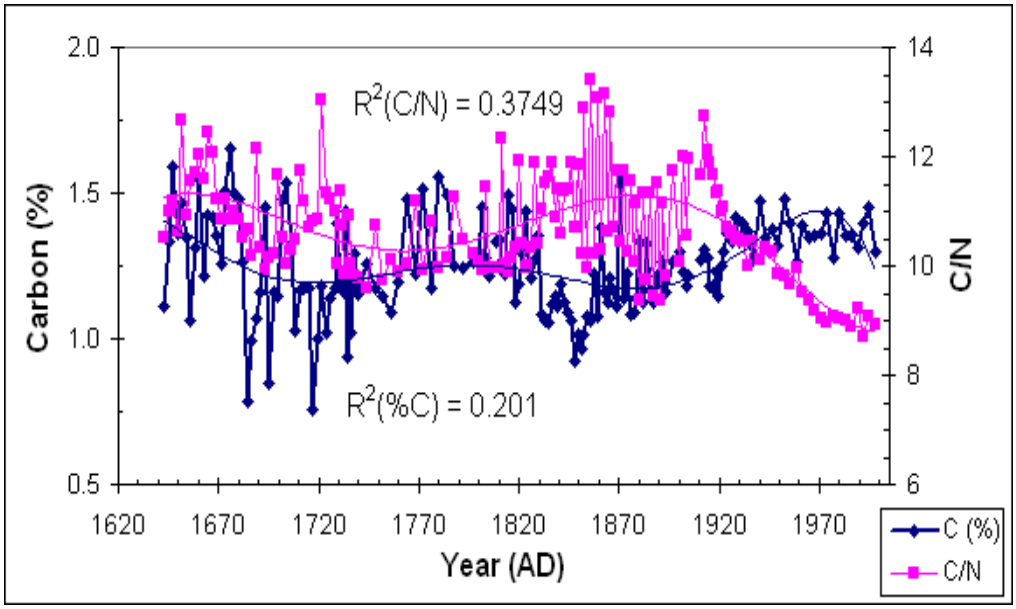

Figure 3b GAK4 Percent Carbon and OC/N Ratios of Marine Sediment Organic Matter

5.2 Carbon and Nitrogen Stable Isotopes ($\delta^{13}C$, $\delta^{15}N$) of Marine Sediment Organic Matter

Carbon stable isotope ratios ($\delta^{13}C$) range from -22.0 to -22.7 ‰ (Bay of Pillars) and -23 to -24.8 ‰ (GAK4) while nitrogen stable isotopes ($\delta^{15}N$) range from 4.5 to 6.0 ‰ (Bay of Pillars) and 3.4 to 5.1 ‰ (GAK4) (Figures 4a – b).

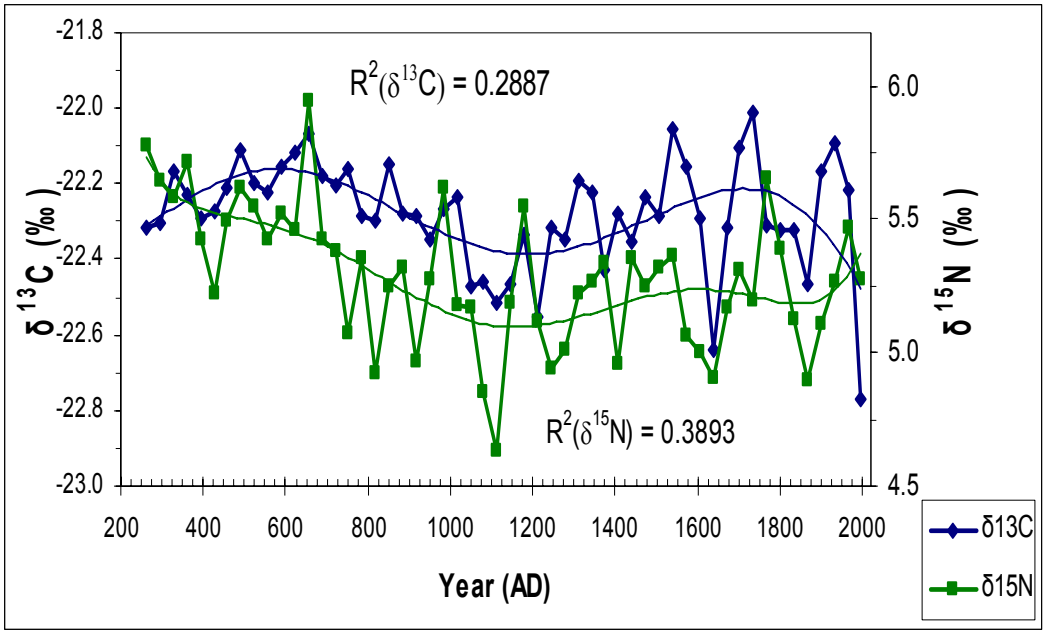

Figure 4a Bay of Pillars $\delta^{13}C$ and $\delta^{15}N$ Signatures of Marine Sediment Organic Matter

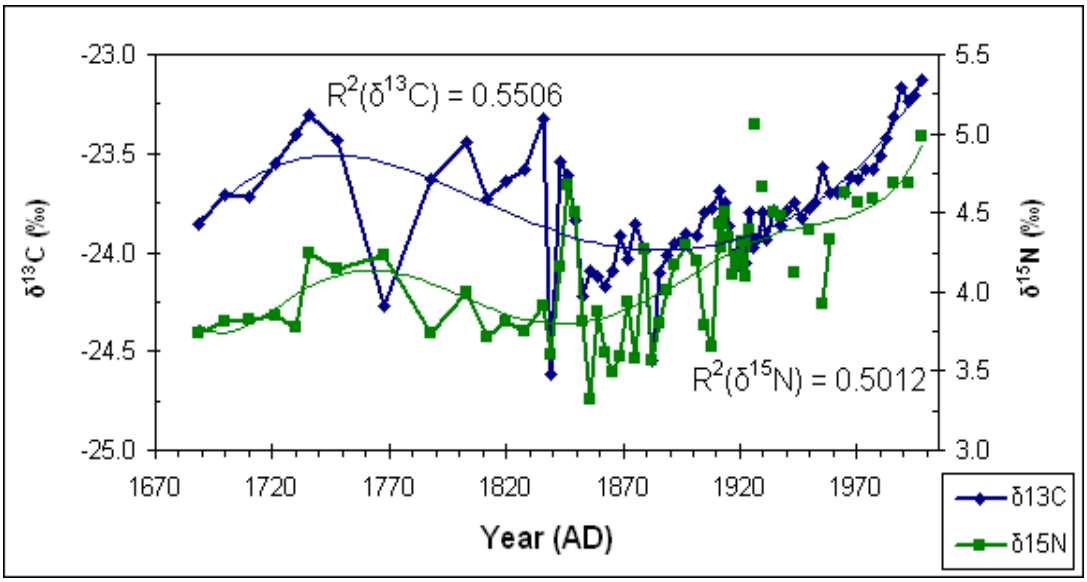

Figure 4b GAK4 $\delta^{13}C$ and $\delta^{15}N$ Signatures of Marine Sediment Organic Matter

Bay of Pillars (Figure 4a) shows approximate 100 – 200 year fluctuations in both $\delta^{15}N$ and $\delta^{13}C$ signatures, with more pronounced variability in the last ~1000 years; GAK4 oscillations do not display a regular pattern. The GAK4 $\delta^{13}C$ (Figure 4b) appears to be increasing (enrichment from -24.1 to -23.1 ‰) during the period from 1920 – 1997 AD. The Suess effect would make values more depleted over this interval; and thus, if corrected, the increase in $\delta^{13}C$ would be greater yet. The GAK4 $\delta^{15}N$ appears to be increasing during this time; however, data gaps make this assumption difficult to assess.

Figure 5 shows scatter plots for both cores comparing the $\delta^{13}C$ and $\delta^{15}N$ signatures to biogenic opal. In each instance (Figures 5a – d), the R^2 values are very low, indicating there is no obvious relationship between these proxies.

a)

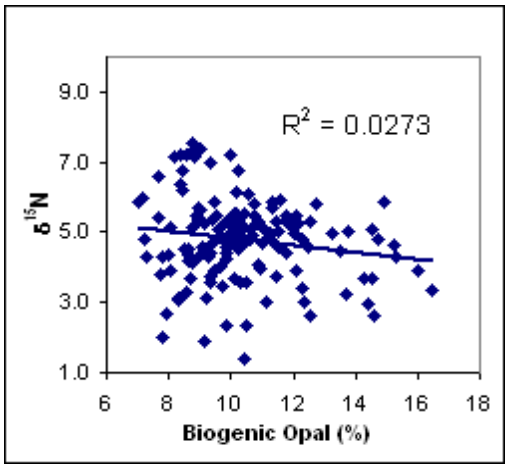

b)

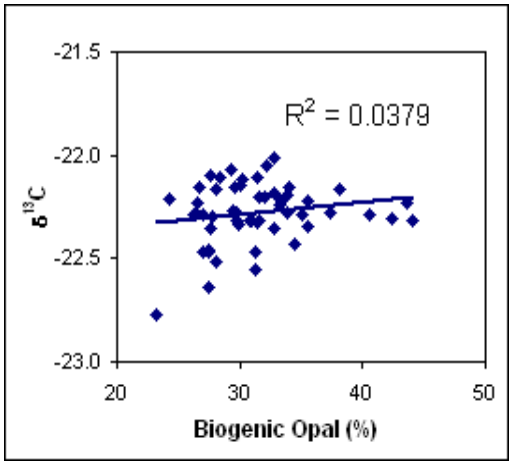

Figures 5a - b Bay of Pillars Comparison of Sediment Opal to a) $\delta^{15}N$ and b) $\delta^{13}C$

c)

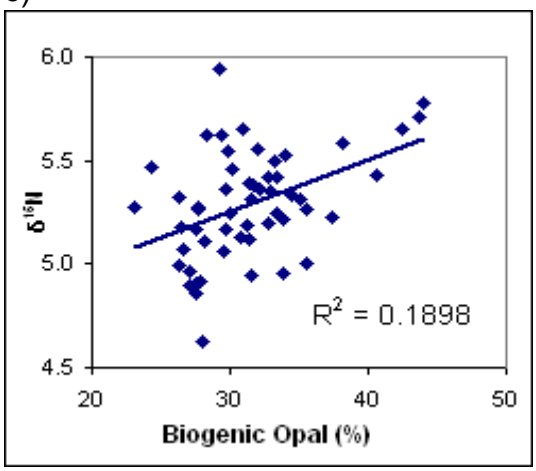

d)

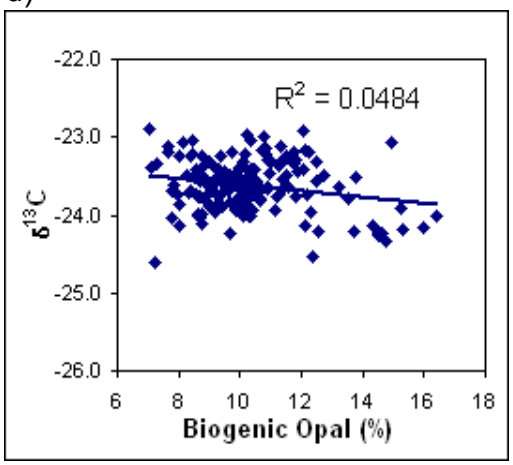

Figures 5c-d GAK 4 Comparison of Sediment Opal to c) δ15N and d)δ13C

5.3 Percent Biogenic Opal of Marine Sediment

Biogenic opal has been plotted with respect to carbon, as both are indications of primary productivity. Opal from the Bay of Pillars core (Figure 6a) was much higher (44.0 – 23.1 %) than the GAK4 core (16.4 – 7.04 %) (Figure 6b).

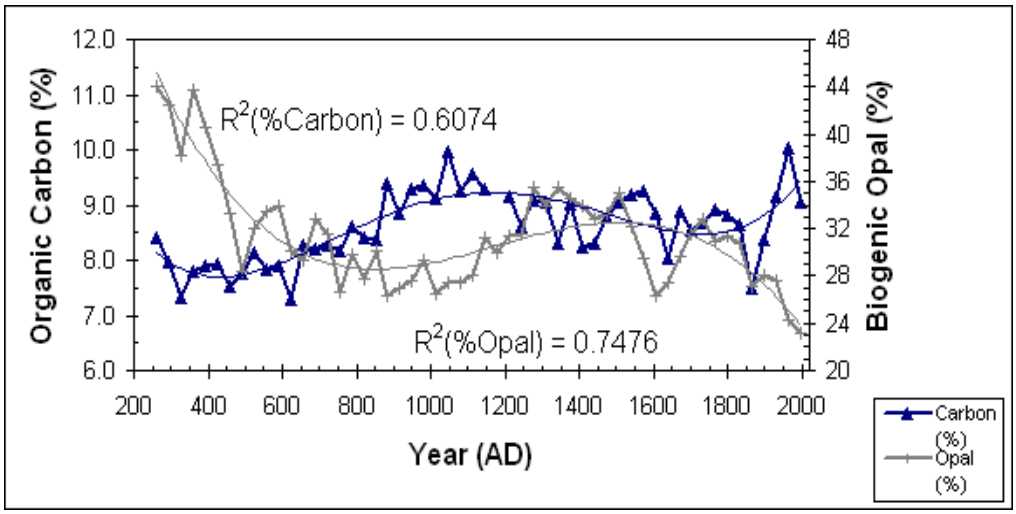

Figure 6a Bay of Pillars Organic Carbon and Biogenic Opal of Marine Sediment

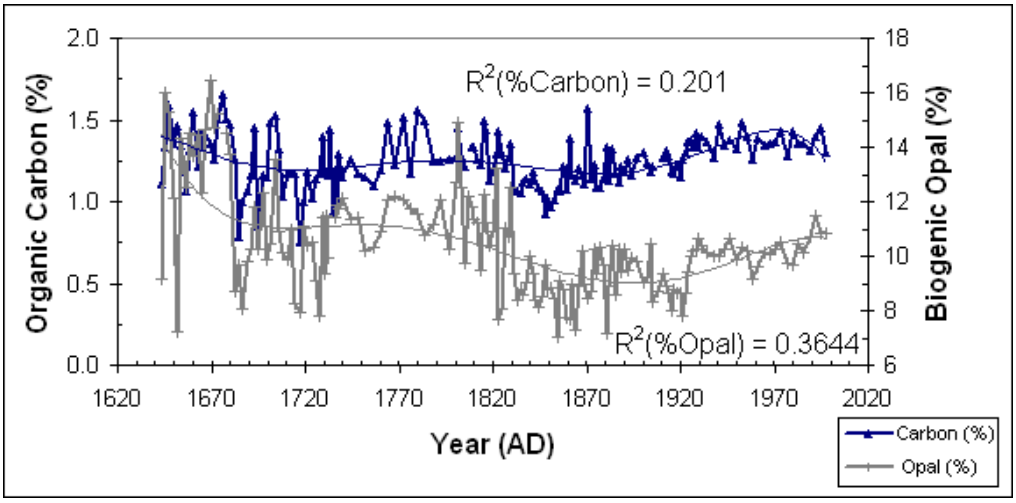

Figure 6b GAK4 Organic Carbon and Biogenic Opal of Marine Sediment

For GAK4, opal percentages are elevated from 1643 – 1684 AD and 1797 – 1829 and have risen about 3 % since 1920. The changes in productivity throughout the past century inferred from the increase in GAK4 $\delta^{13}C$

(Figure 4b) are consistent with biogenic opal percentages from the same time period. Organic carbon and opal show a weak positive linear correlation in the core (Figure 6c).

Bay of Pillars biogenic opal shows a decrease from 44.0 % in 260 AD to 26.9 % in 753 AD; and during the past century, from 28.1 – 23.1 %. There is a weak negative linear relationship between organic carbon and biogenic opal (Figure 6c), opposite of what is observed for the GAK4 data. This is probably due to the high amount of biogenic silica, which dilutes the TOC as it increases.

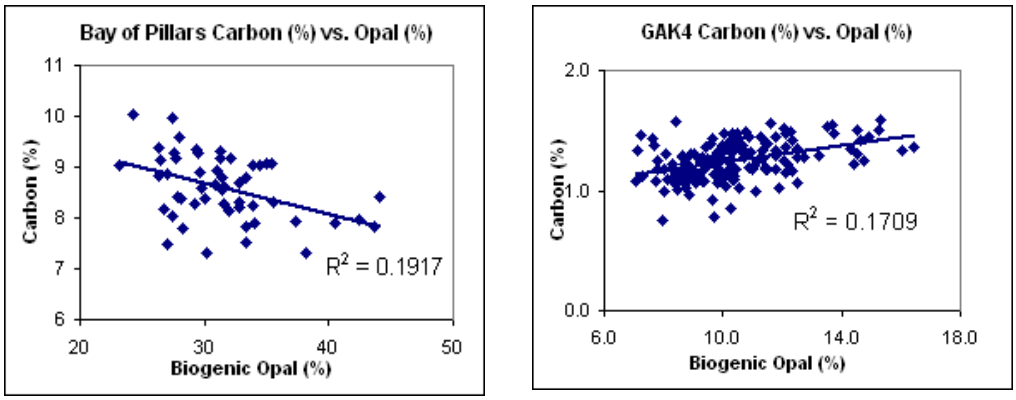

Figure 6c Bay of Pillars and GAK4 Percent Carbon and Biogenic Opal Scatter Plots

5.4 Carbon and Oxygen Stable Isotopes ($\delta^{18}O$, $\delta^{18}C$) of Foraminifera Tests

Carbon isotope ratios from Bay of Pillars benthic foraminfera *(E. excavatum)* tests range from -0.6 to -2.4 ‰; the oxygen isotopic signatures

range from 1.3 to -2.8 ‰ (Figure 7a). The time period from 557 – 1244 AD displays a range of $\delta^{18}O$ of ~1.1 ‰; whereas the period from 1244 – 1833 AD shows a 4 ‰ range.

GAK4 $\delta^{18}O$ ratios for the benthic foraminifera (*C. teretis*) (Figure 7b) ranged from 1.8 to 2.3 ‰; and 1.6 to -3.2 ‰ for the planktonic individuals (*N. pachyderma*) (Figure 7c). Time periods of decreased planktonic $\delta^{18}O$ (Figure 7c) occurred from 1740 – 1800 AD, 1848 – 1874 AD, 1925 – 1966 AD and 1978 – 2003 AD. Note the lack of *C. teretis* individuals during the periods from 1854 – 1868 AD and 1925 – 1978 AD (Figure 7b).

The $\delta^{13}C$ signatures of the GAK4 benthic species ranged from -0.5 to -0.9 ‰; and from 0.9 to -3.29 ‰ for the planktonic species. Time periods in which the planktonic $\delta^{13}C$ signatures were depleted include: 1820 – 1841 and 1930 – 1966. The benthic $\delta^{13}C$ is depleted relative to the planktonic foraminifera from 1848 – 1925 AD.

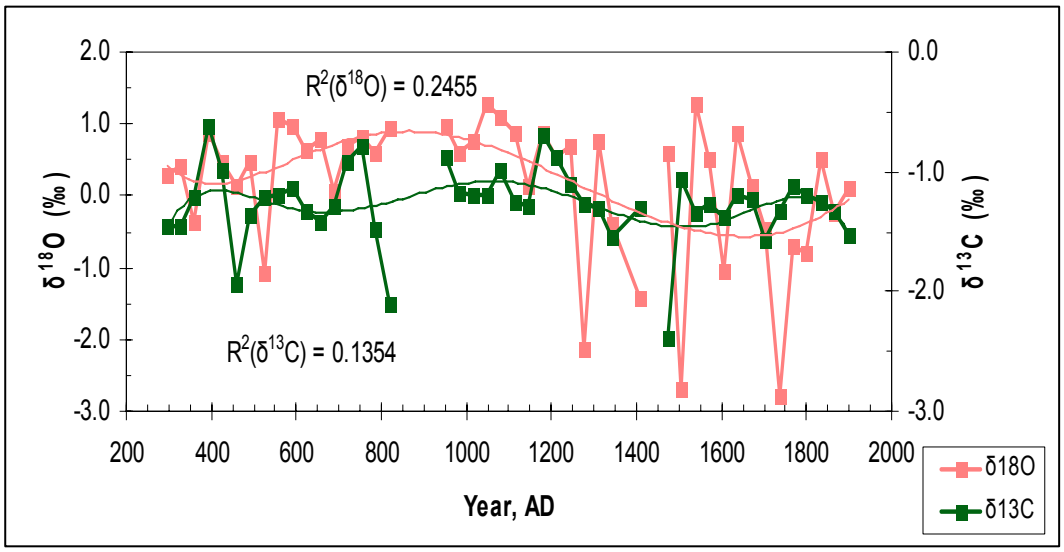

Figure 7a Bay of Pillars δ13C and δ18O Signatures of Benthic Foraminifer *E. excavatum*

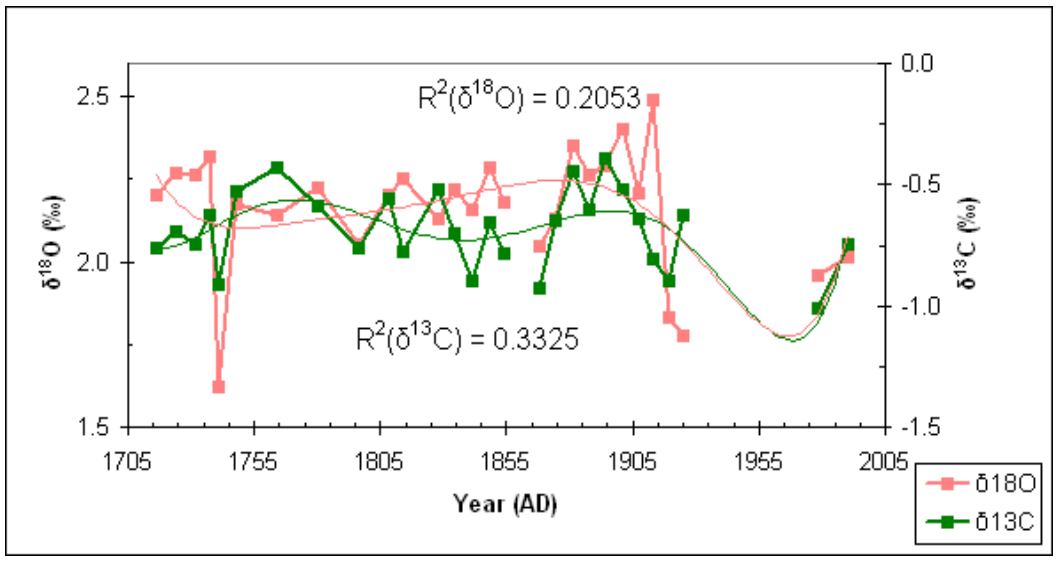

Figure 7b GAK4 δ13C and δ18O Signatures of Benthic Foraminifer *C. teretis*

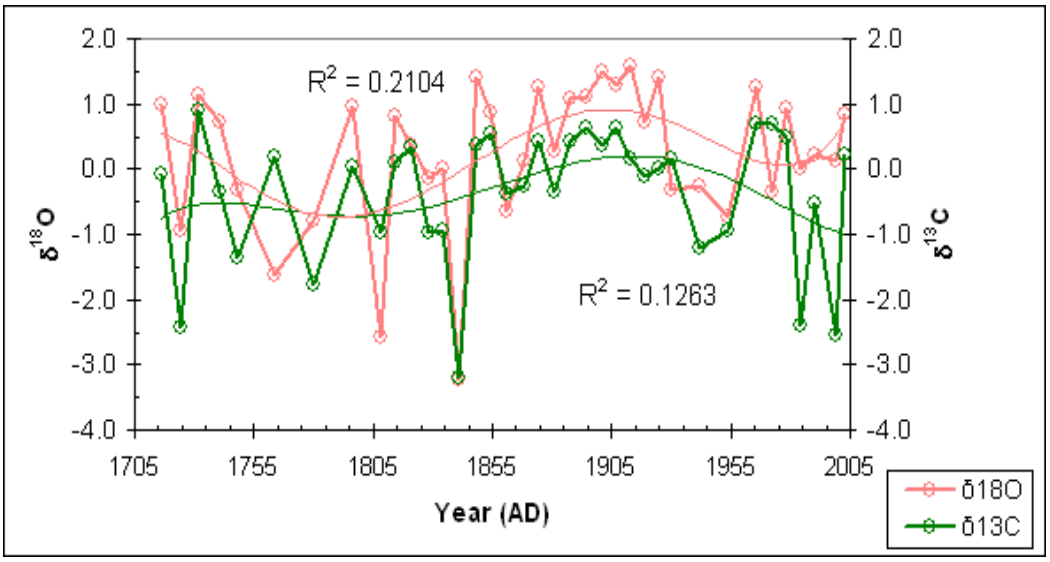

Figure 7c GAK4 δ13C and δ18O Signatures of Planktonic Foraminifer *N. pachyderma*

5.5 Water Column Instrumental Record and Equilibrium of Foraminifera $\delta^{18}O$

When foraminifera secrete their tests, the resulting isotopic signature is a function of the temperature of the water column, the isotopic composition of the water column, and any differing fractionation due to vital effects of the species. A long time-series of water column temperature and salinity from GAK1 (59.85°N, 149.47°W; 270m water depth) is available to asses controls on foraminiferal $\delta^{18}O$ data (Institute of Marine Science, University of Alaska Fairbanks (http://www.ims.uaf.edu/gak1/). The $\delta^{18}O$ of the water column is well correlated with salinity in the coastal Gulf of Alaska (Mix *et al*. 2006). There is a linear relationship between salinity and the $\delta^{18}O$ signature of the water column, therefore, salinity

measurements can be converted to $\delta^{18}O_{PDB}$ (PeeDee Belemnite) according to the following equation (Legrande and Schmidt 2006), where $\delta^{18}O_{SMOW}$ is the $\delta^{18}O$ of water with respect to standard mean ocean water (SMOW):

$$\delta^{18}O_{SMOW} = (\text{localized slope})\ (\text{Salinity}) - 15.13 \quad (6)$$

The localized slope is the linear relationship between the measured salinity and $\delta^{18}O_{SMOW}$ for the study area. In this case, 0.49 was used for the slope, based on regional measurements from the central GOA (Mix *et al*. 2006). The $\delta^{18}O_{SMOW}$ can then be used in the following equation from Duplessy *et al.* (2007) to predict calcite $\delta^{18}O$ ($\delta^{18}O_{PDB}$) signatures that would be at equilibrium within the water column:

$$\delta^{18}O_{calcite(PDB)} = 21.9 - 0.27 + \delta^{18}O_{water\ column} - (310.61 + 10T)^{1/2}; \quad (7)$$

where T is the measured temperature of the water column at the depth in which the foraminifera are assumed to have formed.

Figure 8 shows the theoretical $\delta^{18}O_{calcite}$ (based on equation 6) and the measured $\delta^{18}O_{calcite}$ (based on foraminifera tests) relative to salinity (Figure 8a) and temperature (Figure 8b).

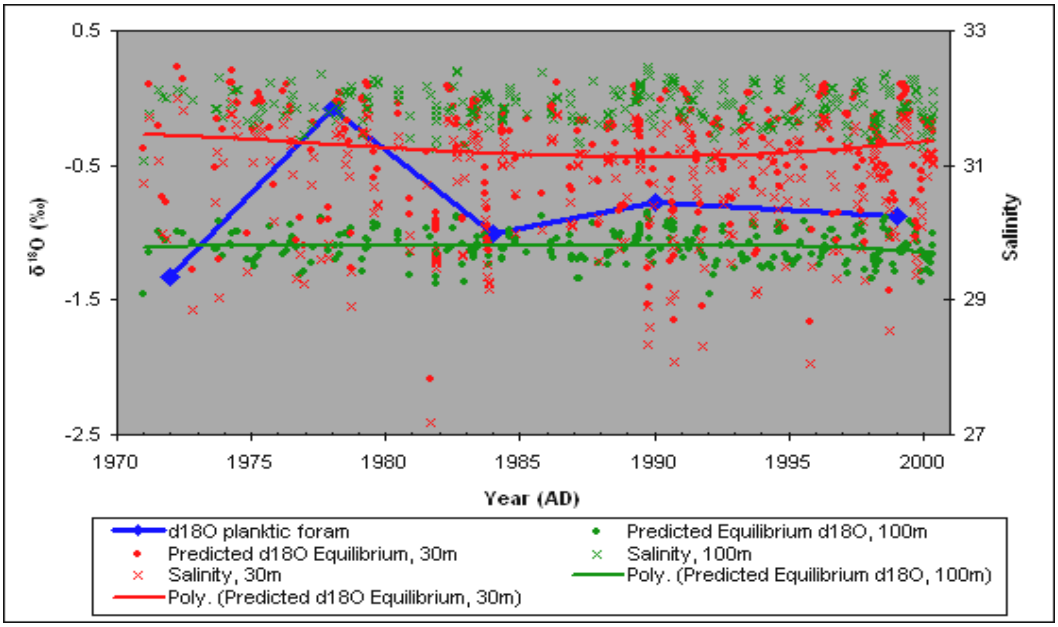

Figure 8a GAK4 Planktic $\delta^{18}O$ (PDB)-Corrected for Vital Effects vs. Water Column Measured Salinity and Predicted Equilibrium $\delta^{18}O$ (PDB)

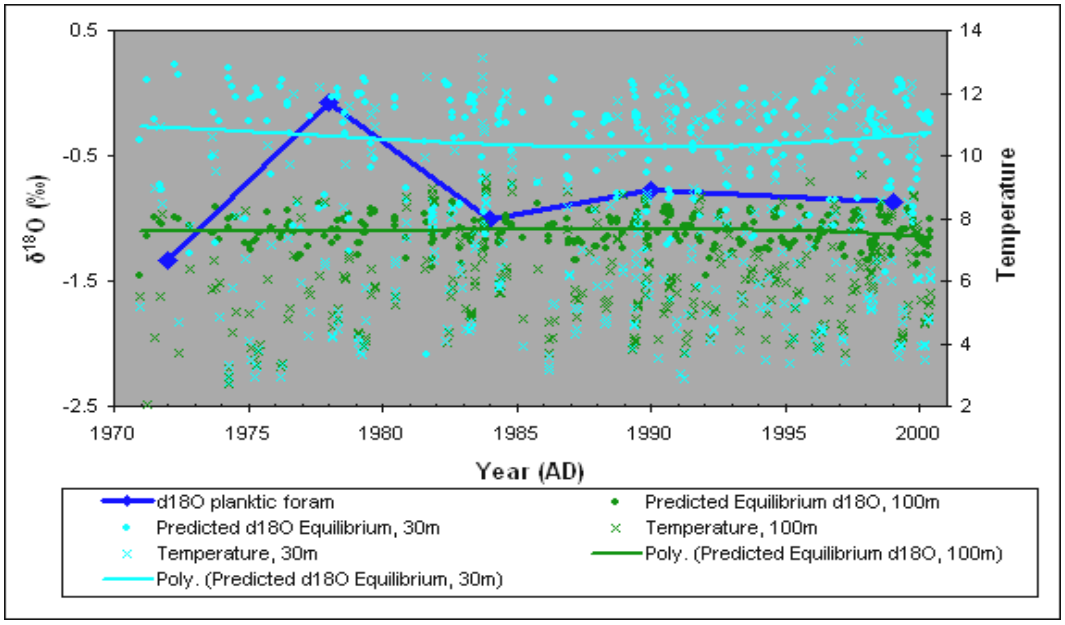

Figure 8b GAK4 Planktic $\delta^{18}O$ (Corrected for Vital Effects) vs. Water Column Measured Temperature and Predicted Equilibrium $\delta^{18}O$ (pdb)

As previously mentioned, a 1 ‰ decrease was applied to the foraminifera data in Figures 7a – b to account for vital effects. The 1976 – 1977 period is used to illustrate the seasonal cycle of temperature and salinity. Since sediment foraminifera samples are available that date to this period, I can compare their values to estimated equilibrium values. *N. pacyderma* is believed to reside at the deep chlorophyll maximum just above the thermocline; therefore, water column data were selected to reflect the range of seasonal shifts: 30 m was used to represent the summer thermocline and 150 m was used to represent the rest of the year.

Figure 9 displays monthly changes in temperature (Figures 9a – b), salinity (Figures 9c – d), and predicted $\delta^{18}O_{calcite}$ (Figures 9e – f) at GAK1

with respect to depth during two periods: 1976 – 1977 and 1999 – 2000. In comparison, after the regime shift year, the same profiles from 1999 – 2000 (Figures 9b, d, f) are colder, more saline, and show less annual variation in both temperature and salinity. There also appears to be a notable difference in the temperature and salinity for the month of October (indicated by bold black line). This suggests that summer stratification extended into October during 1999 – 2000 whereas mixing occurred earlier in 1976 – 1977. Figures 9e – f show the theoretical differences in calcite $\delta^{18}O$ for foraminifera growing under these conditions. The biggest differences are seen in surface water, and changes decrease with depth.

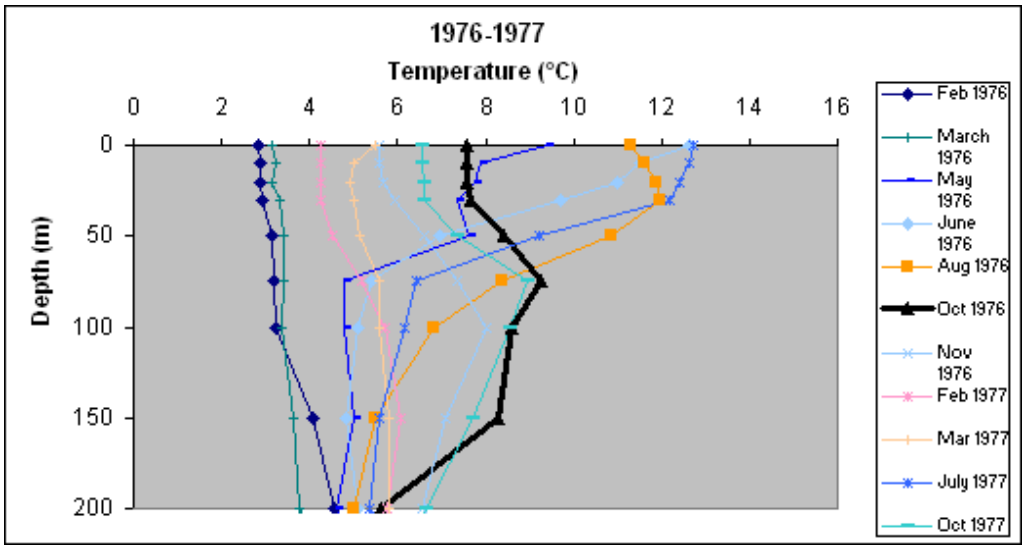

Figure 9a GAK1 Water Column Temperature vs. Depth: 1976 – 1977

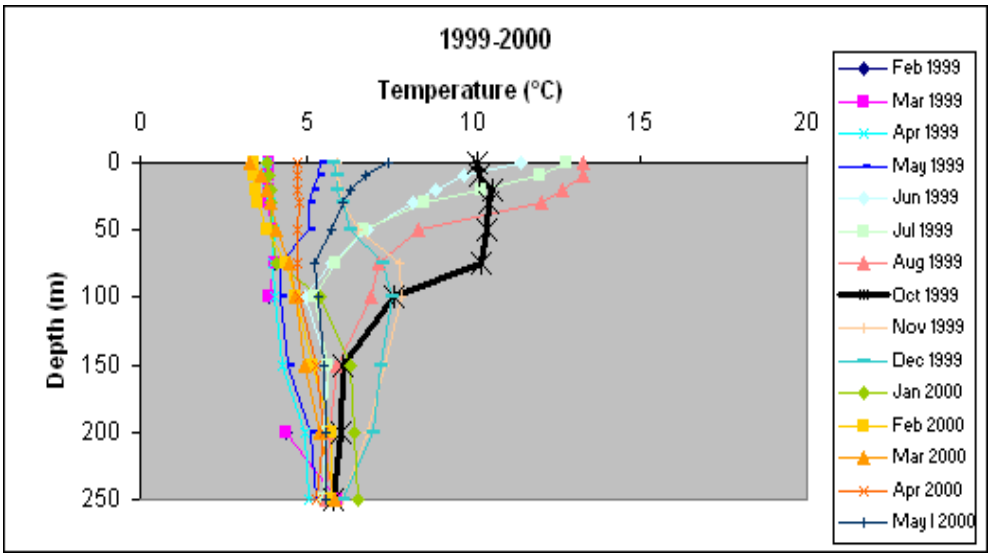

Figure 9b GAK1 Water Column Temperature vs. Depth: 1999 – 2000

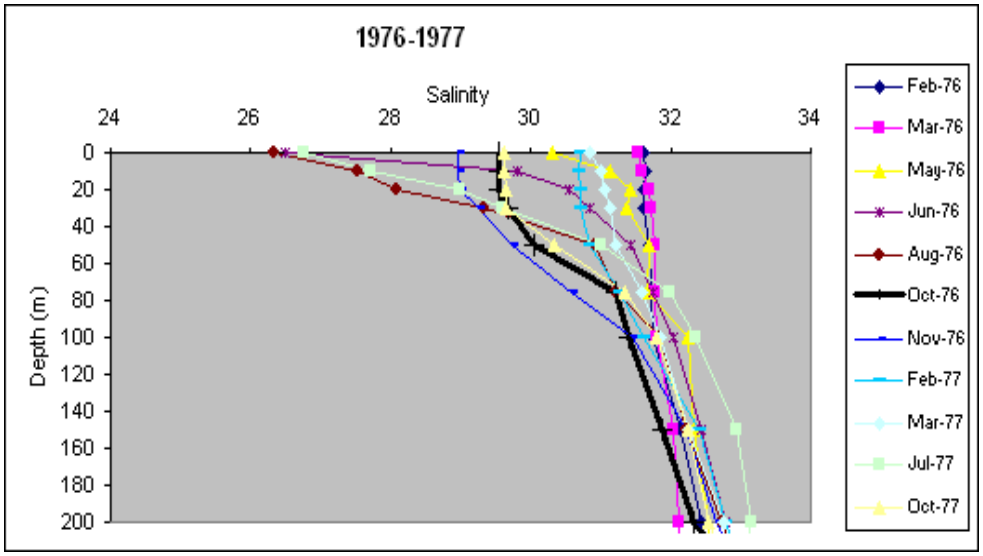

Figure 9c Water Column GAK1 Salinity vs. Depth: 1976 – 1977

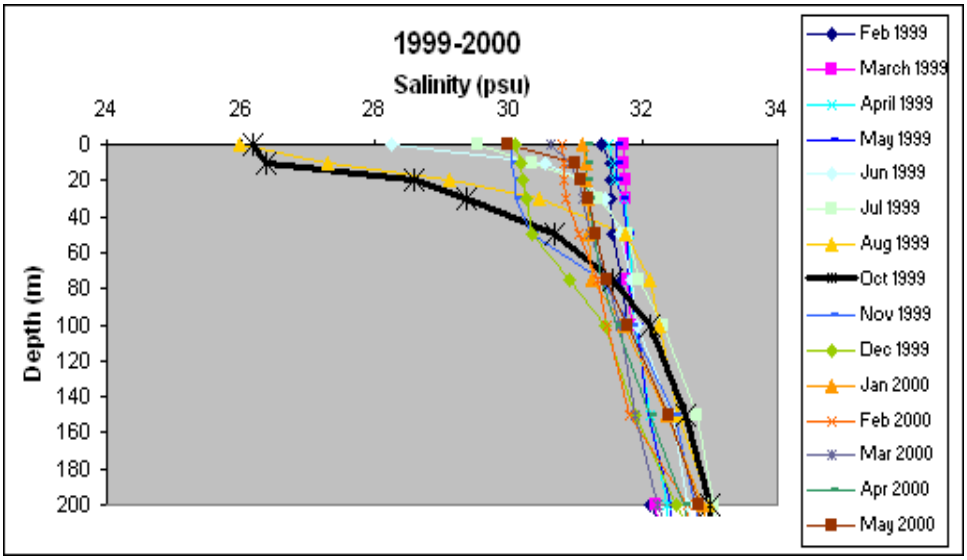

Figure 9d GAK1 Water Column Salinity vs. Depth: 1999 – 2000

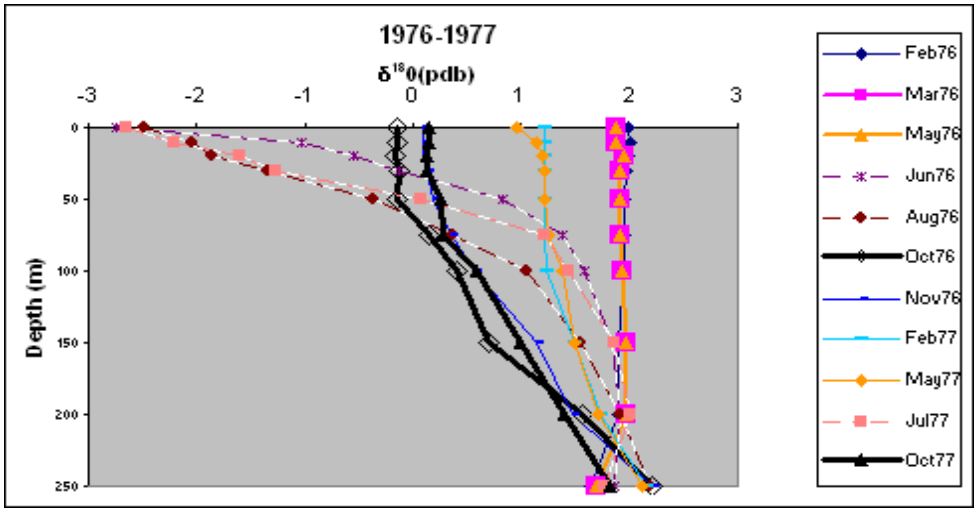

Figure 9e GAK1 Predicted Calcite $\delta^{18}O$ (PDB) vs. Depth: 1976 – 1977

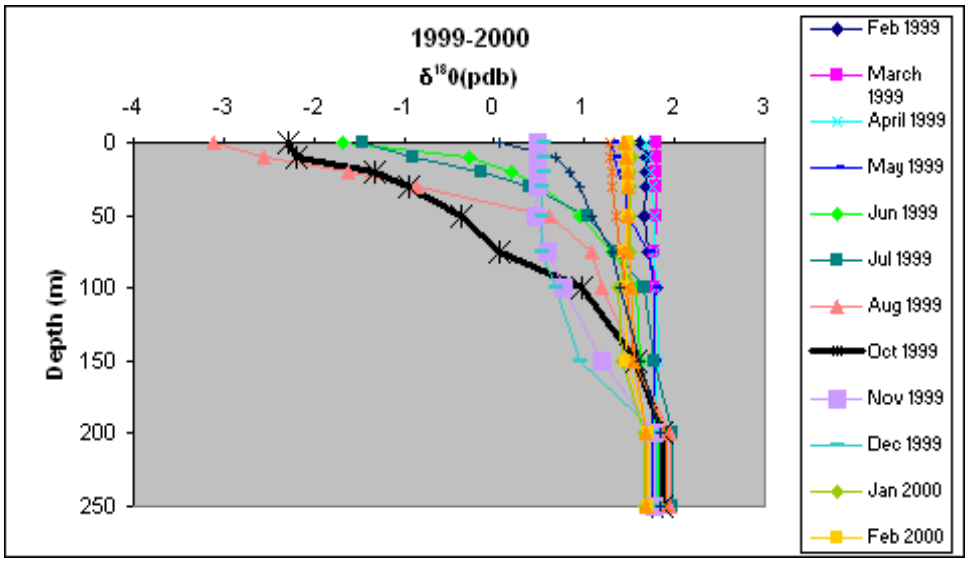

Figure 9f GAK1 Predicted Calcite $\delta^{18}O$ (PDB) vs. Depth: 1999 – 2000

5.6 Foraminifera Faunal Analysis

Individuals were counted from 1 cm^3 bulk sediment samples that were sieved into three size fractions (63 – 125 μm, 125 – 250 μm and >250 μm). The total number of foraminifera, or standing stock, is considered statistically significant when there are at least 300 individuals; although, for fossils, 100 is often an acceptable number (Murray 2006). For these cores, Bay of Pillars standing stock ranged from 0 – 800 (Figure 10a); and GAK4 was much lower ranging from 3 – 209 (Figure 10d). The standing stock for GAK4 was less than 300 at all depths and, although it is not considered statistically significant, relative abundance and size data are included in this thesis (Figures 10e – f).

There were very few individual foraminifera in the Bay of Pillars core during the past century. Since 1931, the total number of foraminifera (from three 1 cm^3 samples) was six. By comparison, in 1898 there were 764 individuals in a single 1 cm^3 sample. Bay of Pillars relative abundance of the two most abundant species, *E. excavatum* and *A. bacarii,* (Figure 10b) show that *E. excavatum* dominates most of the time and *A. bacarii* increases when *E. excavatum* decreases. Shifts in *A. bacarii* relative abundance suggest 80 – 150 year fluctuations in foraminifera diversity.

Relative abundance (Figure 10e) of the planktonic species *N. pachyderma* and the benthic species *C. teretis* were analyzed for GAK4. The relative abundance of *C. teretis* increases when *N. pachyderma* relative abundance decreases.

Based on Figure 10c, there were elevated numbers of large tests from 1407 – 1571 AD and 1833 – 1898 AD. For GAK4 (Figure 10f), the size ratios are fairly consistent throughout the core, the majority being 125 – 249 μm.

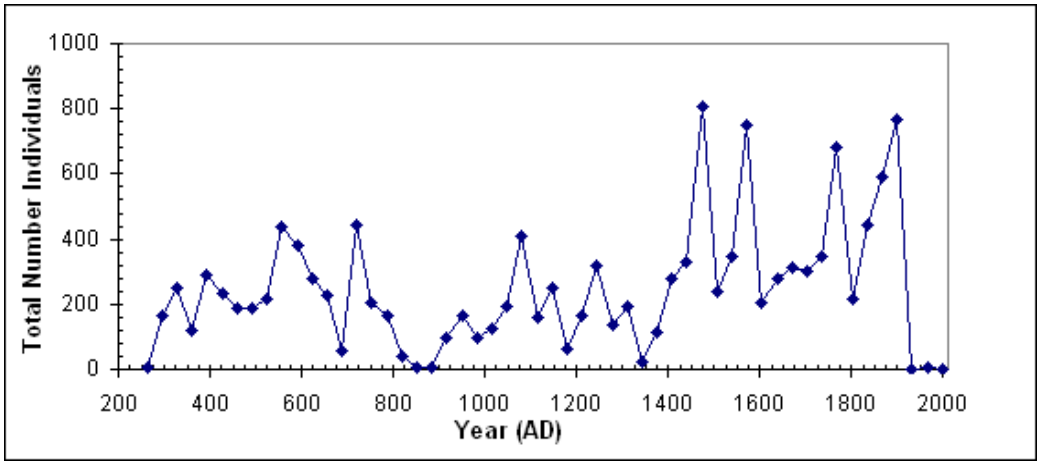

Figure 10a Bay of Pillars Foraminifera Standing Stock

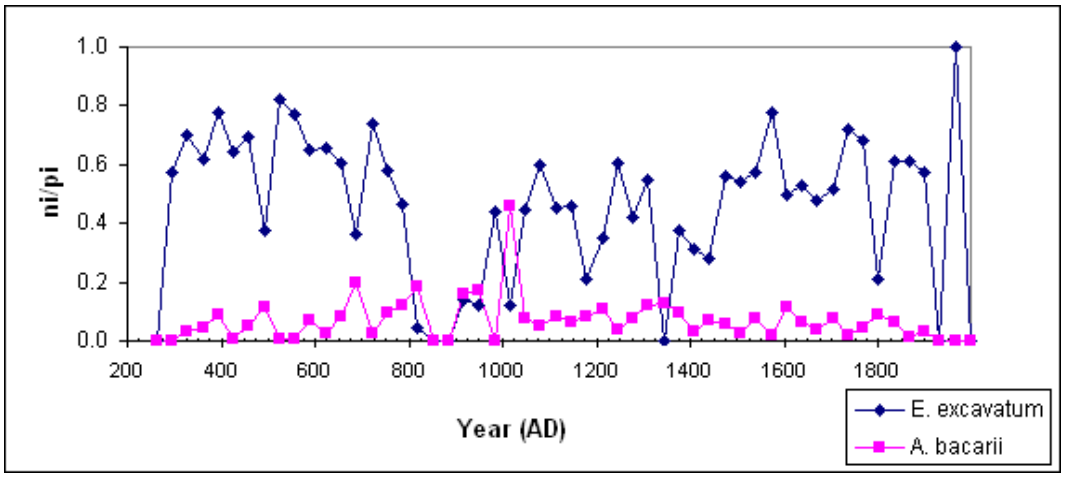

Figure 10b Bay of Pillars: Relative Abundance of *E. excavatum* and *A. bacarii* (125-250 µm size fraction)

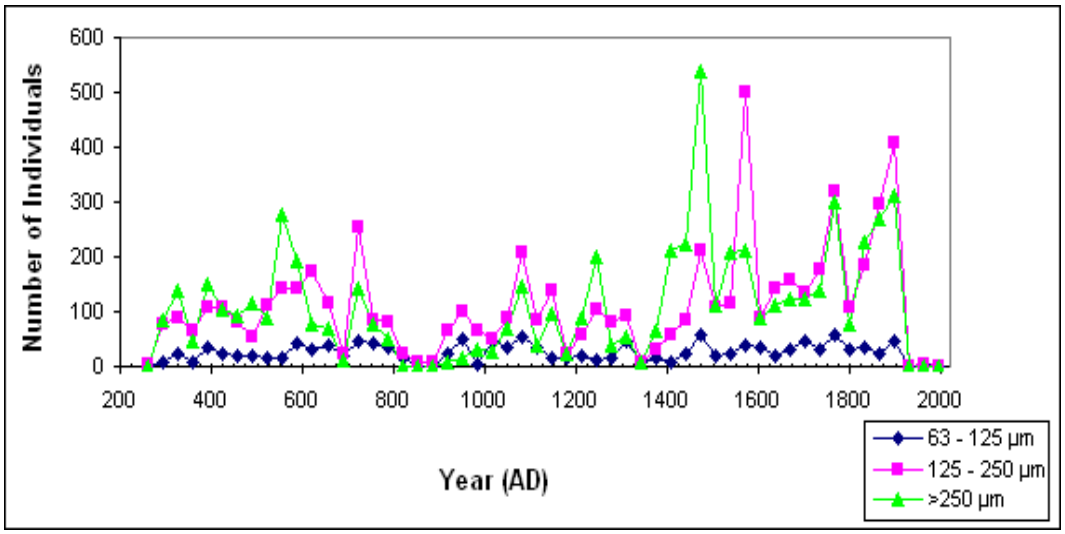

Figure 10c Bay of Pillars Size Variation of Individuals

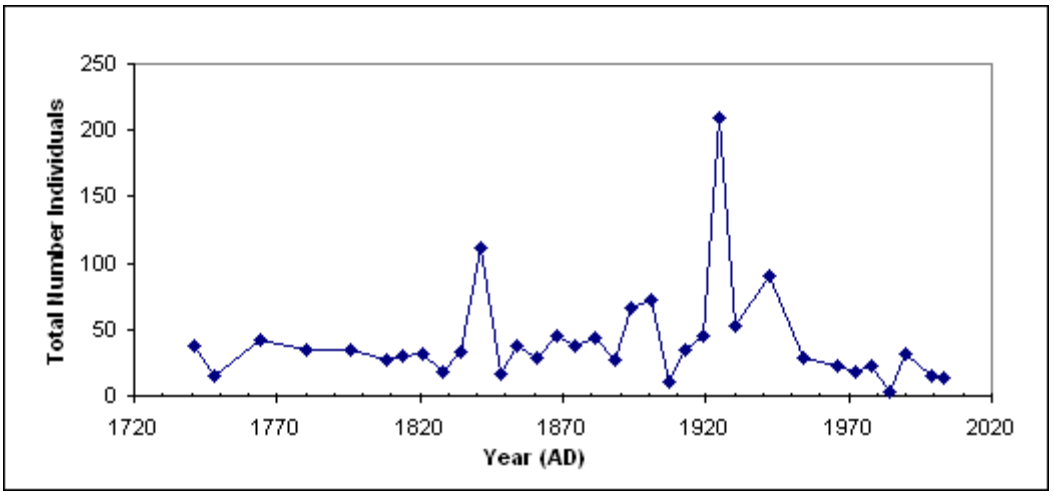

Figure 10d GAK4 Foraminifera Standing Stock

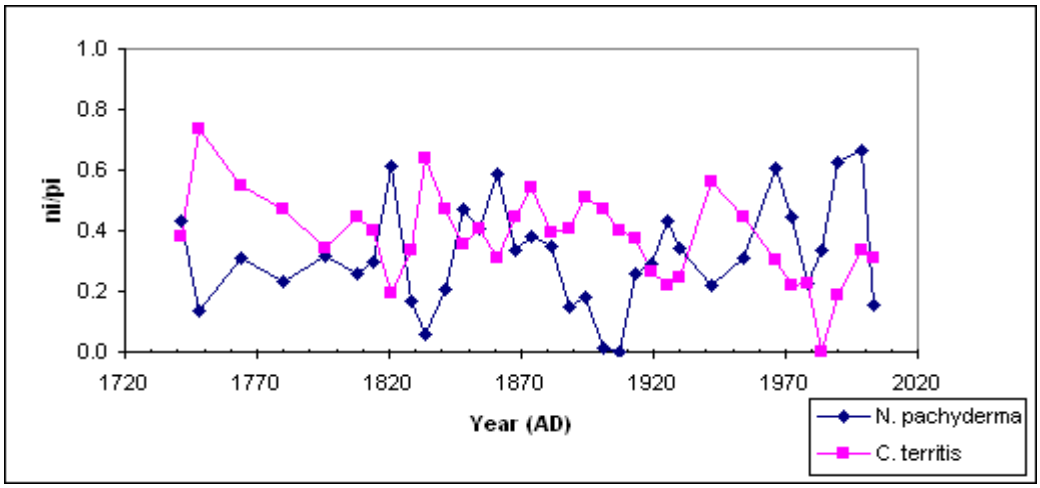

Figure 10e GAK4 Relative of Abundace of *N. pacyderma* (Planktonic) and *C. teretis* (Benthic) (125-250 µm size fraction)

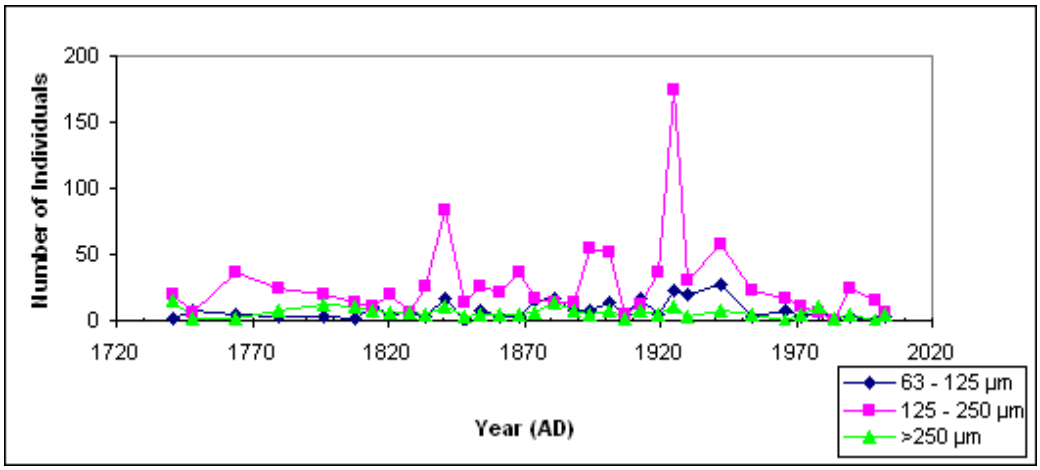

Figure 10f GAK4 Size Variation of Individual Foraminfera

6.0 Discussion

The paleoceanographic data suggest that considerable oceanic variability occurred before the instrumental record. However, the two data sets, which quantify different time periods and have different resolution, reveal varying time scales of change: 20 – 50 years for GAK4 and 100 years for Bay of Pillars. This is attributed to the differing sedimentation rates (0.06 cm y^{-1}, Bay of Pillars; 0.46 cm y^{-1}, GAK4) at the two locations, which resulted in varying sample resolutions: 8 years for GAK4 and 32 years for Bay of Pillars.

Calkin *et al*. (2001) have noted several climatic events that will be assessed in the interpretation of Bay of Pillars data: the Medieval Glaciation (~575 – 1050 AD), the medieval Warm Period (MWP), or Medieval Optimum, (1000 – 1200 AD) and the Little Ice Age (LIA, 1200 – 1900 AD). The GAK4 core has a higher resolution, therefore past PDO shifts should be noted (i.e., 1890, 1925, 1947, 1977, and 1998 AD).

6.1 Paleoceanographic Interpretation from Oxygen Isotopes

As shown for these settings, oxygen isotopes reflect salinity and (to a lesser extent) temperature parameters of the water in which they formed. Therefore, the assumption is made that depleted oxygen isotope ratios indicate fresher and possibly warmer water. Based on Figure 8, the $\delta^{18}O$ of the foraminifera tests remains within the limits of the seasonal shifts of the

water column $\delta^{18}O$, which may reflect some seasonal fluctuations and not regional climatic shifts (Field and Baumgartner 2000).

For the purpose of this study, depleted oxygen isotopes will be hypothesized to reflect more productive periods, based on the assumption that lower salinity enhances stratification. However, the two locations in this study are not controlled by identical physical forces.

There were no planktonic foraminifera in Bay of Pillars sediment, however the benthic $\delta^{18}O$ signature will reflect over-all water column variability due to the shallow (16 m) water depth and close proximity to the fresh water run-off. The $\delta^{18}O$ of the benthic foraminifer (*E. excavatum*) (Figure 7a) appears to fluctuate more and has somewhat more depleted values during the LIA (1200 – 1900 AD) than the time period before (200 – 1200 AD). This indicates greater variation in salinity and overall lower fjord salinity during the LIA. Although this seems somewhat counterintuitive based on the assumption that freshwater influx would decrease during colder periods, some paleoclimate studies in the region have suggested increased coastal precipitation (and presumably runoff) during the Little Ice Age (Mann *et al*. 1998, Hu *et al*. 2003). Greater storm frequency has also been suggested (Mason and Begét 1991), which could increase the occurrence of temporary mixing events and open ocean exchange with the shallow fjord bottom waters. Productivity fluctuations may explain the

increased standing stock of *E. excavatum* (Figure 10) from about 1500 – 1900 AD.

The $\delta^{18}O$ values from the same core during the MWP (1000 – 1200 AD) show less fluctuation (Figure 7a), suggesting that salinity fluctuates less during warmer periods than during cooler periods. Assuming that precipitation was higher during the LIA, as previously mentioned, then decreased $\delta^{18}O$ fluctuation could imply decreased precipitation during the MWP.

GAK4 *N. pacyderma* (planktonic) $\delta^{18}O$ data (Figure 7c) shows three time periods of depleted signatures: 1730 – 1880, 1925 – 1960 and 1980 – 2003, which, within resolution, coincide with the two positive PDO periods during 20th century. This indicates that changes were occurring in the surface currents; and were most likely the result of decreasing salinity due to increased freshwater influx. The OC/N data (Figure 3b) increase approximately two units from 1730 – 1880, which correlates with the increased terriginous sediment source; however, it decreases steadily during the last century. The benthic $\delta^{18}O$ data suggest little variability, where available, during this time period. This contrasts with observed Bay of Pillars $\delta^{18}O$ data; but it is important to note that the GAK4 site is much deeper and in a different setting than Bay of Pillars. Furthermore, there is wide temporal overlap between the records for which to compare.

6.2 Paleoproductivity Interpretation from Organic Carbon and Organic Carbon/Nitrogen Ratios

As indicated in Figures 3a – b, the percentage of organic carbon was much higher for Bay of Pillars than GAK4; yet the OC/N ratios are quite similar suggesting that the organic carbon is mainly of marine (i.e. phytodetritus) rather than terrestrial origin. One reason OC is so high in the Bay of Pillars location is that Baranof Island inhibits some exchange with Alaska Gyre circulation, resulting in estuarine conditions. Another factor contributing to carbon input is the rich ecosystem inhabiting both Kuiu Island, which contributes via riverine input, and a vast benthic community, including sea stars, crab, sea urchins, salmon and halibut (Firman and Bosworth 1990). There is an estimated 3 – 5 black bears/mi^2 that inhabit Kuiu Island to feed on the abundant salmon runs (Peacock 2002), the remains of which have been noted to contribute high amounts of carbon elsewhere in SE Alaska fjords (Sugai 1985, Burrell 1989). In GAK4, the OC is probably carried westward by the swift ACC, whereas at Bay of Pillars it remains within the fjord. Lower values at the GAK4 site also reflect greater microbial breakdown during sedimentation in deeper water, and greater dilution from lithogenic input. In both profiles, increases in carbon are coupled with a decrease in OC/N. This further supports the assumption that an increase in carbon in these cores coincides with increased productivity.

6.3 Paleoproductivity Interpretation from Carbon and Nitrogen Stable Isotopes ($\delta^{13}C$ and $\delta^{15}N$) of Organic Matter

Based on these cores (Figures 4a – b), increased $\delta^{13}C$ and $\delta^{15}N$ signatures correlate with increased productivity in Bay of Pillars. Both proxies in this interpretation represent enrichment by phytoplankton (carbon) and higher trophic levels (represented by particulate organic nitrogen). In GAK4 sediment, while increased $\delta^{13}C$ implies increased productivity, the $\delta^{15}N$ is more difficult to interpret. It is possible that primary productivity is high (which decreases $\delta^{15}N$) while at the same time, high microbial breakdown is occurring post-deposition (which increases the $\delta^{15}N$); thus cancelling out any apparent shifts. This could explain why there is no apparent relationship between the $\delta^{13}C$ and $\delta^{15}N$ with respect to opal (Figure 5).

GAK4 (Figure 4b) displays an enrichment in $\delta^{13}C$ of organic matter over the past century. One possible explanation for the increased $\delta^{13}C$ could be due to overall increasing productivity during this time frame. Salmon productivity has increased in general over the last ~50 years in this region (Adkison and Finney 2003). Although population declines of some marine mammals have been noted during this period, such as stellar sea lions, harbor seals and fur seals (Schell 2000, Newsome *et al.* 2007), these data are from sites west of the GAK4 site in the Gulf of Alaska and the Bering Sea.

An alternative explanation for the increased $\delta^{13}C$ in GAK4 sediment over the past century could be that terrestrial input is decreasing. This could be from decreased precipitation and consequent meltwater, decreased glacial cover, or increased logging. However, salinity measurements from GAK1 do not indicate that salinity is increasing, which would be expected if freshwater influx decreased. Figure 11 shows a slight freshening in the water column, with the exception of the 0m depth, which has a positive slope of y = 0.0002x + 28.947.

When considering the Seuss effect, it is possible that the $\delta^{13}C$ increased up to 1.6 ‰ more than indicated by the data. This would more than double the increase portrayed in Figure 4b, thus indicating even further fractionation has occurred.

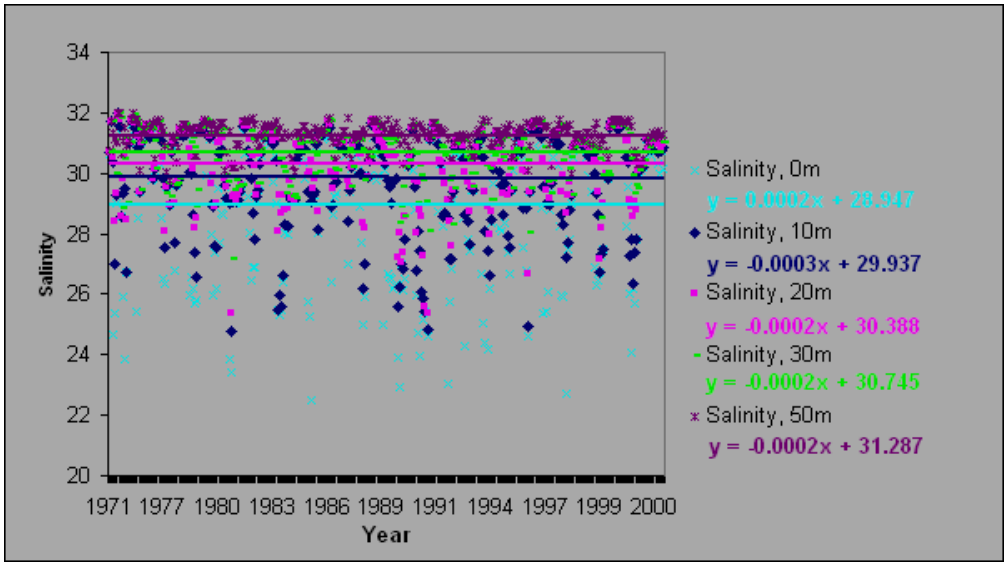

Figure 11 GAK1 Water Column Salinity: 1971-2000
Note the slope of each line indicates very little change in salinity over the past 30 years.

6.4 Paleoproductivity Interpretation from Percent Biogenic Opal

During the past century, opal percentages are increasing in the GAK4 core but decreasing in the Bay of Pillars core, though due to sample resolution, only three samples date to this period (Figure 6). Bay of Pillars opal is higher during the LIA (1200 – 1900) and lower during the MWP (1000 – 1200). Percentages do not increase during the Medieval Galciation (575 – 1050 AD), as might be expected, however this event is not well understood in terms of climatic conditions in this region. The opal percentages from the GAK4 core do not seem to correlate with any of the PDO events, except perhaps for the post 1976 increase.

6.5 Implications of Carbon Pump Efficiency based on Foraminifera Carbon Stable Isotopes

Figure 12 shows the carbon isotopes from both foram species, *N. pachyderma* (planktonic) and *C. teretis* (benthic). Each species is plotted on separate y-axes to display the relative change, therefore vital effects are irrelevant. The higher variability in the planktonic species most likely reflects the seasonal variation in temperature and salinity in the surface layer.

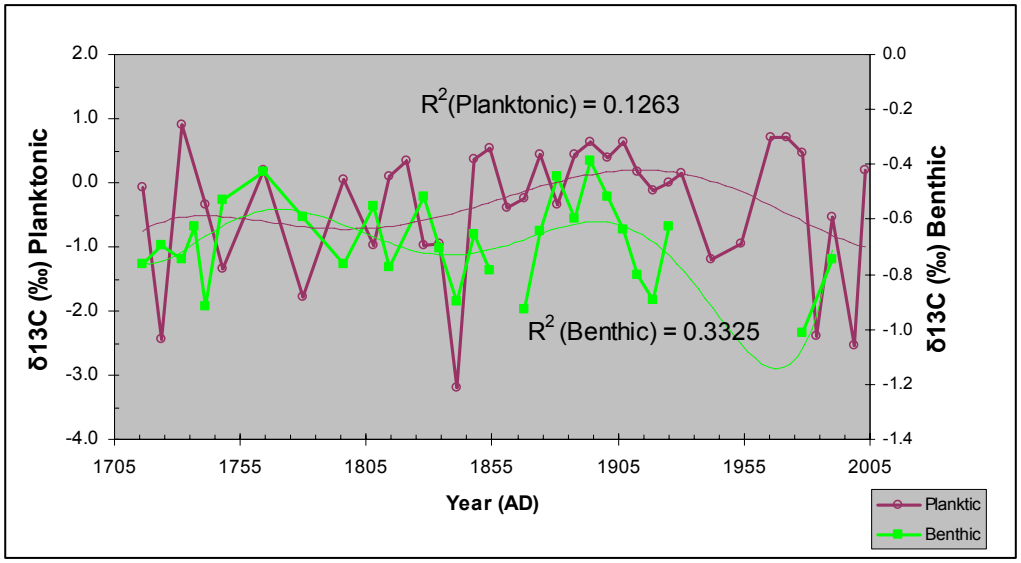

Figure 12 GAK4 relative comparison of *N. pachyderma* (planktonic) and *C. teretis* (benthic) foraminifera

The carbon isotope data suggest a less efficient pump from 1828 – 1848 and 1907 – 1966 AD, as indicated by depleted $\delta^{13}C$ signatures of both planktonic and benthic species. The majority of the core, from 1705 – 1907 AD, is fairly consistent, which would be expected in a region with an overall efficient carbon pump.

There were no planktonic foraminifera in the Bay of Pillars core so this relationship could not be examined. For GAK4, there were no benthic foraminifera from 1920 – 1970. During this period, planktonic tests were depleted in $\delta^{13}C$, indicating decreased productivity in surface waters and therefore less available carbon at the seafloor for benthos. This idea is contradicted by an increase in opal from 1920 – 1950, which indicates increased productivity. The decrease in standing stock in both cores over

the past century is probably due to the epibenthic dwelling of these forams. *E. excavatum* has been documented to live in the top 4 cm of sediment (Thomas *et al*. 2000); however, the standing stock in GAK4 is very low in the top 33 cm of the core. One explanation is that increasing atmospheric CO_2 could be impacting the GOA carbon pump and decreasing calcite precipitation.

6.6 Paleoproductivity Summary

Globally, warmer oceans are less productive because stratification increases and upwelling is diminished. However, GLOBEC research has suggested that in the downwelling GOA, stratification is beneficial to productivity. This appears to hold true during different periods for both the Bay of Pillars and GAK4 proxy data. For GAK4, the data suggest increasing temperatures and freshwater influx are occurring while productivity is increasing. For example, increased stratification is indicated by the water column parameters (Figure 9), yet $\delta^{13}C$ (Figure 4) and opal (Figure 6) are increasing.

During the Little Ice Age in the Bay of Pillars data, increased stratification is suggested by lower $\delta^{18}O$; and higher productivity is suggested by higher opal and $\delta^{13}C$ of organic matter. Productivity fluctuations from this core are generally higher during the Medieval Glaciation and LIA and lower during the MWP. The past century, however,

in this region appears to be decreasing in productivity. There is a marked decrease in all proxies ($\delta^{13}C$, $\delta^{15}N$, opal TOC of sediment and $\delta^{13}C$ and $\delta^{18}O$ of tests) from approximately 1535 – 1735.

7.0 Conclusion

Basic conclusions regarding past changes in oceanographic conditions, which can be drawn from this study include:

1. Overall freshening/mixing during LIA relative to the previous period can be inferred from Bay of Pillars $\delta^{18}O$ data. The freshening occurs in a series of pulses, and is not uniform.
2. Within the LIA, GAK $\delta^{18}O$ data indicate GOA waters were freshest from 1750 – 1880. Somewhat lower salinity can be inferred from 1925 to present, with fluctuations that coincide with PDO regimes.

Conclusions regarding paleoproductivity variability include:

1. Increased productivity correlates with the Medieval Glaciation and the LIA according to Bay of Pillars proxies opal, $\delta^{13}C$, and $\delta^{15}N$.
2. Based on the same proxies from GAK4, GOA productivity has been increasing over the past century. Periods of high productivity also occurred during parts of the LIA.

Proxy data from the Bay of Pillars location suggest colder periods are generally more productive in this region. Proxy data from GAK4 suggest that this is not always true, particularly in the last century. This can most likely be attributed to different modes of physical forcing that occur in the area. It has recently been suggested that ocean-atmosphere circulation reorganized in this region at the transition into and out of the LIA (Finney *et al*. 2008). Therefore, the contrasting relationships between temperature and productivity which I observed before and after the 20th century may be due to different modes of circulation that predominated during these periods.

As mentioned, the use of proxies to infer past conditions relies on many assumptions; and proxies can often be interpreted in various ways depending on what set of controlling factors are most important. Figure 13 summarizes proxy interpretations, which often contradict during the same time period. This study suggests that single proxy studies may be less reliable that previously believed.

Since glaciers in SE Alaska have decreased substantially in the past century, it is possible that the forcing mechanisms behind present oceanographic (and therefore productivity) parameters have altered. For example, it has been proposed that the PDO shifted in 1998. According to past ecological observations, productivity in the GOA should decrease while productivity along the west coast of Washington, Oregon, and

California should increase. However, little change relative to the past regime has occurred yet. Productivity in the GOA has remained similar and salmon fisheries along the US west coast have considerably decreased and even been banned during the 2008 season in California and Oregon (Koopman 2008). The Pacific Salmon Fishery Management Council news release dated February 28, 2008, predicted a disastrously low salmon forecast.

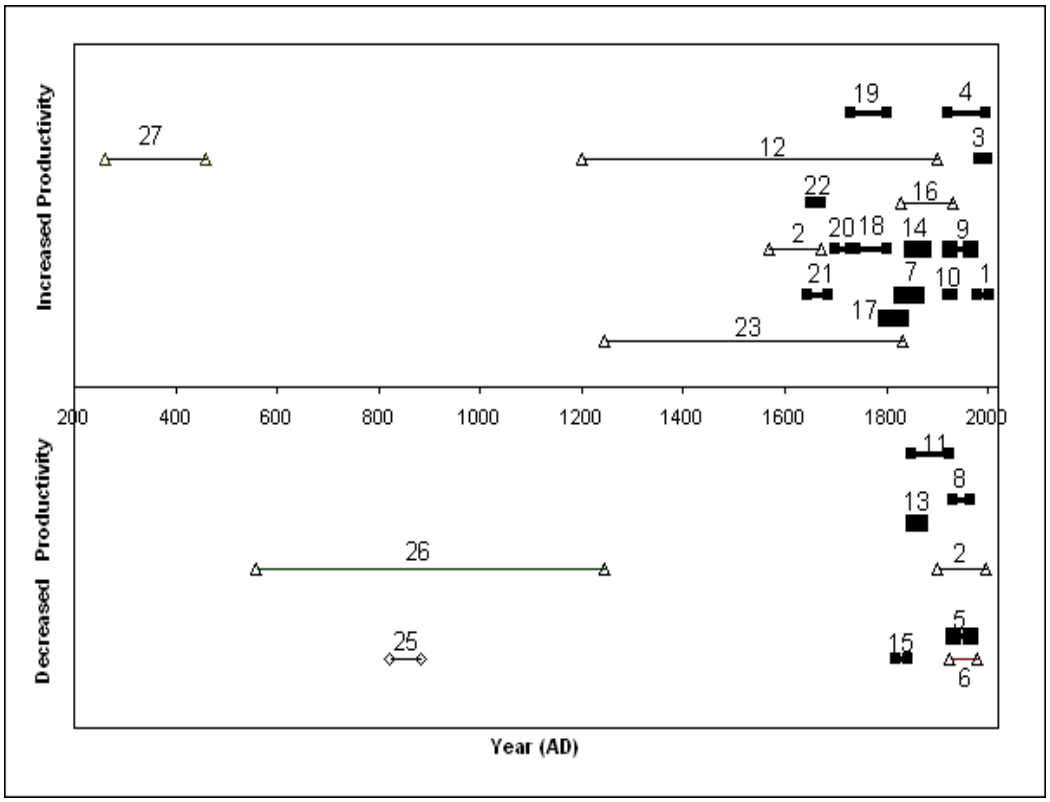

Figure 13a Proxy Data Summary: 200 - 2000 AD
Triangles indicate Bay of Pillars proxy data; bold squares indicate GAK4 proxy data.

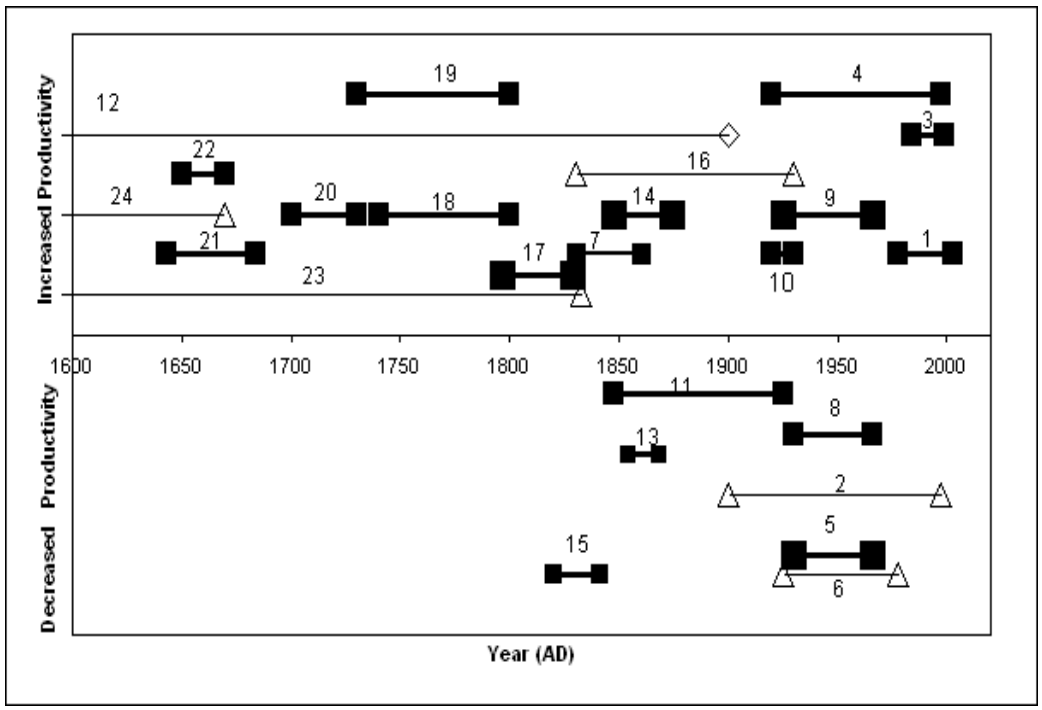

Figure 13b Proxy Data Summary: 1600 - 2000 AD
Triangles indicate Bay of Pillars proxy data; bold squares indicate GAK4 proxy data. Note: Figures 13a and 13b display the same proxies. The timeline on Figure 13b has been reduced for clarity.

Legend for Figure 13 – Summary of Assumptions

No.	Core	Proxy	Ocean Temp.	Product-ivity	Assumption
1	GAK4	↓Planktonic Foram $\delta^{18}O$	Warmer		Depleted planktonic δ18O = fresher surface waters (=Increased GOA Productivity)
2	BoP	↓ Standing Stock		Lower	Very low standing stock = low nutrient availability
3	GAK4	↓Planktonic Foram $\delta^{18}O$	Warmer		Depleted planktonic δ18O = fresher surface waters (=Increased GOA Productivity)
4	GAK4	↑ $\delta^{13}C$ (Marine Sediment OC)		Higher	Enriched $\delta^{13}C$-increased productivity
5	GAK4	Planktonic $\delta^{13}C$ Depleted		Lower	Decreased primary productivity in surface waters
6	BoP	↓ Standing Stock		Lower	Low standing stock = low nutrient availability
7	GAK4	%C, C/N (Marine Sediment OC)		Higher	High %C and Low C/N indicate Increased Marine Productivity
8	GAK4	Planktonic $\delta^{13}C$ Depleted		Lower	Decreased primary productivity in surface waters
9	GAK4	↓Planktonic Foram $\delta^{18}O$	Warmer		Depleted planktonic δ18O = fresher surface waters (=Increased GOA Productivity)
10	GAK4	↑ Standing Stock		Higher	Increased standing stock= increased nutrient availability
11	GAK4	Benthic $\delta^{13}C$ Depleted		Lower	Benthic $\delta^{13}C$ depleted relative to planktonic implies carbon not utilized at surface
12	BoP	↑ Biogenic Opal		Higher	Elevated Opal indicates diatom blooms = increased productivity
13	GAK4	↓ Standing Stock		Lower	Very low standing stock = low nutrient availability
14	GAK4	↓ Planktonic Foram $\delta^{18}O$	Warmer		Depleted planktonic δ18O = fresher surface waters (=Increased GOA Productivity)
15	GAK4	Planktonic $\delta^{13}C$ Depleted		Lower	Decreased primary productivity in surface waters
16	BoP	%C, C/N (Marine Sediment OC)		Higher	High %C and Low C/N indicate Increased Marine Productivity
17	GAK4	↑ Biogenic Opal		Higher	Elevated Opal indicates diatom blooms = increased productivity
18	GAK4	↓ Planktonic Foram $\delta^{18}O$	Warmer		Depleted planktonic δ18O = fresher surface waters (=Increased GOA Productivity)
19	GAK4	↓ Planktonic Foram $\delta^{18}O$	Warmer		Depleted planktonic δ18O = fresher surface waters (=Increased GOA Productivity)
20	GAK4	%C, C/N (Marine Sediment OC)		Higher	High %C and Low C/N indicate Increased Marine Productivity
21	GAK4	↑ Biogenic Opal		Higher	Elevated Opal indicates diatom blooms = increased productivity
22	GAK4	%C, C/N (Marine Sediment OC)		Higher	High %C and Low C/N indicate Increased Marine Productivity
23	BoP	Benthic $\delta^{18}O$ Enriched	Cooler		Cooler/Saltier at depth-increased mixing with open ocean
24	BoP	%C, C/N (Marine Sediment OC)		Higher	High %C and Low C/N indicate Increased Marine Productivity
25	BoP	↓ Standing Stock		Lower	Very low standing stock = low nutrient availability
26	BoP	Benthic $\delta^{18}O$ Depleted	Warmer		Increased freshwater input
27	BoP	↑ Biogenic Opal		Lower	Elevated Opal indicates diatom blooms = increased productivity

BoP – Bay of Pillars

Overall, productivity and climatic shifts have occurred during the past two millennia. The exact duration of these fluctuations is difficult to pinpoint through proxy studies because there is a high margin of error associated with interpretive assumptions. However, it is important to note that these fluctuations occurred under stable atmospheric pCO_2 conditions. It is uncertain what consequences may lay ahead for future generations as anthropogenic CO_2 continues to increase in both the ocean and atmosphere. Further understanding of how increasing carbon emissions will affect atmospheric circulation and the carbon pump is paramount given the oceans' ability to regulate global temperatures and provide important food resources to human populations.

8.0 References

Adkison MD and Finney BP. 2003. The long-term outlook for salmon returns to Alaska. *Alaska Fishery Research Bulletin*, 10(2): 83-94.

Altabet MA and François R. 1994. Sedimentary nitrogen isotopic ratio as a recorder for surface ocean nitrate utilization. *Global Biogeochemical Cycles*, 8: 103-116.

Altabet MA, Pilskaln C, Thunnel R, Pride C, Sigman D, Chavez F, François R. 1999. The nitrogen isotope biogeochemistry of sinking particles from the margin of the Eastern North Pacific. *Deep Sea Research I*, 46(4): 655-679.

An S, Kug J, Timmermann A, Kang I, Timm O. 2007. Influence of ENSO on the Generation of Decadal Variability in the North Pacific. *Journal of Climate*, 20: 667-680.

Anderson TF and Arthur MA. 1983. Stable isotope of oxygen and carbon and their application to sedimentologic and paleoenvironmental problems. *In* Stable Isotopes in Sedimentary Geology, *SEPM Short Course* 10: pp1-1-1 through 1-1-151. Arthur MA, Anderson TF, Kaplan IR, Veizer J, and Land LS (eds.).

Anderson JB and Molnia BF. 1989. Glacial-Marine Sedimentation*, In* Short Course in Geology, Volume 9*:* 129 pages. Crawford ML and Padovani E (eds.), American Geophysical Union, Washington DC.

Anderson PJ and Piatt JF. 1999. Community reorganization in the Gulf of Alaska following ocean climate regime shift. *Marine Ecology Progress Series*, 189: 117-123.

Barker P, Fontes JC, Gasse F, Druart JC. 1994. Experimental Dissolution of Diatom Silica in Concentrated Salt Solutions and Implications for Paleoenvironmental Reconstruction. *Limnology and Oceanography*, 39(1): 99-110.

Bauch D, Carstens J, Wefer G. 1996. Oxygen isotope composition of living *Neogloboquadrina pachyderma* (sin.) in the Arctic Ocean. *Earth and Planetary Science Letters*, 146: 47-58.

Beamish RJ, Neville CE, Cass AJ. 1997. Production of Fraser River sockeye salmon (*Oncorhynchus nerka*) in relation to decadal-scale

changes in the climate and the ocean. *Canadian Journal of Fisheries and Aquatic Sciences*, 54: 543-554.

Brady HB. 1881. On some Arctic Foraminifera from soundings obtained on the Austro-Hungarian North Polar Expedition of 1872-76. *Annual Magazine of Natural History,* 5(8): 393-418.

Burrell DC. 1989. *Biogeochemistry of a Boreal Fjord Boca de Quadra, Southeast Alaska.* Occasional Publication No. 6, Institute of Marine Science, University of Alaska Fairbanks.

Buzas MA and Hayek LC. 2005. On richness and evenness within and between communities. *Paleobiology*, 31(2): 199-220.

Calkin PE, Wiles GC, Barclay DJ. 2001. Holocene coastal glaciation of Alaska. *Quaternary Science Reviews*, 20: 449-461.

Childers AR. 2005. Nutrient Dynamics in the Northern Gulf of Alaska and Prince William Sound: 1998-2001. Dissertation, University of Alaska Fairbanks. ProQuest/UMI, AAT 3206050: 141 pages.

Childers AR, Whitledge TE, Stockwell DA. 2005. Seasonal and interannual variability in the distribution of nutrients and chlorophyll *a* across the Gulf of Alaska shelf: 1998-2000. *Deep Sea Research II*, 52: 193-216.

D'Arrigo R, Mashig E, Frank D, Wilson R, Jacoby G. 2005. Temperature variability over the past millennium inferred from Northwestern Alaska tree rings. *Climate Dynamics*, 24: 227-236.

Deines P. 1980. The isotopic composition of reduced organic carbon. *In Handbook of Environmental Geochemistry: The Terrestrial Environment*: 329-406*.* Fritz P and Fontes JC (eds.). Elsevier.

DeNiro MJ and Epstein S. 1977. Mechanism of carbon isotope fractionation associated with lipid synthesis. *Science*, 197: 261-263.

DeNiro MJ and Epstein S. 1978. Influence of diet on the distribution of carbon isotopes in animals. *Geochimica et Cosmochimica Acta*, 42: 495-506.

Duplessy JC**,** Roche DM, Kageyama M. 2007. The deep ocean during the last interglacial period. *Science*, 316: 89-91.

Emiliani C. 1954. Depth habitats of some species of pelagic foraminifers as indicated by oxygen isotope ratios. *American Journal of Science*, 252: 149-158.

Field DB and Baumgartner TR. 2000. A 900 year stable isotope record of interdecadal and centennial change from the California Current. *Paleoceanography*, 15(6): 695-708.

Finney BP, Alheit J, Christian-Kay E, Field D, Gutierrez D, Struck U. 2008. Paleocological studies on variability in marine fish populations: A long-term perspective on the impacts of climate change on marine fisheries. *Journal of Marine Systems*, (in press).

Firman A and Bosworth RG. 1990. Harvest and use of fish and wildlife by residents of Kake, Alaska. Technical Paper No. 145, Alaska Department of Fish and Game, Division of Subsistence.

Francis RC, Hare SR, Hollowed AB, Wooster WS. 1998. Effects of interdecadal climate variability on the oceanic ecosystems of the NE Paciific. *Fisheries Oceanography*, 7: 1-21.

Francis RC and Hare SR. 1994. Decadal-scale regime shifts in the large marine ecosystems of the Northeast Pacific: a case for historical science. *Fisheries Oceanography*, 3: 279-291.

Freeman KH. 2001. Isotopic Biogeochemistry of Marine Organic Carbon. *Reviews in Mineralogy and Geochemistry*, 43:579-605.

Friedli H, Lotcher H, Oeschger H, Siegenthaler U and Stauffer B. 1986. Ice Core record of the $^{13}C/^{12}C$ ratio of atmospheric CO_2 in the past two centuries. *Nature*, 324: 237-238.

Gedalof Z and Smith DJ. 2001. Interdecadal climate variability and regime-scale shifts in Pacific North America. *Geophysical Research Letters*, 28(8): 1515-1518.

Gedalof Z and Mantua NJ. 2002. A multi-century perspective of variability in the Pacific Decadal Oscillation: new insights from tree rings and coral. *Geophysical Research Letters*, 29(24): 57-1 – 57-4.

GLOBEC GAK1 CTD Time Series Data. Maintained by Dr. Tom Weingartner of the Institute of Marine Science at the School of Fisheries and Ocean, University of Alaska Fairbanks. http://www.ims.uaf.edu/gak1/

Hare SR and Mantua NJ. 2000. Empirical evidence for North Pacific regime shifts in 1997 and 1989. *Progress in Oceanogrpahy*, 47(2-4): 103-146.

Harrison,PJ, Whitney FA, Atushi T, Saito H, and Tadokoro K. 2004. Nutrient and Plankton Dynamics in the NE and NW Gyres of the Subarctic Pacific Ocean. *Journal of Oceanography,* 20(1):93-117.

Herguera JC and Berger WH. 1991. Paleoproductivity from benthic foraminifera abundance: Glacial to post-glacial change in the west-equatorial Pacific. *Geology* 19: 1173-1176.

Hu FS, Kaufman D, Yoneji S, Nelson D, Shemesh A, Huang Y, Tian J, Bond G, Clegg B, Brown T. 2003. Cyclic variation and solar forcing in the Alaskan subarctic. *Science*, 301: 1890-1893.

Jaeger J, Vienne W, Channel J, Stoner J, and Finney BP. Exploring the use of environmental magnetism and sediment texture as proxies of sediment transport on the Gulf of Alaska continental shelf. *Marine Geology, In Progress.*

Jaeger JM, CA. Nittrouer, ND Scott, JD Milliman. 1998. Sediment accumulation along a glacially impacted mountainous coastline: north-east Gulf of Alaska. *Basin Research,*10: 155-173.

Jennings, AE*,* Weiner NJ, Helgadottir G, Andrews JT. 2004. Modern foraminiferal faunas of the Southwestern to Northern Iceland shelf: Oceanographic and environmental controls. *Journal of Foraminiferal Research*, 34(3): 180-207.

Keeling CD, Mook WG, Tans PP. 1979. Recent trends in the $^{13}C/^{12}C$ ratio of atmospheric carbon dioxide. *Nature*, 277: 121-123.

Keeling CD, Whorf TP, Wahlen M, VanDerPlichtt J. 1995. Interannual extremes in the rate of rise of atmospheric carbon dioxide since 1980. *Nature*, 375: 666-670.

Koopman J. April 11, 2008. Salmon fishing closed for California, Oregon. *San Francisco Chronicle*. Online article: http://www.sfgate.com/cgi-bin/article.cgi?f=/c/a/2008/04/11/MNO6103NBB.DTL

Korsun S and Hald M. 2000. Seasonal dynamics of benthic foraminifera in a glacially fed fjord of Svalbard, European Arctic. *Journal of Foraminiferal Research*, 30(4): 251-271.

Laws EA, Popp BN, Bidigare RR, Kennicutt MC, Macko SA. 1995. Dependence of phytoplankton carbon isotopic coposition on growth rate and $[CO_2]_{aq}$: theoretical considerations and experimental results. *Geochimica et Cosmochimica Acta,* 59(6): 1131-1138.

Legrande AN and Schmidt GA. 2006. Global gridded data set of the oxygen isotopic composition in seawater. *Geophysical Research Letters,* 33: 1-5.

Litzow MA. 2006. Climate regime shifts and community reorganization in the Gulf of Alaska: how do recent shifts compare with 1976/1977? *ICES Journal of Marine Science*, 63: 1386-1396.

MacDonald GM and Case RA. 2005. Variations in the Pacific Decadal Oscillation over the past millennium. *Geophysical Research Letters*, 32: L08703.

MacDonald SO and JA Cook. 1996. The land mammal fauna of Southeast Alaska. *Canadian Field-Naturalist,* 110:571–599.

Mann DH, Crowell AL, Hamilton TD, Finney BP. 1998. Holocene geologic and climatic history around the Gulf of Alaska. *Arctic Anthropology*, 35(1): 112-131.

Mantua NJ, Hare SR, Zhang Y, Wallace JM, Francis RC. 1997. A Pacific interdecadal climate oscillation with impacts on salmon production. *Bulletin of the American Meteorological Society*, 78(6): 1069-1079.

Mason OK and Begét JE. 1991. Late Holocene flood history of the Tanana River, Alaska, USA. *Arctic and Alpine Research*, 23(4): 392-403.

Melsom A, Meyer SD, Hurlburt HE, Metzger JE, O'Brien JJ. 1999. ENSO effects on Gulf of Alaska eddies. *Earth Interactions*, 3: 1-30.
Meyers, PA. 1994. Preservation of elemental and isoptopic source identification of sedimentary organic matter. *Chemical Geology,* 114: 289-302.

Minobe S. 1997. A 50-70 year climatic oscillation over the North Pacific and North America. *Geophysical Research Letters*, 24(6): 683–686.

Mix AC, Prahl FG, Finney BP. 2006. Oxygen isotope and salinity relationships from SE Alaska track freshwater sources in the NE Pacific. *Eos Trans. AGU, 87*(52), Fall Meet. Suppl., Abstract PP51C-1154.

Mortlock RA and Froelich PN. 1989. A simple method for the rapid determination of biogenic opal in pelagic marine sediments. *Deep Sea Research*, 35(9): 1415-1426.

Murray J. 2006. *Ecology and Applications of Benthic Foraminifera*. Cambridge University Press.

Naidu AS, Scalan RS, Feder HM, Goering JJ, Hameedi MJ, Parker PL, Behrens EW, Caughey ME, Jewett SC. 1993. Stable organic carbon isotopes in sediments of the north Bering-south Chukchi seas, Alaskan-Soviet Arctic Shelf. *Continental Shelf Research*, 13: 669–691.

Newsome SD, Etnier MA, Gifford-Gonzalez D, Phillips DL, vanTuinen M, Hadly EA, Costa DP, Kennett DJ, Guilderson TP, Koch PL. 2007. The shifting baseline of northern fur seal ecology in the northeast Pacific Ocean. *PNAS* ,104 (23): 9709-9714.

Noto and Yasuda. 1999. Population decline of the Japanese sardine, *Sardinops melanostictus*, in relation to sea surface temperature in the Kuroshio Extension. *Canadian Journal of Fisheries and Aquatic Science*, 56(6): 973–983.

Overland JE and Stabeno PJ. 2004. Is the climate of the Bering Sea warming and affecting the ecosystem? *EOS Transactions of the American Geophysical Union,* 85: 309–316.

Overland JE, Adams JM and Bond NA. 1999. Decadal variability of the Aleutian Low and its relation to high-latitude circulation. *Journal of Climate*, 12(5): 1542-1548.

Pacific Fishery Management Council News Release. Feburary 28, 2008. http://www.pcouncil.org/newsreleases/Feb_2008_Sacramento_News_Release.pdf.

Peacock E. 2002. Kuiu Island black bear population estimation using biomarking and DNA, 1 July 2001 – 30 June 2002. Alaska Department of Fish and Game. Federal aid in wildlife restoration research performance report, grant W-27-5, Project 17.7. Juneau, Alaska.

Perry RI, Thompson PA, Mackas DL, Harrison PJ, Yelland DR. 1999. Stable carbon isotopes as pelagic food web tracers in adjacent shelf and slope regions off British Columbia, Canada. *Canadian Journal of Fisheries and Aquatic Sciences,* 56(12): 2477-2486

Rember R and Trefry J. 2005. Sediment and organic carbon focusing in the Shelikof Strait, Alaska. *Marine Geology*, 224: 83-101.

Reynolds LA and Thunell RC. 1986. Seasonal production and morphologic variation of N. pachyderma (Ehrenberg) in the Northeast Pacific. *Micropaleontology*, 32(1): 1-18.

Royer TC, Grosch CE, Mysak LA. 2001. Interdecadal variability of Northeast Pacific coastal freshwater and its implications on biological productivity. *Progress in Oceanography*, 49: 95-111.

Sambrotto RN and Lorenzen CJ. 1987. Phytoplankton and phytoplankton production in the coastal and oceanic areas of the Gulf of Alaska, p. 249-282. *In The Gulf of Alaska: Physical environment and biological resources.* D.W. Hood and S.T. Zimerman [eds.], US Department of Commerce.

Schell, DM. 2000. Declining carrying-capacity in the Bering Sea: Isotopic evidence from whale baleen. *Limnology and Oceanography*, 45(2): 459-462.

Schell DM, Barnett BA, Vinette KA. 1998. Carbon and nitrogen isotope ratios in zooplankton of Bering, Chukchi, and Beaufort Seas. *Marine Ecology Progress Series*, 162: 11-23.

Shackleton NJ. 1974. Attainment of isotopic equilibrium between ocean water and the benthonic foraminifera genus *Uvigerina*: Isotopic changes in the ocean during the last glacial. Colloques internationaux du Centre national de la recherche scientifique, 219: 203-209.

Shackleton NJ and Pisias NG. 1985. Atmospheric carbon dioxide, orbital forcing, and climate. *In* The carbon cycle and atmospheric CO_2: Natural variations Archean to Present, *Geophysical Monograph Series*, 32: 303–317. Eds. Sundquist ET and Broecker WS, American Geophysical Union, Washington, DC.

Shulski M and Wendler G. 2007. *The Climate of Alaska.* University of Alaska Press.

Spero HJ, Bijma J, Lea DW, Bemis BE. 1997. Effect of seawater carbonate concentration on foraminiferal carbon and oxygen isotopes. *Nature*, 390: 497-500.

Strom SL, Olson MB, Marci EL, Mordy CW. 2006. Cross-shelf gradient in phytoplankton community structure, nutrient utilization, and growth rate in the coastal Gulf of Alaska. *Marine Ecology Progress Series*, 328: 75-92.

Strom SL, Marci EL, Olsen MB. 2007. Microzooplankton grazing in the coastal Gulf of Alaska: Variations in top-down control of phytoplankton. *Limnology and Oceanography*, 52(4): 1480-1494.

Sugai SF. 1985. Processes controlling trace metal and nutrient geochemistry in two Southeast Alaskan fjords. Dissertation, University of Alaska Fairbanks. ProQuest/UMI, AAT 8612265: 156 pages.

Teranes JL and Bernasconi SM. 2000. The record of nitrate utilization and productivity limitation provided by δ^{15}N values in lake organic matter—A study of sediment trap and core sediments from Baldeggersee, Switzerland. *Limnology and Oceanography,* 45(4): 801-813.

Thomas E, Gapotchenko T, Varekamp JC, Mecray EL, Buchholtz ten Brink MR. 2000. Benthic foraminifera and environmental changes in Long Island Sound. *Journal of Coastal Research*, 16(3): 641-655.

Trenberth KE. 2001. Climate variability and global warming. *Science*, 293: 48-49.

Urey HC, Lowenstam HA, Epstein S, McKinney CR. 1951. Measurements of paletemperatures and temperatures of the upper cretaceous of England, Denmark, and the Southeastern United States. *Bulletin of the Geological Society of America*, 62: 319-416.

Verburg P. 2007. The need to correct for the Suess effect in the application of δ^{13}C in sediment of autotrophic Lake Tanganyika, as a productivity proxy in the Anthropocene. *Journal of Paleolimnology*, 37:591-602.

Weingartner TJ, Coyle K, Finney B, Hopcroft R, Whitledge T, Brodeur R, Dagg M, Farley E, Haidvogel D, Haldorson L, Hermann A, Hinckley S, Napp J, Stabeno P, Kline T, Lee C, Lessard E, Royer T, Strom S. 2002. The northeast Pacific GLOBEC Program: Coastal Gulf of Alaska. *Oceanography*, 15(2): 48.

Appendix A
Bay of Pillars Proxy Data

Table A – 1

Bay of Pillars Organic Matter Stable Isotopes, C/N, Biogenic Opal

Depth (cm)	Year	N (%)	C (%)	C (%)/N (%)	$\delta^{15}N$	$\delta^{13}C$	Opal (%)
0	1997	0.83	9.05	10.84	5.279	-22.768	23.15
2	1964.27	0.96	10.05	10.48	5.465	-22.216	24.29
4	1931.54	0.85	9.16	10.83	5.267	-22.095	27.67
6	1898.81	0.72	8.37	11.69	5.11	-22.167	28.12
8	1866.08	0.65	7.49	11.60	4.899	-22.465	27.08
10	1833.35	0.75	8.66	11.55	5.127	-22.32	30.82
12	1800.62	0.80	8.80	10.97	5.387	-22.322	31.41
14	1767.89	0.81	8.92	10.97	5.653	-22.312	30.98
16	1735.16	0.79	8.68	10.96	5.194	-22.014	32.75
18	1702.43	0.79	8.54	10.80	5.313	-22.103	31.47
20	1669.7	0.81	8.90	11.02	5.168	-22.316	29.69
22	1636.97	0.66	8.04	12.09	4.905	-22.641	27.47
24	1604.24	0.78	8.84	11.31	4.998	-22.291	26.3
26	1571.51	0.82	9.26	11.23	5.063	-22.154	29.53
28	1538.78	0.85	9.18	10.85	5.36	-22.052	32.15
30	1506.05	0.82	9.06	11.06	5.317	-22.288	35.03
32	1473.32	0.80	8.79	11.06	5.249	-22.236	33.32
34	1440.59	0.75	8.30	11.14	5.352	-22.353	32.85
36	1407.86	0.72	8.25	11.41	4.956	-22.277	33.92
38	1375.13	0.79	9.03	11.41	5.335	-22.431	34.48
40	1342.4	0.75	8.32	11.09	5.262	-22.225	35.55
42	1309.67	0.78	9.04	11.55	5.22	-22.189	33.85
44	1276.94	0.80	9.08	11.28	5.007	-22.345	35.48
46	1244.21	0.72	8.62	12.04	4.942	-22.319	31.58
48	1211.48	0.77	9.17	11.97	5.119	-22.551	31.34
50	1178.75	0.32	3.52	11.04	5.544	-22.336	29.89
52	1146.02	0.82	9.30	11.36	5.184	-22.468	31.25
54	1113.29	0.77	9.57	12.41	4.629	-22.516	28
56	1080.56	0.77	9.27	12.10	4.854	-22.456	27.51
58	1047.83	0.85	9.95	11.73	5.167	-22.472	27.48
60	1015.1	0.79	9.13	11.63	5.181	-22.233	26.48
62	982.37	0.85	9.36	10.97	5.623	-22.267	29.37
64	949.64	0.80	9.29	11.55	5.273	-22.35	27.63
66	916.91	0.77	8.85	11.54	4.965	-22.285	27.03
68	884.18	0.83	9.37	11.24	5.321	-22.279	26.36
70	851.45	0.73	8.38	11.43	5.25	-22.15	30.05
72	818.72	0.72	8.41	11.75	4.92	-22.299	27.8

Depth (cm)	Year MagSusc	N (%)	C (%)	C (%)/N (%)	$\delta^{15}N$	$\delta^{13}C$	Opal (%)
74	785.99	0.76	8.60	11.28	5.358	-22.283	29.75
76	753.26	0.70	8.18	11.62	5.071	-22.159	26.69
78	720.53	0.74	8.28	11.18	5.381	-22.206	31.62
80	687.8	0.73	8.20	11.30	5.422	-22.182	32.79
82	655.07	0.77	8.26	10.78	5.942	-22.069	29.27
84	622.34	0.66	7.30	11.05	5.458	-22.116	30.2
86	589.61	0.72	7.88	10.90	5.522	-22.153	34
88	556.88	0.71	7.82	11.05	5.424	-22.224	33.38
90	524.15	0.72	8.14	11.25	5.552	-22.2	32
92	491.42	0.70	7.78	11.05	5.62	-22.11	28.32
94	458.69	0.68	7.52	11.05	5.492	-22.208	33.28
96	425.96	0.67	7.93	11.78	5.226	-22.274	37.35
98	393.23	0.70	7.89	11.32	5.428	-22.292	40.54
100	360.5	0.71	7.81	11.00	5.712	-22.228	43.68
102	327.77	0.66	7.32	11.10	5.581	-22.167	38.16
104	295.04	0.73	7.96	10.85	5.648	-22.303	42.4
106	262.31	0.77	8.40	10.89	5.776	-22.318	44.04

Table A – 2
Bay of Pillars Foraminifera Stable Isotopes

ID	Core depth (cm)	$\delta^{18}O$ year (AD)	ID2	$\delta^{13}C$ (permil, vs VPDB)	$\delta^{18}O$ (permil, vs VPDB)	Notes	Date run
NBS-19			std	1.93	-2.15		3/31/2004
NBS-19			std	1.98	-2.11		3/31/2004
NBS-19			std	1.94	-2.40		3/31/2004
NBS-19			std	1.91	-2.24		3/31/2004
BoP-G-2 6	6		E. excav.	-1.54	0.12		3/31/2004
BoP-G-2 8	8		E. excav.	-1.33	-0.24		3/31/2004
BoP-G-2 10	10		E. excav.	-1.25	0.50		3/31/2004
BoP-G-2 12	12		E. excav.	-1.20	-0.79		3/31/2004
BoP-G-2 14	14		E. excav.	-1.12	-0.70		3/31/2004
BoP-G-2 16	16		E. excav.	-1.33	-2.77		3/31/2004
BoP-G-2 18	18		E. excav.	-1.57	-0.44		3/31/2004
BoP-G-2 20	20		E. excav.	-1.22	0.13		3/31/2004
BoP-G-2 22	22		E. excav.	-1.20	0.88		3/31/2004
BoP-G-2 24	24		E. excav.	-1.39	-1.04		3/31/2004
BoP-G-2 26	26		E. excav.	-1.26	0.51		3/31/2004
BoP-G-2 28	28		E. excav.	-1.35	1.28		3/31/2004
BoP-G-2 30	30		E. excav.	-1.07	-2.68		3/31/2004
BoP-G-2 32	32		E. excav.	-2.38	0.62		3/31/2004
BoP-G-2 34	34		E. excav.			Lost trap error	3/31/2004
BoP-G-2 36	36		E. excav.	-1.30	-1.41		3/31/2004
NBS-19			std	1.94	-2.17		3/31/2004
NBS-19			std	1.92	-2.24		3/31/2004
BoP-G-2 40	40		E. excav.	-1.55	-0.39		3/31/2004
BoP-G-2 42	42		E. excav.	-1.30	0.75		3/31/2004
BoP-G-2 46	46		E. excav.	-1.11	0.71		3/31/2004
BoP-G-2 48	48		E. excav.	-0.88	0.53		3/31/2004
BoP-G-2 50	50		E. excav.	-0.69	0.88		3/31/2004
BoP-G-2 52	53		E. excav.	-1.29	0.14		3/31/2004
BoP-G-2 54	54		E. excav.	-1.25	0.89		3/31/2004
BoP-G-2 56	56		E. excav.	-0.98	1.09		3/31/2004
BoP-G-2 58	68		E. excav.	-1.20	1.28		3/31/2004
BoP-G-2 60	60		E. excav.	-1.18	0.75		3/31/2004
BoP-G-2 62	62		E. excav.	-1.18	0.60		3/31/2004
BoP-G-2 64	64		E. excav.	-0.88	0.97		3/31/2004
BoP-G-2 72	72		E. excav.	-2.10	0.93		3/31/2004
BoP-G-2 74	74		E. excav.	-1.48	0.62		3/31/2004
BoP-G-2 76	76		E. excav.	-0.78	0.82		3/31/2004
BoP-G-2 78	78		E. excav.	-0.92	0.68		3/31/2004

ID	Core depth (cm)	$\delta^{18}O$ year (AD)	ID2	$\delta^{13}C$ (permil, vs VPDB)	$\delta^{18}O$ (permil, vs VPDB)	Notes	Date run
BoP-G-2 82	82		E. excav.	-1.41	0.80		3/31/2004
BoP-G-2 84	84		E. excav.	-1.33	0.62		3/31/2004
BoP-G-2 86	86		E. excav.	-1.13	0.96		3/31/2004
BoP-G-2 88	88		E. excav.	-1.19	1.08		3/31/2004
NBS-19			std	1.99	-2.08		3/31/2004
NBS-19			std	1.98	-2.20		3/31/2004
NBS-19			std	1.95	-2.15		4/2/2004
NBS-19			std	1.96	-2.23		4/2/2004
NBS-19			std	1.96	-2.14		4/2/2004
NBS-19			std	1.95	-2.24		4/2/2004
BoP-G-2 90	90		E. excav.	-1.22	-1.07		4/2/2004
BoP-G-2 92	92		E. excav.	-1.37	0.48		4/2/2004
BoP-G-2 100	100		E. excav.	-1.22	-0.35		4/2/2004
BoP-G-2 102	102		E. excav.	-1.46	0.43		4/2/2004
BoP-G-2 104	104		E. excav.	-1.45	0.28		4/2/2004
NBS-19			std	1.93	-2.25		4/2/2004

Table A-3

Bay of Pillars Foraminifera Faunal Analysis

Depth (cm)	Size fraction (µm)	Community Totals (Individuals)	Community Totals (Percent)	*Elphidium excavatum*	*Ammonia becarii*	Buliminella elegantissima	*Textularia spp.*	*Rosalzna ornatissima*	*Nonionell bradii*	*Nonion commune*	*Bolvina subaenariensis*
0	> 63	0									
	125-250	0									
	>250	0									
	Sum:	0									
2	> 63	3	50	3							
	125-250	3	50				3				
	>250	0	0								
	Sum:	6	100	3			3				
4	> 63	0									
	125-250	0									
	>250	0									
	Sum:	0	0								
6	> 63	46	6.01	19	14	9	4				
	125-250	406	53.07	234	154	7	11				
	>250	313	40.92	285	28						
	Sum:	765	100	538	196	16	15	0			
8	> 63	23	3.90	11	4	7	1				
	125-250	296	50.17	181	108	4	1	2			
	>250	271	45.93	247	22			2			
	Sum:	590	100	439	134	11	2	4			
10	> 63	33	7.45	15	12	5	1				
	125-250	184	41.53	112	61	7		3	1		
	>250	226	51.02	209	14				3		
	Sum:	443	100	336	87	12	1	3	4		

Depth (cm)	Size fraction (µm)	Community Totals (Individuals)	Community Totals (Percent)	Elphidium excavatum	Ammonia becarii	Buliminella elegantissima	Textularia spp.	Rosalzna ornatissima	Nonionell bradii	Nonion commune	Bolvina subaenariensis
12	> 63	29	13.49	11	10	5	1			2	
	125-250	109	50.70	23	74	1	11				
	>250	77	35.81	64	13						
	Sum:	215	100.00	98	97	6	12	0	0	2	
14	> 63	58	8.53	33	15	9	1				
	125-250	321	47.21	219	79	9	6	3	2	3	
	>250	301	44.26	276	24				1		
	Sum:	680	100.00	528	118	18	7	3	3	3	
16	> 63	29	8.36	16	3	6	1		3		
	125-250	178	51.30	128		45	1		4		
	>250	140	40.35	132		8					
	Sum:	347	100.00	276	3	59	2	0	7	0	
18	> 63	45	15.00	23	10	10	1		1		
	125-250	133	44.33	69	55	2	2	1	2	2	
	>250	122	40.67	115	7						
	Sum:	300	100.00	207	72	12	3	1	3	2	
20	> 63	29	9.35	13	6	8	2				
	125-250	156	50.32	75	69	5	3	2	1	1	
	>250	125	40.32	119	6						
	Sum:	310	100.00	207	81	13	5	2	1	1	
22	> 63	20	7.22	7	9	4					
	125-250	144	51.99	76	61	3	1	1	1	1	
	>250	113	40.79	110	3						
	Sum:	277	100.00	193	73	7	1	1	1	1	

Depth (cm)	Size fraction (µm)	Community Totals (Individuals)	Community Totals (Percent)	Elphidium excavatum	Ammonia becarii	Buliminella elegantissima	Textularia spp.	Rosalzna ornatissima	Nonionell bradii	Nonion commune	Bolvina subaenariensis
24	> 63	33	15.94	10	10	8	4		1		
	125-250	87	42.03	43	36	2	2	3		1	
	>250	87	42.03	73	8				6		
	Sum:	207	100.00	126	54	10	6	3	7	1	
26	> 63	38	5.07	12	9	10	6	1			
	125-250	500	66.76	389	95	6	4	2	4		
	>250	211	28.17	196	10			1	4		
	Sum:	749	100.00	597	114	16	10	4	8	0	
28	> 63	22	6.36	8	9	5					
	125-250	117	33.82	67	41	4	1	1	1	2	
	>250	207	59.83	196	8			1	2		
	Sum:	346	100.00	271	58	9	1	2	3	2	
30	> 63	20	8.33	10	3	5	1			1	
	125-250	107	44.58	58	41	4		1	2	1	
	>250	113	47.08	95	18						
	Sum:	240	100.00	163	62	9	1	1	2	2	
32	> 63	58	7.20	37	12	7	2				
	125-250	210	26.05	118	73	6	3	5	1	3	1
	>250	538	66.75	513	21				4		
	Sum:	806	100.00	668	106	13	5	5	5	3	1
34	> 63	24	7.27	14	6	3			1		
	125-250	83	25.15	23	56	2	1	1			
	>250	223	67.58	209	10				4		
	Sum:	330	100.00	246	72	5	1	1	5	0	

Depth (cm)	Size fraction (µm)	Community Totals (Individuals)	Community Totals (Percent)	*Elphidium excavatum*	*Ammonia becarii*	Buliminella elegantissima	*Textularia spp.*	*Rosalzna ornatissima*	*Nonionell bradii*	*Nonion commune*	*Bolvina subaenariensis*
36	> 63	7	2.53	4	2	1					
	125-250	58	20.94	18	32	1	1		6		
	>250	212	76.53	198	6			1	7		
	Sum:	277	100.00	220	40	2	1	1	13	0	
38	> 63	14	12.39	4	3	7					
	125-250	32	28.32	12	13	2	1		3	1	
	>250	67	59.29	61	3				3		
	Sum:	113	100.00	77	19	9	1	0	6	1	
40	> 63	8	34.78		1	5	2				
	125-250	8	34.78		3	4	1				
	>250	7	30.43	4	3						
	Sum:	23	100.00	4	7	9	3	0	0	0	
42	> 63	47	24.48	18	11	17	1				
	125-250	91	47.40	50	34	3			4		
	>250	54	28.13	48	4				2		
	Sum:	192	100.00	116	49	20	1	0	6	0	
44	> 63	17	12.32	5	6	6					
	125-250	81	58.70	34	37	7			3		
	>250	40	28.99	36	3				1		
	Sum:	138	100.00	75	46	13	0	0	4	0	
46	> 63	13	4.10	6	4	2	1				
	125-250	103	32.49	62	31	4	3		2	1	
	>250	201	63.41	187	12				2		
	Sum:	317	100.00	255	47	6	4	0	4	1	

Depth (cm)	Size fraction (µm)	Community Totals (Individuals)	Community Totals (Percent)	*Elphidium excavatum*	*Ammonia becarii*	Buliminella elegantissima	*Textularia spp.*	*Rosalzna ornatissima*	*Nonionell bradii*	*Nonion commune*	*Bolvina subaenariensis*
48	> 63	19	11.45	6	6	5	1		1		
	125-250	57	34.34	20	30	3	3				1
	>250	90	54.22	72	16				2		
	Sum:	166	100.00	98	52	8	4	0	3	0	1
50	> 63	14	23.33	5	2	5	1				1
	125-250	24	40.00	5	13	3	3				
	>250	22	36.67	17	1		2	1	1		
	Sum:	60	100.00	27	16	8	6	1	1	0	1
52	> 63	17	6.75	2	9	6					
	125-250	139	55.16	64	68		3	3	1		
	>250	96	38.10	90	4			1	1		
	Sum:	252	100.00	156	81	6	3	4	2	0	
54	> 63	33	20.89	14	7	4	7			1	
	125-250	86	54.43	39	42	4	1				
	>250	39	24.68	36	3						
	Sum:	158	100.00	89	52	8	8	0	0	1	
56	> 63	53	12.96	27	11	13	2				
	125-250	208	50.86	125	72	4	2	2	3		
	>250	148	36.19	128	18				2		
	Sum:	409	100.00	280	101	17	4	2	5	0	
58	> 63	36	18.65	18	7	9	2				
	125-250	88	45.60	39	40	3	3	1	2		
	>250	69	35.75	65	4						
	Sum:	193	100.00	122	51	12	5	1	2	0	

Depth (cm)	Size fraction (µm)	Community Totals (Individuals)	Community Totals (Percent)	*Elphidium excavatum*	*Ammonia becarii*	Buliminella elegantissima	*Textularia spp.*	*Rosalzna ornatissima*	*Nonionell bradii*	*Nonion commune*	*Bolvina subaenariensis*
60	> 63	47	37.90	6	23	17	1				
	125-250	50	40.32	6	34	2	5	2		1	
	>250	27	21.77	19	8						
	Sum:	124	100.00	31	65	19	6	2	0	1	
62	> 63	2	2.04				2				
	125-250	66	67.35	29	21	6	4	2	4		
	>250	30	30.61	24	6						
	Sum:	98	100.00	53	27	6	6	2	4	0	
64	> 63	49	30.25	2	17	29	1				
	125-250	99	61.11	12	66	13	3	3	2		
	>250	14	8.64	13	1						
	Sum:	162	100.00	27	84	42	4	3	2	0	
66	> 63	23	24.21	2	10	7	4				
	125-250	64	67.37	9	40	9	3	2	1		
	>250	8	8.42	4	2			2			
	Sum:	95	100.00	15	52	16	7	4	1	0	
68	> 63	0	0.00								
	125-250	7	100.00		3	1	1	2			
	>250	0	0.00								
	Sum:	7	100.00	0	3	1	1	2	0	0	0
70	> 63	0	0.00								
	125-250	6	100.00		4	1		1			
	>250	0	0.00								
	Sum:	6	100.00	0	4	1	0	1	0	0	0

Depth (cm)	Size fraction (µm)	Community Totals (Individuals)	Community Totals (Percent)	Elphidium excavatum	Ammonia becarii	Buliminella elegantissima	Textularia spp.	Rosalzna ornatissima	Nonionell bradii	Nonion commune	Bolvina subaenariensis
72	> 63	17	43.59	4	4	9					
	125-250	22	56.41	1	10	4	6	1			
	>250	0	0.00								
	Sum:	39	100.00	5	14	13	6	1	0	0	
74	> 63	33	19.88	4	10	16	2		1		
	125-250	82	49.40	38	36	3	2	1	2		
	>250	51	30.72	43	8						
	Sum:	166	100.00	85	54	19	4	1	3	0	
76	> 63	41	20.20	17	8	15				1	
	125-250	86	42.36	50	28	3	3		2		
	>250	76	37.44	68	4				4		
	Sum:	203	100.00	135	40	18	3	0	6	1	
78	> 63	47	10.61	18	7	17	1		1	1	2
	125-250	254	57.34	188	50	7	4		5		
	>250	142	32.05	132	9				1		
	Sum:	443	100.00	338	66	24	5	0	7	1	2
80	> 63	20	35.71	5	5	9	1				
	125-250	25	44.64	9	13	1	1		1		
	>250	11	19.64	9	2						
	Sum:	56	100.00	23	20	10	2	0	1	0	
82	> 63	40	17.78	16	10	9	3		1		1
	125-250	117	52.00	71	27	17			2		
	>250	68	30.22	60	4		4				
	Sum:	225	100.00	147	41	26	7	0	3	0	1

Depth (cm)	Size fraction (µm)	Community Totals (Individuals)	Community Totals (Percent)	*Elphidium excavatum*	*Ammonia becarii*	Buliminella elegantissima	*Textularia spp.*	*Rosalzna ornatissima*	*Nonionell bradii*	*Nonion commune*	*Bolvina subaenariensis*
84	> 63	29	10.39	14	4	9			1		1
	125-250	173	62.01	113	44	11	2		3		
	>250	77	27.60	70	5				2		
	Sum:	279	100.00	197	53	20	2	0	6	0	1
86	> 63	44	11.64	13	10	13	3		5		
	125-250	143	37.83	93	29	4	4	1	12		
	>250	191	50.53	184	4			1	2		
	Sum:	378	100.00	290	43	17	7	2	19	0	
88	> 63	14	3.22	10	1	3					
	125-250	143	32.87	110	22	5	1	1	4		
	>250	278	63.91	262	10			1	5		
	Sum:	435	100.00	382	33	8	1	2	9	0	
90	> 63	14	6.54	6	1	6			1		
	125-250	113	52.80	93	14	3	1		2		
	>250	87	40.65	76	7			1	3		
	Sum:	214	100.00	175	22	9	1	1	6	0	
92	> 63	21	11.17	5	6	8	2				
	125-250	53	28.19	20	21	10	2				
	>250	114	60.64	104	8				2		
	Sum:	188	100.00	129	35	18	4	0	2	0	
94	> 63	19	10.05	5	4	7	2		1		
	125-250	79	41.80	55	17	5	1	1			
	>250	91	48.15	85	6						
	Sum:	189	100.00	145	27	12	3	1	1	0	

Depth (cm)	Size fraction (µm)	Community Totals (Individuals)	Community Totals (Percent)	*Elphidium excavatum*	*Ammonia becarii*	Buliminella elegantissima	*Textularia spp.*	*Rosalzna ornatissima*	*Nonionell bradii*	*Nonion commune*	*Bolvina subaenariensis*
96	> 63	24	10.30	5	1	14	2		1	1	
	125-250	106	45.49	68	20	7	1		10		
	>250	103	44.21	97	3				3		
	Sum:	233	100.00	170	24	21	3	0	14	1	
98	> 63	33	11.34	12	10	9			2		
	125-250	109	37.46	85	15	3	2		4		
	>250	149	51.20	139	4				6		
	Sum:	291	100.00	236	29	12	2	0	12	0	
100	> 63	9	7.56	2	3	3	1				
	125-250	65	54.62	40	22	3					
	>250	45	37.82	43	2						
	Sum:	119	100.00	85	27	6	1	0	0	0	
102	> 63	25	9.92	10	3	7	4		1		
	125-250	90	35.71	63	19	2	1	1	4		
	>250	137	54.37	133	1				3		
	Sum:	252	100.00	206	23	9	5	1	8	0	
104	> 63	6	3.61			2	4				
	125-250	77	46.39	44	27	2	1	2		1	
	>250	83	50.00	80	2					1	
	Sum:	166	100.00	124	29	4	5	2	0	2	
106	> 63	0	0.00								
	125-250	4	100.00				3	1			
	>250	0	0.00								
	Sum:	4	100.00	0	0	0	3	1	0	0	0

Table A – 4
Bay of Pillars Radiocarbon Dates

CENTER FOR ACCELERATOR MASS SPECTROMETRY
Lawrence Livermore National Laboratory
^{14}C results

Date	CAMS #	Core Depth (cm)	Macrofossil Type	$d^{13}C$	Fraction Modern	±	$D^{14}C$	±	^{14}C age	±
16-Nov-2004	111119	68 - 69	Terrestrial	-25	0.8651	0.0043	-134.9	4.3	1165	40
16-Jan-2000	61558	95 - 96	Terrestrial	-25	0.8679	0.0136	-132.1	13.6	1140	130
16-Jan-2000	61559	95 - 96	Carbonate	0	0.7518	0.0037	-248.2	3.7	2290	40
25-May-1999	55699	105 - 106	Terrestrial	-25	0.351	0.0135	-649	13.5	8410	310
25-May-1999	55667	105 - 106	Carbonate	0	0.7589	0.0031	-241.1	3.1	2220	40

1) Delta 13C values are the assumed values according to Stuiver and Polach (Radiocarbon, v. 19, p.355, 1977) when given without decimal places. Values measured for the material itself are given with a single decimal place.

2) The quoted age is in radiocarbon years using the Libby half life of 5568 years and following the conventions of Stuiver and Polach
(ibid.).

3) Radiocarbon concentration is given as fraction Modern, D14C, and conventional radiocarbon age.

4) Sample preparation backgrounds have been subtracted, based on measurements of samples of 14C-free coal and
calcite. Backgrounds were scaled relative to sample size.

5) Comment: The large uncertainties for some of these results are due to small sample sizes (less than 0.1 mg C).

Appendix B
GAK4 Proxy Data

Table B – 1
GAK4 Organic Matter Stable Isotopes, OC/N, Biogenic Opal

Depth (cm)	Year AD	MagSusc	N %	C%	δ15N	δ13C	C/N	Opal %
2	1997.9	115.96	0.146	1.299	5.303	-23.133	8.914	10.85
3	1994.9	218.26	0.160	1.450	5.328	-23.210	9.077	10.86
4	1991.9	290.81	0.161	1.397	5.036	-23.233	8.687	11.49
5	1988.9	324.03	0.142	1.311	5.476	-23.158	9.209	10.73
6	1985.8	335.18	0.152	1.354	5.548	-23.312	8.904	10.11
7	1982.8	338.74	0.150	1.351	5.529	-23.420	9.015	10.46
8	1979.8	336.3	0.158	1.427	5.117	-23.513	9.020	9.66
9	1976.7	333.38	0.140	1.274	4.818	-23.615	9.081	9.71
10	1973.7	331.86	0.159	1.428	6.089	-23.577	8.969	10.54
11	1970.7	334.25	0.151	1.364	4.834	-23.647	9.040	10.23
12	1967.6	338.49	0.147	1.352	4.950	-23.625	9.179	10.05
13	1964.6	345.3	0.144	1.344	4.776	-23.705	9.353	10.16
14	1961.6	354.81	0.146	1.388	5.082	-23.701	9.522	9.61
15	1958.6	362.72	0.127	1.261	5.226	-23.538	9.947	9.18
16	1955.5	363.73	0.144	1.393	5.530	-23.672	9.685	10.20
17	1952.5	361.45	0.151	1.480	5.005	-23.689	9.811	10.31
18	1949.5	358.37	0.134	1.323	4.565	-23.817	9.854	9.84
19	1946.4	357.4	0.134	1.374	4.787	-23.826	10.258	10.64
20	1943.4	359.66	0.130	1.346	4.619	-23.780	10.316	10.26
21	1940.4	362.29	0.146	1.472	4.879	-23.677	10.094	10.01
22	1937.3	365.42	0.122	1.268	4.644	-23.559	10.430	10.01
23	1934.3	368.15	0.137	1.365	5.483	-23.800	9.985	10.13
24	1931.3	368.47	0.134	1.397	5.136	-23.933	10.439	10.41
25	1929.6	369.24	0.128	1.337	5.096	-23.789	10.472	10.65
26	1928.1	369.58	0.135	1.415	5.308	-23.929	10.476	10.24
27	1926.7	368.67	0.125	1.331	5.173	-23.935	10.635	10.18
28	1925.3	368.93	0.130	1.376	5.353	-23.971	10.582	10.01
29	1923.9	369.03	0.127	1.363	5.885	-23.887	10.719	9.44
30	1922.4	372.07	0.117	1.296	4.361	-24.000	11.084	8.64
31	1921.0	376.67	0.114	1.253	4.321	-24.048	10.999	7.79
32	1919.6	382.42	0.101	1.149	4.175	-23.995	11.381	8.63
33	1918.1	384.02	0.108	1.226	4.215	-24.047	11.352	8.68
34	1916.7	379.99	0.101	1.176	4.104	-24.124	11.655	8.78
35	1915.3	373.63	0.099	1.183	4.338	-23.863	11.897	8.00
36	1913.9	369.69	0.106	1.278	4.497	-23.752	12.103	8.66
37	1912.4	369.3	0.103	1.309	4.279	-23.829	12.726	8.93
38	1911.0	372.08	0.109	1.272	3.716	-23.842	11.666	9.33
39	1908.2	374.26			3.658	-23.776		8.69
40	1905.0	376.1	0.102	1.215	3.113	-23.719	11.967	8.32
41	1904.0	377.51	0.112	1.184	4.791	-23.591	10.538	10.44
42	1902.0	377.22	0.103	1.232	4.324	-23.732	11.999	9.25
43	1900.0	376.38	0.129	1.298	4.561	-23.589	10.092	9.05
44	1897.0	377.12	0.108	1.265	4.247	-23.488	11.731	9.83

Depth (cm)	Year AD	MagSusc	N %	C%	$\delta^{15}N$	$\delta^{13}C$	C/N	Opal %
45	1893.6	379.05	0.118	1.158	5.275	-23.442	9.800	9.93
46	1891.9	381.82	0.113	1.261	3.924	-23.596	11.158	9.46
47	1890.3	384.79	0.126	1.185	4.511	-23.510	9.386	10.24
48	1888.7	384.81	0.105	1.215	4.675	-23.442	11.520	9.39
49	1887.0	381.56	0.119	1.123	4.600	-23.535	9.432	10.24
50	1885.4	376.98	0.103	1.167	3.287	-23.747	11.342	8.57
51	1883.7	373.76	0.136	1.328	4.661	-24.002	9.746	10.37
52	1882.1	375.62	0.100	1.126	5.353	-23.604	11.318	8.93
53	1880.5	381.26	0.142	1.331	5.970	-23.401	9.361	7.13
54	1878.8	387.29	0.102	1.137	4.911	-23.848	11.143	9.68
55	1877.2	392.83	0.108	1.090	4.856	-23.417	10.092	10.32
56	1875.5	400.28	0.094	1.083	5.336	-23.499	11.541	9.37
57	1873.9	406.99	0.119	1.221	6.763	-23.544	10.274	10.24
58	1872.3	412.08	0.097	1.137	4.280	-23.560	11.739	8.72
59	1870.6	417.8	0.150	1.569	6.177	-23.054	10.451	8.42
60	1869.0	423.43	0.095	1.113	5.658	-23.881	11.747	9.00
61	1867.3	427.98	0.109	1.165	6.122	-23.392	10.686	10.17
62	1865.7	430.16	0.094	1.205	5.467	-23.532	12.833	8.88
63	1864.1	428.96	0.106	1.127	4.286	-23.343	10.624	7.28
64	1862.4	428.09	0.088	1.158	5.723	-23.720	13.161	8.97
65	1860.8	435.99	0.134	1.382	6.584	-23.122	10.291	7.68
66	1859.2	454.67	0.082	1.077	3.805	-23.699	13.078	7.76
67	1857.5	474.41	0.119	1.220	5.145	-23.500	10.223	8.76
68	1855.9	491.69	0.079	1.065	4.562	-23.371	13.407	9.10
69	1854.2	504.17	0.108	1.079	5.886	-22.900	9.945	7.04
70	1852.6	510.64	0.078	1.011	6.737	-23.227	12.893	8.46
71	1851.0	513.44	0.094	0.966	7.172	-23.525	10.229	8.84
72	1849.3	515.96	0.086	1.016	7.535	-23.391	11.866	8.75
73	1847.7	512.95	0.086	0.920	4.008	-23.500	10.696	9.67
74	1846.0	493.49	0.089	1.061	4.544	-23.519	11.899	8.49
75	1844.4	460.4	0.096	1.090	7.171	-23.062	11.413	8.16
76	1842.8	431.55	0.099	1.125	6.386	-23.688	11.354	8.36
77	1841.1	418.9	0.112	1.184	6.990	-23.254	10.604	9.34
78	1839.5	418.64	0.097	1.110	7.179	-23.771	11.415	9.99
79	1837.8	423.65	0.105	1.143	7.380	-23.327	10.900	9.01
80	1836.2	429.96	0.094	1.121	7.188	-23.411	11.883	8.60
81	1834.6	432.58	0.091	1.058	7.344	-23.237	11.626	8.77
82	1832.9	426.58	0.093	1.065	7.219	-23.248	11.501	8.36
83	1831.3	415.19	0.098	1.082	3.566	-23.409	11.031	9.33
84	1829.6	407.51	0.130	1.354	4.601	-23.571	10.420	12.51
85	1828.0	405.28	0.107	1.272	4.900	-23.660	11.872	10.70
86	1826.4	400.68	0.117	1.207	5.124	-23.326	10.340	11.02
87	1824.7	395.47	0.130	1.305	5.143	-23.236	10.006	8.05
88	1823.1	394.27	0.144	1.434	5.409	-23.181	9.955	7.65
89	1821.4	395.93	0.124	1.293	4.979	-23.633	10.414	13.25
90	1819.8	398.33	0.100	1.188	4.101	-23.677	11.936	10.90
91	1818.2	399.39	0.109	1.127	4.649	-23.415	10.322	10.38
92	1816.5	396.21	0.142	1.441	4.958	-23.368	10.154	11.25
93	1814.9	391.86	0.151	1.496	4.784	-23.189	9.880	12.26
94	1813.3	385.59	0.122	1.224	5.460	-23.433	10.044	9.51

Depth (cm)	Year AD	MagSusc	N %	C%	$\delta^{15}N$	$\delta^{13}C$	C/N	Opal %
95	1811.6	380.22	0.102	1.261	4.904	-23.728	12.334	11.24
96	1810.0	377.06	0.134	1.337	5.699	-23.117	9.948	11.33
97	1808.3	376.14	0.134	1.332	5.500	-23.288	9.974	11.80
98	1806.7							12.21
99	1805.1	373.71	0.122	1.218	5.215	-23.198	9.956	9.72
100	1803.4	371.54	0.111	1.274	5.277	-23.318	11.435	12.52
101	1801.8	369.23	0.146	1.451	5.865	-23.066	9.925	14.92
102	1800.1	365.49	0.126	1.273	5.825	-23.489	10.068	12.71
103	1797.0	362.37	0.124	1.262	4.996	-22.980	10.215	10.24
104	1792.0	361.86	0.119	1.246	4.965	-23.418	10.499	12.05
105	1788.0	364.16	0.111	1.251	4.860	-23.766	11.278	11.19
106	1784.0	366.75	0.147	1.490	5.814	-22.987	10.166	10.76
107	1780.0	362.88	0.156	1.556	5.945	-23.628	9.965	11.58
108	1776.0	355.64	0.108	1.174	5.476	-23.342	10.832	11.77
109	1772.0	350.67	0.153	1.514	5.455	-22.920	9.926	12.08
110	1768.0	351.85	0.109	1.224	5.240	-23.750	11.197	12.18
111	1764.0	357.76	0.148	1.480	3.924	-23.180	10.034	12.10
112	1760.0	361.06	0.121	1.198	5.223	-23.292	9.894	10.88
113	1756.0	360.5	0.108	1.094	4.669	-23.055	10.103	10.35
114	1752.0	363.74	0.118	1.147	5.010	-23.221	9.752	10.18
115	1748.0	370.14	0.109	1.174	4.688	-23.539	10.743	11.42
116	1744.0	374.8	0.131	1.258	5.871	-23.306	9.610	11.35
117	1740.0	376.4	0.118	1.151	5.329	-23.166	9.765	12.10
118	1737.5	376.26	0.131	1.288	5.321	-23.196	9.799	11.76
119	1736.5	375.85	0.102	1.021	5.208	-23.452	10.041	11.89
120	1735.5	376.84	0.109	1.192	5.283	-23.294	10.932	11.45
121	1734.5	377.16	0.095	0.940	5.323	-23.315	9.899	
122	1733.5	375.52	0.145	1.438	5.081	-23.055	9.892	
123	1732.5	373.28	0.118	1.158	5.414	-23.389	9.802	9.95
124	1731.5	370.92	0.110	1.179	4.570	-23.481	10.738	11.49
125	1730.5	368.66	0.106	1.202	4.387	-23.732	11.388	9.37
126	1728.9	366.71	0.139	1.396	3.714	-23.636	10.025	11.44
127	1727.8	366.6	0.107	1.177	1.993	-23.612	11.010	7.82
128	1725.7	369.25	0.101	1.139	1.886	-23.604	11.221	9.12
129	1723.5	372.25	0.090	1.018	2.320	-23.612	11.329	10.52
130	1721.3	373.36	0.090	1.178	1.374	-23.734	13.037	10.42
131	1719.1	372.79	0.092	0.997	2.989	-23.934	10.845	11.12
132	1717.0	373.38	0.070	0.756	2.672	-23.731	10.817	7.94
133	1714.8	375.24	0.110	1.174	3.088	-23.496	10.697	8.29
134	1712.6	378.95	0.105	1.173	4.672	-23.463	11.173	10.98
135	1710.4	381.89	0.100	1.167	4.879	-23.895	11.727	9.88
136	1708.3	383.72	0.098	1.028	3.703	-24.011	10.491	10.11
137	1706.1	385.3	0.129	1.324	3.960	-23.644	10.293	10.92
138	1703.9	388.45	0.152	1.532	4.465	-23.794	10.051	13.52
139	1701.7	393.18	0.141	1.481	3.569	-23.734	10.533	10.46
140	1699.6	398.86	0.098	1.146	2.327	-23.820	11.650	9.84
141	1697.4	403.65	0.113	1.161	3.401	-23.966	10.236	12.32
142	1695.2	409.73	0.084	0.849	3.558	-24.008	10.145	10.27
143	1693.0	416.71	0.147	1.453	4.398	-23.755	9.913	11.79
144	1690.9	417.7	0.112	1.158	5.201	-23.854	10.340	10.23

Depth (cm)	Year AD	MagSusc	N %	C%	$\delta^{15}N$	$\delta^{13}C$	C/N	Opal %
145	1688.7	410.55	0.088	1.070	4.434	-23.948	12.164	9.83
146	1686.5	401.91	0.098	0.996	3.905	-24.149	10.188	8.04
147	1684.4	396.01	0.073	0.782	3.482	-24.225	10.662	9.69
148	1682.2	380.57	0.120	1.262	4.155	-23.984	10.512	8.73
149	1680.0	334.23	0.136	1.477	5.035	-23.509	10.870	13.75
150	1677.8	245.9	0.137	1.502	5.108	-24.226	10.993	14.52
151	1675.6	133.48	0.153	1.654	2.870	-23.971	10.834	
152	1673.5		0.134	1.505	4.606	-23.921	11.224	15.24
153	1671.3		0.116	1.255	4.797	-24.335	10.833	14.74
154	1669.1		0.121	1.357	3.340	-24.014	11.205	16.43
155	1667.0		0.117	1.414	2.634	-24.228	12.071	14.62
156	1664.8		0.114	1.421	3.018	-24.538	12.443	12.34
157	1662.6		0.105	1.217	2.960	-24.174	11.608	14.42
158	1660.4		0.129	1.549	3.261	-24.201	12.029	13.70
159	1658.3		0.112	1.310	3.658	-24.269	11.707	14.51
160	1656.1		0.092	1.062	2.613	-24.206	11.574	12.53
161	1653.9		0.123	1.349	3.703	-24.132	10.928	14.30
162	1651.7		0.115	1.464	4.808	-24.619	12.684	7.21
163	1649.6		0.128	1.359	5.244	-24.140	10.620	12.10
164	1647.4		0.142	1.590	4.319	-24.181	11.163	15.29
165	1645.2		0.121	1.333	3.932	-24.171	10.995	16.01
166	1643.0		0.105	1.110	3.099	-23.952	10.528	9.19

Table B – 2

GAK4 Foraminifera Stable Isotopes

ID	Core depth (cm)	δ18O year (AD)	ID other	δ13C (permil VPDB)	δ18O (permil PDB)	Notes	Date run
Planktonic							
NBS-19			std	1.98	-2.18		3/25/2004
NBS-19			std	2.01	-2.14		3/25/2004
NBS-19			std	2.00	-2.23		3/25/2004
NBS-19			std	1.98	-2.20		3/25/2004
GAK-4-A-P 0	0	2003	Planktic	0.21	0.84		3/25/2004
GAK-4-A-P 2	2	1999	Planktic	-2.54	0.13		3/25/2004
GAK-4-A-P 5	5	1990	Planktic	-0.53	0.22		3/25/2004
GAK-4-A-P 7	7	1984	Planktic	-2.39	0.00		3/25/2004
GAK-4-A-P 9	9	1978	Planktic	0.47	0.92		3/25/2004
GAK-4-A-P 11	11	1972	Planktic	0.70	-0.33		3/25/2004
GAK-4-A-P 13	13	1966	Planktic	0.70	1.26		3/25/2004
GAK-4-A-P 17	17	1954	Planktic	-0.95	-0.74		3/25/2004
GAK-4-A-P 21	21	1942	Planktic	-1.20	-0.26		3/25/2004
GAK-4-A-P 25	25	1930	Planktic	0.16	-0.31		3/25/2004
GAK-4-A-P 29	29	1925	Planktic	0.00	1.40		3/25/2004
GAK-4-A-P 33	33	1919	Planktic	-0.12	0.73		3/25/2004
GAK-4-A-P 37	37	1913	Planktic	0.17	1.57		3/25/2004
GAK-4-A-P 41	41	1907	Planktic	0.65	1.29		3/25/2004
GAK-4-A-P 45	45	1901	Planktic	0.38	1.48		3/25/2004
GAK-4-A-P 49	49	1894	Planktic	0.64	1.11		3/25/2004
NBS-19			std	1.75	-2.29		3/25/2004
NBS-19			std			error	3/25/2004
GAK-4-A-P 53	53	1888	Planktic	0.43	1.08		3/25/2004
GAK-4-A-P 57	57	1881	Planktic	-0.35	0.27		3/25/2004
GAK-4-A-P 61	61	1874	Planktic	0.43	1.25		3/25/2004
GAK-4-A-P 65	65	1868	Planktic	-0.25	0.14		3/25/2004
GAK-4-A-P 69	69	1861	Planktic	-0.39	-0.63		3/25/2004
GAK-4-A-P 73	73	1854	Planktic	0.53	0.86		3/25/2004
GAK-4-A-P 77	77	1848	Planktic	0.36	1.42		3/25/2004
GAK-4-A-P 81	81	1841	Planktic	-3.19	-3.22		3/25/2004
GAK-4-A-P 85	85	1834	Planktic	-0.95	0.00		3/25/2004
GAK-4-A-P 89	89	1828	Planktic	-0.97	-0.14		3/25/2004
GAK-4-A-P 93	93	1821	Planktic	0.34	0.36		3/25/2004
GAK-4-A-P 97	97	1814	Planktic	0.09	0.82		3/25/2004
GAK-4-A-P 101	101	1808	Planktic	-0.97	-2.57		3/25/2004
GAK-4-A-P 105	105	1796	Planktic	0.05	0.95		3/25/2004
GAK-4-A-P 109	109	1780	Planktic	-1.79	-0.78		3/25/2004
GAK-4-A-P 113	113	1764	Planktic	0.20	-1.62		3/25/2004
GAK-4-A-P 117	117	1748	Planktic	-1.34	-0.32		3/25/2004

ID	Core depth (cm)	δ18O year (AD)	ID other	δ13C (permil VPDB)	δ18O (permil PDB)	Notes	Date run
GAK-4-A-P 121	121	1741	Planktic	-0.33	0.73		3/25/2004
GAK-4-A-P 129	129	1732	Planktic	0.90	1.15		3/25/2004
GAK-4-A-P 133	133	1724	Planktic	-2.44	-0.94		3/25/2004
GAK-4-A-P 137	137	1716	Planktic	-0.08	0.98		3/25/2004
NBS-19			std	1.98	-2.15		3/25/2004
NBS-19			std	1.94	-2.22		3/25/2004
Benthic							
NBS-19			std	2.00	-2.12		3/28/2004
NBS-19			std	1.97	-2.09		3/28/2004
NBS-19			std	1.98	-2.15		3/28/2004
NBS-19			std	1.95	-2.10		3/28/2004
GAK-4-A-B 5	5	1990	C. teretis	-0.75	2.02		3/28/2004
GAK-4-A-B 9	9	1978	C. teretis	-1.01	1.96		3/28/2004
GAK-4-A-B 17	17	1954	C. teretis			Too small	3/28/2004
GAK-4-A-B 21	21	1942	C. teretis			Lost computer error	3/28/2004
GAK-4-A-B 25	25	1930	C. teretis			Lost computer error	3/28/2004
GAK-4-A-B 29	29	1925	C. teretis	-0.63	1.78		3/28/2004
GAK-4-A-B 33	33	1919	C. teretis	-0.90	1.83		3/28/2004
GAK-4-A-B 37	37	1913	C. teretis	-0.81	2.49		3/28/2004
GAK-4-A-B 41	41	1907	C. teretis	-0.64	2.21		3/28/2004
GAK-4-A-B 45	45	1901	C. teretis	-0.52	2.40		3/28/2004
GAK-4-A-B 49	49	1894	C. teretis	-0.39	2.29		3/28/2004
GAK-4-A-B 53	53	1888	C. teretis	-0.60	2.26		3/28/2004
GAK-4-A-B 57	57	1881	C. teretis	-0.44	2.35		3/28/2004
GAK-4-A-B 61	61	1874	C. teretis	-0.65	2.13		3/28/2004
GAK-4-A-B 65	65	1868	C. teretis	-0.93	2.05		3/28/2004
GAK-4-A-B 69	69	1861	C. teretis			Too small	3/28/2004
NBS-19			std	1.91	-2.27		3/28/2004
NBS-19			std	1.91	-2.37		3/28/2004
GAK-4-A-B 73	73	1854	C. teretis	-0.78	2.18		3/28/2004
GAK-4-A-B 77	77	1848	C. teretis	-0.66	2.28		3/28/2004
GAK-4-A-B 81	81	1841	C. teretis	-0.90	2.16		3/28/2004
GAK-4-A-B 85	85	1834	C. teretis	-0.70	2.22		3/28/2004
GAK-4-A-B 89	89	1828	C. teretis	-0.52	2.13		3/28/2004
GAK-4-A-B 97	97	1814	C. teretis	-0.77	2.25		3/28/2004
GAK-4-A-B 101	101	1808	C. teretis	-0.55	2.20		3/28/2004

ID	Core depth (cm)	δ18O year (AD)	ID2	δ13C (permil VPDB)	δ18O (permil PDB)	Notes	Date run
GAK-4-A-B 105	105	1796	C. teretis	-0.76	2.05		3/28/2004
GAK-4-A-B 109	109	1780	C. teretis	-0.59	2.22		3/28/2004
GAK-4-A-B 113	113	1764	C. teretis	-0.43	2.14		3/28/2004
GAK-4-A-B 117	117	1748	C. teretis	-0.53	2.17		3/28/2004
GAK-4-A-B 121	121	1741	C. teretis	-0.91	1.62		3/28/2004
GAK-4-A-B 125	125	1737	C. teretis	-0.63	2.32		3/28/2004
GAK-4-A-B 129	129	1732	C. teretis	-0.74	2.26		3/28/2004
GAK-4-A-B 133	133	1724	C. teretis	-0.70	2.27		3/28/2004
GAK-4-A-B 137	137	1716	C. teretis	-0.76	2.20		3/28/2004
NBS-19			std	1.92	-2.29		3/28/2004
NBS-19			std	1.97	-2.21		3/28/2004

Table B – 3

GAK4 Foraminifera Faunal Analysis

Depth (cm)	Size fraction (µm)	Community Totals (Individuals)	Community Totals (Percent)	*Neogloboquadrina pachyderma*	*Globigerina bulloides*	*Cassidulina teretis*	*Ammonia becarii*	*Elphidium excavatum*	*Nonion commune*	*Uvigerina peregrina*	*Quinquelo culina sp.*	Buliminella elegantissima	*Globobulimina auriculata*
5	> 63	3	23.08			2			1				
	125-250	6	46.15	2		1	1		1	1			
	>250	4	30.77			1			2	1			
	Sum:	13	100.00	2	0	4	1	0	4	2	0	0	
9	> 63	0	0.00										
	125-250	15	100.00	10		5							
	>250	0	0.00										
	Sum:	15	100.00	10	0	5	0	0	0	0	0	0	
13	> 63	3	9.38	2								1	
	125-250	24	75.00	16	2	4		1			1		
	>250	5	15.63	2		2		1					
	Sum:	32	100.00	20	2	6	0	2	0	0	1	1	
17	> 63	1	33.33	1									
	125-250	0	0.00										
	>250	2	66.67		1						1		
	Sum:	3	100.00	1	1	0	0	0	0	0	1	0	
21	> 63	6	27.27			4	2						
	125-250	6	27.27	5		1							
	>250	10	45.45						1		9		
	Sum:	22	100.00	5	0	5	2	0	1	0	9	0	
25	> 63	3	16.67			3							
	125-250	11	61.11	8		1			1	1			
	>250	4	22.22						3		1		
	Sum:	18	100.00	8	0	4	0	0	4	1	1	0	

Depth (cm)	Size fraction (µm)	Community Totals (Individuals)	Community Totals (Percent)	*Neogloboquadrina pachyderma*	*Globigerina bulloides*	*Cassidulina teretis*	*Ammonia becarii*	*Elphidium excavatum*	*Nonion commune*	*Uvigerina peregrina*	*Quinqueloculina sp.*	Buliminella elegantissima	*Globobulimina auriculata*
29	> 63	7	30.43	1		4						2	
	125-250	16	69.57	13		3							
	>250	0	0.00										
	Sum:	23	100.00	14	0	7	0	0	0	0	0	2	
33	> 63	3	10.34		1			1	1				
	125-250	22	75.86	9		13							
	>250	4	13.79						2		2		
	Sum:	29	100.00	9	1	13	0	1	3	0	2	0	
37	> 63	27	29.67	5		18	2	1	1				
	125-250	57	62.64	15		33			2	6	1		
	>250	7	7.69						1	5	1		
	Sum:	91	100.00	20	0	51	2	1	4	11	2	0	
41	> 63	20	37.74	3	1	13	2		1				
	125-250	30	56.60	15	8			1	4	1		1	
	>250	3	5.66						2			1	
	Sum:	53	100.00	18	9	13	2	1	7	1	0	2	
45	> 63	23	11.00	12	3	5	1		1		1		
	125-250	175	83.73	79	35	41		1	10	8	1		
	>250	11	5.26		2				9				
	Sum:	209	100.00	91	40	46	1	1	20	8	2		
49	> 63	4	8.89			3		1					
	125-250	36	80.00	11	3	9			8	5			
	>250	5	11.11	2					3				
	Sum:	45	100.00	13	3	12		1	11	5			

Depth (cm)	Size fraction (µm)	Community Totals (Individuals)	Community Totals (Percent)	*Neogloboquadrina pachyderma*	*Globigerina bulloides*	*Cassidulina teretis*	*Ammonia becarii*	*Elphidium excavatum*	*Nonion commune*	*Uvigerina peregrina*	*Quinqueloculina sp.*	Buliminella elegantissima	*Globobulimina auriculata*
	125-250	12	34.29	5		7							
	>250	7	20.00	1				2	2	1		1	
	Sum:	35	100.00	9	3	13		4	3	1	1	1	
57	> 63	4	40.00			4							
	125-250	5	50.00						1	4			
	>250	1	10.00							1			
	Sum:	10	100.00			4			1	5			
61	> 63	14	19.44			3			1	10			
	125-250	51	70.83	1		31		1	12	6			
	>250	7	9.72						6			1	
	Sum:	72	100.00	1		34		1	19	16		1	
65	> 63	8	11.94			7			1				
	125-250	55	82.09	12		27		1	4	11			
	>250	4	5.97							4			
	Sum:	67	100.00	12		34		1	5	15			
69	> 63	7	25.93	2		5							
	125-250	13	48.15	2		6			3	2			
	>250	7	25.93						1	5		1	
	Sum:	27	100.00	4		11			4	7		1	
73	> 63	16	37.21	4	1	7	2	1			1		
	125-250	13	30.23	7		6							
	>250	14	32.56	4		4			1	5			
	Sum:	43	100.00	15	1	17	2	1	1	5	1		
77	> 63	15	40.54	4		10		1					
	125-250	16	43.24	6		10							
	>250	6	16.22	4					1			1	
	Sum:	37	100.00	14		20		1	1			1	

Depth (cm)	Size fraction (µm)	Community Totals (Individuals)	Community Totals (Percent)	*Neogloboquadrina pachyderma*	*Globigerina bulloides*	*Cassidulina teretis*	*Ammonia becarii*	*Elphidium excavatum*	*Nonion commune*	*Uvigerina peregrina*	*Quinqueloculina sp.*	Buliminella elegantissima	*Globobulimina auriculata*
	125-250	37	82.22	14		18			1	3		1	
	>250	5	11.11	1		1			1		2		2
	Sum:	45	100.00	15		20		2	2	3	2	1	2
85	> 63	3	10.34	1		2							
	125-250	21	72.41	14		7							
	>250	5	17.24	2	1			1		1			1
	Sum:	29	100.00	17	1	9		1		1			1
89	> 63	7	18.92	4		3							
	125-250	26	70.27	11		12			1	2			
	>250	4	10.81						1	3			
	Sum:	37	100.00	15		15			2	5			
93	> 63	0	0.00										
	125-250	14	82.35	8		6							
	>250	3	17.65		1				1		1		1
	Sum:	17	100.00	8	1	6			1		1		1
97	> 63	17	15.32	1		15		1					
	125-250	84	75.68	22	2	36		1	10	13			
	>250	10	9.01			1			4	5			4
	Sum:	111	100.00	23	2	52		2	14	18			4
101	> 63	3	9.09			3							
	125-250	26	78.79	2		18			1	4	1		
	>250	4	12.12		1				2	1			
	Sum:	33	100.00	2	1	21			3	5	1		
105	> 63	6	33.33		2	3		1					
	125-250	6	33.33	1		3			1	1			
	>250	6	33.33	2	1				3				
	Sum:	18	100.00	3	3	6		1	4	1			

Depth (cm)	Size fraction (µm)	Community Totals (Individuals)	Community Totals (Percent)	*Neogloboquadrina pachyderma*	*Globigerina bulloides*	*Cassidulina teretis*	*Ammonia becarii*	*Elphidium excavatum*	*Nonion commune*	*Uvigerina peregrina*	*Quinqueloculina sp.*	Buliminella elegantissima	*Globobulimina auriculata*
109	> 63	5	16.13	1	1	2	1						
	125-250	20	64.52	13		4			3				
	>250	6	19.35	5					1				
	Sum:	31	100.00	19	1	6	1		4				
113	> 63	11	36.67	3		6		2					
	125-250	11	36.67	5		6							
	>250	8	26.67	1	1				6				1
	Sum:	30	100.00	9	1	12		2	6				1
117	> 63	2	7.41	1		1							
	125-250	14	51.85	2		10			2				
	>250	11	40.74	4		1		1	3	2			1
	Sum:	27	100.00	7		12		1	5	2			1
121	> 63	3	8.57			3							
	125-250	20	57.14	7		7			2	3	1		
	>250	12	34.29	4	1	2		1	1	3			
	Sum:	35	100.00	11	1	12		1	3	6	1		
125	> 63	3	8.82			3							
	125-250	24	70.59	7		13		2	2				
	>250	7	20.59	1				1	4		1		1
	Sum:	34	100.00	8		16		3	6		1		1
129	> 63	5	11.90			5							
	125-250	36	85.71	13		18			2	2	1		
	>250	1	2.38						1				3
	Sum:	42	100.00	13		23			3	2	1		3
133	> 63	7	46.67			6	1						
	125-250	6	40.00	1		5							
	>250	2	13.33	1							1		
	Sum:	15	100.00	2		11	1				1		

Depth (cm)	Size fraction (µm)	Community Totals (Individuals)	Community Totals (Percent)	*Neogloboquadrina pachyderma*	*Globigerina bulloides*	*Cassidulina teretis*	*Ammonia becarii*	*Elphidium excavatum*	*Nonion commune*	*Uvigerina peregrina*	*Quinqueloculina sp.*	Buliminella elegantissima	*Globobulimina auriculata*
137	> 63	2	5.41			2							
	125-250	20	54.05	5		12	2		1				
	>250	15	40.54	11					2	2			
	Sum:	37	100.00	16		14	2		3	2			

Appendix C
GAK1 Water Column Data

Table C – 1

GAK1 Water Column Data 1976-1977

TEMPERATURE									
Depth	Feb-76	Mar-76	May-76	May-76	Jun-76	Aug-76	Oct-76	Nov-76	Feb-77
0	2.84	3.154	9.384	10.751	12.647	11.3	7.56	5.592	4.257
10	2.86	3.232	7.89	8.029	11.544	11.61	7.57	5.606	4.26
20	2.89	3.134	7.763	7.78	10.97	11.89	7.59	5.651	4.268
30	2.93	3.339	7.357	7.386	9.722	11.98	7.68	5.954	4.269
50	3.14	3.393	7.628	7.428	6.957	10.84	8.4	6.618	4.514
75	3.18	3.405	4.804	4.84	5.388	8.37	9.27	7.379	5.171
100	3.24	3.381	4.8	4.794	5.098	6.82	8.58	8.012	5.704
150	4.08	3.647	5.012	4.926	4.824	5.51	8.27	7.086	6.072
200	4.55	3.788	4.613	4.649	5.083	4.99	5.65	6.539	5.769
250	5.023	4.98	5.271	5.241	5.208	4.826	4.823	4.835	4.942
SALINITY									
0	31.6	31.529	30.303	28.513	26.491	26.34	29.551	28.949	30.718
10	31.627	31.591	31.129	31.088	29.813	27.521	29.545	28.959	30.694
20	31.616	31.691	31.427	31.361	30.546	28.087	29.549	28.977	30.704
30	31.621	31.731	31.376	31.302	30.852	29.323	29.675	29.243	30.71
50	31.702	31.775	31.697	31.519	31.414	30.917	30.048	29.741	30.849
75	31.725	31.78	31.675	31.728	31.75	31.214	31.219	30.569	31.257
100	31.746	31.804	32.249	31.961	32.042	31.851	31.388	31.457	31.613
150	32.132	32.031	32.331	32.338	32.443	32.221	31.87	32.213	32.402
200	32.439	32.129	32.528	32.497	32.778	32.719	32.321	32.654	32.792
250	32.107	32.209	32.548	32.649	32.718	33.245	33.319	33.3	33.237
PREDICTED δ^{18}O pdb (water column)									
0	1.9917	1.8754	1.8754	-0.2776	-2.7504	-2.4921	-0.1497	0.0925	1.2228
10	1.9982	1.8816	1.8816	0.4607	-1.0232	-2.0477	-0.1549	0.0933	1.2114
20	1.9852	1.9521	1.9521	0.6240	-0.5612	-1.8663	-0.1582	0.0895	1.2137
30	1.9765	1.9144	1.9144	0.7049	-0.1199	-1.3442	-0.1257	0.1276	1.2161
50	1.9553	1.9192	1.9192	0.7771	0.8239	-0.3662	-0.1436	0.1749	1.2122
75	1.9546	1.9181	1.9181	1.4989	1.3783	0.3769	0.1537	0.3442	1.2183
100	1.9477	1.9352	1.9352	1.7525	1.5829	1.0513	0.4006	0.5741	1.2355
150	1.8921	1.9635	1.9635	1.7327	1.8315	1.5536	0.6907	1.1424	1.4869
200	1.9022	1.9688	1.9688	1.9247	1.9107	1.9092	1.5611	1.4770	1.7373
250	1.6312	1.6874	1.6874	1.7601	1.8514	2.1839	2.2172	2.2057	2.1498

TEMPERATURE					
Depth	Mar-77	Jul-77	Oct-77	Oct-77	**AVERAGE**
0	5.495	12.7	6.562	6.456	**7.592**
10	5.008	12.62	6.559	6.484	**7.175**
20	4.901	12.419	6.592	6.492	**7.103**
30	5.012	12.2	6.588	6.5	**6.994**
50	5.137	9.198	7.368	8.739	**6.874**
75	5.573	6.424	8.972	7.785	**6.197**
100	5.574	6.176	8.535	8.5	**6.093**
150	5.793	5.595	7.716	7.783	**5.870**
200	5.803	5.383	6.667	6.499	**5.383**
250	5.012	5.88	5.819	5.816	**5.206**
SALINITY					
0	30.842	26.759	29.625	29.799	**29.309**
10	30.996	27.714	29.628	29.793	**30.008**
20	31.062	28.982	29.64	29.803	**30.265**
30	31.133	29.605	29.638	29.833	**30.465**
50	31.209	30.99	30.347	30.826	**31.003**
75	31.58	31.985	31.341	31.108	**31.456**
100	31.863	32.367	31.798	31.794	**31.841**
150	32.248	32.945	32.246	32.22	**32.280**
200	32.764	33.161	32.531	32.613	**32.610**
250	33.222	32.908	32.998	32.901	**32.874**
PREDICTED δ^{18}O pdb (water column)					
0	0.95086	-2.6452	0.13835	0.24225	**0.006**
10	1.1464	-2.2058	0.14044	0.23239	**0.278**
20	1.20363	-1.5998	0.13722	0.23472	**0.401**
30	1.20563	-1.2731	0.13737	0.24586	**0.506**
50	1.20619	0.071	0.24936	0.1135	**0.762**
75	1.25519	1.2124	0.28179	0.47813	**1.076**
100	1.37945	1.4446	0.59238	0.59941	**1.264**
150	1.49172	1.85	0.99636	0.96792	**1.505**
200	1.71616	2.0005	1.38994	1.46932	**1.764**
250	2.12479	1.7595	1.81495	1.77305	**1.911**

Table C – 2

GAK1 Water Column Data 1999-2000

Depth	Feb-99	Mar-I 1999	March II 1999	April I 1999	April II 1999	April II 1999	April IV 1999	May I 1999	May II 1999
TEMPERATURE									
0	3.865	3.713	3.564	3.817	3.951	4.518	4.811	5.403	5.964
10	3.871	3.734	3.564	3.791	3.963	4.299	4.794	5.333	5.636
20	3.873	3.79	3.586	3.818	3.968	4.113	4.751	5.172	5.157
30	3.875	3.801	3.603	3.937	3.951	4	4.674	5.035	5.112
50	3.942	3.806	3.68	4.011	3.968	3.971	4.627	5.041	5.274
75	4.045	3.914	3.744	3.989	3.981	3.979	4.369	4.206	5.168
100	3.846	3.993	3.784	4.054	4.01	3.922	4.377	4.189	4.239
150				4.288	4.254	4.163	4.65	4.434	4.43
200	4.401	4.463		4.918	4.658	4.457	4.929	5.142	5.118
250	5.915	4.872		5.029	4.972	4.98	5.293	5.264	5.326
SALINITY									
0	31.365	31.705	31.7	31.477	31.686	31.385	31.555	31.593	31.574
10	31.516	31.712	31.7	31.538	31.695	31.465	31.563	31.592	31.615
20	31.525	31.727	31.704	31.58	31.706	31.676	31.566	31.6	31.612
30	31.527	31.73	31.708	31.704	31.733	31.684	31.583	31.673	31.622
50	31.542	31.733	31.722	31.797	31.761	31.739	31.667	31.77	31.703
75	31.668	31.761	31.747	31.815	31.78	31.793	31.816	31.772	31.76
100	31.773	31.825	31.77	31.885	31.799	31.845	31.879	31.912	31.868
150				32.096	32.088	31.992	32.063	32.086	32.061
200	32.113	32.175		32.348	32.215	32.149	32.295	32.395	32.38
250	32.769	32.319		32.434	32.398	32.398	32.548	32.529	32.566
PREDICTED EQUILIBRIUM FORAM δ^{18}O pdb									
0	1.6121	1.8024	1.8402	1.6742	1.73034	1.4470	1.4442	1.3053	1.1506
10	1.6769	1.7998	1.8402	1.7080	1.7310	1.5403	1.4523	1.3232	1.2541
20	1.6803	1.7914	1.8360	1.7192	1.7346	1.6827	1.4649	1.3690	1.3782
30	1.6807	1.7898	1.8332	1.7420	1.75102	1.7163	1.4928	1.4371	1.3944
50	1.6693	1.7898	1.8187	1.7631	1.7588	1.7483	1.5422	1.4782	1.3875
75	1.6973	1.7732	1.8125	1.7769	1.76369	1.7699	1.6761	1.7001	1.4404
100	1.7967	1.7802	1.8119	1.7904	1.76430	1.8080	1.7017	1.7662	1.7336
150				1.8209	1.82643	1.8084	1.7103	1.7777	1.7677
200	1.6892	1.7643		1.7735	1.77275	1.7706	1.7543	1.7536	1.7536
250	1.6892	1.7643		1.7735	1.77275	1.7706	1.7543	1.7536	1.7536

Depth	Jun-1999	Jul-1999	Aug I 1999	Aug II 1999	Oct I 1999	Oct II 1999	Oct III 1999	Nov I 1999	Nov II 1999
TEMPERATURE									
0	11.424	12.809	13.27	13.214	10.117	9.727	9.618	5.893	5.823
10	9.735	12.011	13.293	13.345	10.165	10.169	9.623	5.884	5.919
20	8.859	10.25	12.668	12.875	10.563	10.547	10.011	6.035	5.949
30	8.156	8.517	12.031	12.282	10.45	10.463	10.12	6.058	6.094
50	6.822	6.724	8.37	9.069	10.383	10.601	9.987	6.531	6.194
75	5.746	5.829	7.161	6.965	10.237	9.816	10.199	7.804	6.93
100	4.919	5.206	6.921	6.559	7.591	8.68	8.713	7.824	7.529
150	5.631	5.64	5.9	5.922	6.103	6.05	5.971	7.339	7.729
200	5.523	5.59	5.675	5.674	6.017	5.973	5.859	6.831	7.011
250	5.551	5.491	5.571	5.549	5.775	5.769	5.763	6.099	6.127
SALINITY									
0	28.255	29.531	25.997	24.093	26.167	25.713	27.795	30.025	30.145
10	30.524	30.341	27.287	27.806	26.362	27.367	27.799	30.027	30.191
20	31.073	31.078	29.1	28.915	28.594	29.062	28.794	30.076	30.202
30	31.434	31.308	30.461	29.921	29.358	29.625	29.499	30.089	30.252
50	31.64	31.771	31.746	31.56	30.681	30.731	30.511	30.334	30.286
75	31.817	31.929	32.106	32.133	31.53	31.457	31.356	31.388	30.635
100	31.899	32.29	32.238	32.276	32.104	32.113	31.96	31.82	31.28
150	32.443	32.807	32.514	32.675	32.636	32.617	32.549	32.458	31.987
200	32.67	33.043	32.999	33.038	32.985	32.974	32.976	32.778	32.541
250	32.841	33.183	33.147	33.167	33.079	33.066	33.072	33.087	33.092
PREDICTED EQUILIBRIUM FORAM $\delta^{18}O$ pdb									
0	-1.6796	-1.4515	-3.1162	-3.9407	-2.2788	-2.3823	-1.439	0.4875	0.5585
10	-0.2674	-0.9038	-2.5541	-2.3380	-2.2049	-1.7636	-1.438	0.4907	0.5538
20	0.1921	-0.1508	-1.6074	-1.7383	-1.3206	-1.1107	-1.096	0.4731	0.5509
30	0.5276	0.3813	-0.8557	-1.1537	-0.9567	-0.8424	-0.8135	0.4728	0.5352
50	0.9580	1.0408	0.611	0.3539	-0.3581	-0.3896	-0.3354	0.4583	0.5242
75	1.3143	1.3419	1.0761	1.1382	0.0512	0.1230	-0.0159	0.5965	0.4881
100	1.5671	1.6637	1.1957	1.3055	0.9656	0.6945	0.6189	0.7815	0.6188
150	1.6197	1.7775	1.5809	1.6460	1.5818	1.5872	1.5778	1.1856	0.8791
200	1.8157	1.9819	1.9451	1.9597	1.8620	1.8578	1.8620	1.7813	1.7762
250	1.8157	1.9819	1.9451	1.9597	1.8620	1.8578	1.8620	1.7813	1.7762

Depth	Dec I 99	Dec II 99	Jan-00	Feb-00	Mar I 00	Mar II 00	Mar III 00	Apr I 00	Apr II 00
TEMPERATURE									
0	5.776	5.615	3.823	3.42	3.296	3.186	3.858	4.722	4.736
10	5.889	5.646	3.84	3.436	3.657	3.45	3.858	4.714	4.742
20	5.908	6.078	3.897	3.441	3.806	3.857	3.865	4.706	4.751
30	6.085	6.072	3.937	3.502	3.915	3.913	4	4.75	4.756
50	6.287	6.205	3.947	3.796	4.084	4.125	4.289	4.695	4.762
75	7.247	8.065	4.066	4.388	4.494	4.497	4.639	4.703	4.74
100	7.575	7.205	5.386	4.637	4.656	4.666	4.657	4.801	4.846
150	7.236	7.184	6.295	5.147	4.937	4.908	4.999	5.274	5.122
200	7.016	7.078	6.403	5.765	5.426	5.416	5.373	5.534	5.558
250	6.106	6.335	6.542	5.731	5.832	5.816	5.787	5.273	5.279
SALINITY									
0	30.089	30.214	31.097	30.8	30.617	30.604	31.044	31.142	31.139
10	30.176	30.225	31.15	30.808	30.912	30.819	31.045	31.152	31.142
20	30.188	30.39	31.16	30.804	31.027	31.046	31.048	31.157	31.152
30	30.248	30.398	31.168	30.833	31.083	31.077	31.132	31.19	31.167
50	30.328	30.486	31.177	31.039	31.194	31.214	31.337	31.276	31.199
75	30.909	31.51	31.242	31.308	31.461	31.463	31.617	31.364	31.326
100	31.443	31.765	31.716	31.471	31.647	31.662	31.654	31.592	31.43
150	31.881	32.08	32.362	31.802	31.871	31.852	31.907	32.098	31.96
200	32.502	32.433	32.889	32.658	32.225	32.214	32.208	32.617	32.493
250	33.124	32.912	33.052	32.716	32.704	32.711	32.673	32.867	32.853
PREDICTED EQUILIBRIUM FORAM $\delta^{18}O$ pdb									
0	0.54619	0.6431	1.5054	1.4829	1.4358	1.4598	1.4727	1.2860	1.28106
10	0.5550	0.6399	1.5241	1.4821	1.4685	1.4832	1.4731	1.2926	1.28079
20	0.5554	0.6001	1.5133	1.4790	1.4791	1.4738	1.4726	1.2969	1.28282
30	0.5358	0.6051	1.5061	1.4753	1.4746	1.4725	1.4734	1.2998	1.28810
50	0.5186	0.6094	1.5074	1.4871	1.4783	1.4762	1.4866	1.3521	1.30059
75	0.5275	0.5841	1.5042	1.4476	1.4868	1.4868	1.5170	1.3887	1.36228
100	0.6788	0.9149	1.3639	1.4533	1.5257	1.5296	1.5285	1.4632	1.38005
150	0.9580	1.0588	1.4115	1.4644	1.5501	1.5493	1.5496	1.5613	1.54057
200	1.7958	1.6432	1.6513	1.7137	1.6822	1.6894	1.6802	1.9000	1.89226
250	1.7958	1.6432	1.6513	1.7137	1.6822	1.6894	1.6802	1.9000	1.89226

TEMPERATURE					**AVERAGE**
Depth	Apr III 00	May I 00	May II 00	May III 00	
0	5.72	7.454	7.331	8.25	**6.4093**
10	4.932	6.755	7.298	7.323	**6.2796**
20	4.877	6.319	6.793	6.764	**6.1628**
30	4.803	6.068	6.343	6.121	**6.0137**
50	4.772	5.744	5.819	5.579	**5.7131**
75	5.082	5.203	5.026	5.494	**5.6686**
100	5.217	5.324	6.131	5.612	**5.5184**
150	5.28	5.514	5.654	5.634	**5.5603**
200	5.509	5.551	5.538	5.531	**5.5979**
250	5.343	5.558	5.562	5.58	**5.6030**
SALINITY					
0	30.286	29.975	30.741	30.161	**29.9894**
10	30.663	30.997	30.752	30.832	**30.4120**
20	30.944	31.079	30.878	30.969	**30.7559**
30	31.157	31.168	31.01	31.038	**30.9542**
50	31.41	31.279	31.251	31.281	**31.2634**
75	31.566	31.451	31.65	31.69	**31.5748**
100	31.709	31.758	32.087	31.881	**31.8178**
150	31.985	32.371	32.47	32.365	**32.2170**
200	32.372	32.819	32.835	32.832	**32.5724**
250	32.807	32.927	32.949	32.994	**32.8328**
PREDICTED EQUILIBRIUM FORAM δ^{18}O pdb					
0	0.6474	0.0637	0.4321	-0.0561	**0.3537**
10	1.0198	0.6923	0.4454	0.4742	**0.5720**
20	1.1580	0.8408	0.6302	0.6777	**0.7519**
30	1.2712	0.9450	0.8042	0.8740	**0.8761**
50	1.3907	1.0781	1.0462	1.1220	**1.0862**
75	1.3777	1.2953	1.4294	1.3242	**1.2341**
100	1.4051	1.3986	1.3330	1.3774	**1.3780**
150	1.5100	1.6186	1.6256	1.5846	**1.5404**
200	1.8552	1.8517	1.8604	1.8755	**1.7989**
250	1.8552	1.8517	1.8604	1.8755	**1.7989**